

Discovery and Structure–Activity Relationship of Potent and Selective Covalent Inhibitors of Transglutaminase 2 for Huntington's Disease

Michael E. Prime,[†] Ole A. Andersen,[†] John J. Barker,[†] Mark A. Brooks,[†] Robert K. Y. Cheng,[†] Ian Toogood-Johnson,[†] Stephen M. Courtney,[†] Frederick A. Brookfield,[†] Christopher J. Yarnold,[†] Richard W. Marston,[†] Peter D. Johnson,[†] Siw F. Johnsen,[†] Jordan J. Palfrey,[†] Darshan Vaidya,[†] Sayeh Erfan,[†] Osamu Ichihara,[†] Brunella Felicetti,[†] Shilpa Palan,[†] Anna Pedret-Dunn,[†] Sabine Schaertl,[‡] Ina Sternberger,[‡] Andreas Ebnet,[‡] Andreas Scheel,[‡] Dirk Winkler,[‡] Leticia Toledo-Sherman,[§] Maria Beconi,[§] Douglas Macdonald,[§] Ignacio Muñoz-Sanjuan,[§] Celia Dominguez,[§] and John Wityak^{*,§}

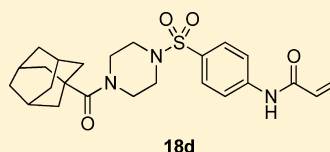
[†]Evotec (UK) Ltd., 114 Milton Park, Abingdon, OX14 4SA, U.K.

[‡]Evotec AG, Schnackenburgallee 114, Hamburg, Germany

[§]CHDI Management/CHDI Foundation, Los Angeles, California, United States

S Supporting Information

ABSTRACT: Tissue transglutaminase 2 (TG2) is a multifunctional protein primarily known for its calcium-dependent enzymatic protein cross-linking activity via isopeptide bond formation between glutamine and lysine residues. TG2 overexpression and activity have been found to be associated with Huntington's disease (HD); specifically, TG2 is up-regulated in the brains of HD patients and in animal models of the disease. Interestingly, genetic deletion of TG2 in two different HD mouse models, R6/1 and R6/2, results in improved phenotypes including a reduction in neuronal death and prolonged survival. Starting with phenylacrylamide screening hit **7d**, we describe the SAR of this series leading to potent and selective TG2 inhibitors. The suitability of the compounds as *in vitro* tools to elucidate the biology of TG2 was demonstrated through mode of inhibition studies, characterization of druglike properties, and inhibition profiles in a cell lysate assay.



TG2 IC₅₀ = 0.010 μM
mTG2 IC₅₀ = 0.016 μM
TG1 IC₅₀ = 3.4 μM
TG3 IC₅₀ >80 μM
FXIIIa IC₅₀ = 0.18 μM
TG6 IC₅₀ = 0.84 μM

■ INTRODUCTION

Tissue transglutaminase 2 (TG2, TGM2, human gene no. 7052) is a multifunctional enzyme primarily known for its calcium-dependent intra- and intermolecular cross-linking activity via isopeptide bond formation between a γ -carboxamide of a glutamine residue of the acyl-donor substrate and an ϵ -amino group of a lysine residue of the acyl-acceptor substrate.¹ TG2 has also been reported to display simple amidase, GTPase, ATPase, and protein disulfide isomerase activities.^{2–4} The protein is the most ubiquitously expressed of the transglutaminase family and has been observed to be localized in the cytosol, cell nucleus, cell membrane, and extracellular compartments.^{5,6} Genetic deletion of TG2 in mice suggests a role for TG2 activity in mitochondrial energy function.⁷ TG2 overactivity has been most closely associated with Celiac disease and Huntington's disease, and there is growing support for roles in inflammation and cancer.^{8–11}

TG2 has been reported to exist in at least two major conformations. These are the transamidation competent Ca²⁺-activated open form and the guanosine nucleotide bound, non-transamidating closed form. An open-inactive form characterized by formation of a Cys370–Cys371 cysteine bridge has also been described.¹² The “open” and “closed” forms are the most studied, and X-ray crystal structures have been reported for each. Liu et al. reported a GTP-bound form having a compact

shape with the transamidation catalytic site obscured within the core domain (Protein Data Bank accession number 1KV3).¹³ An open form was reported by Pinkas et al. (Protein Data Bank accession number 2Q3Z) of an enzyme–inhibitor complex in which TG2 has undergone a substantial conformational rearrangement in which it possesses a linear arrangement of the constituent domains.¹⁴ The structure of the open form protein was obtained in the presence of 10 mM Ca²⁺ and the pentapeptide gluten protein mimic **1** bound covalently to the catalytic cysteine (Cys277). The open form is favored under high Ca²⁺ concentration, while the closed form predominates in the presence of GTP/GDP.

Several groups have reported TG2 inhibitors (Figure 1); these include gluten inspired pentapeptides such as **1** or functionalized amino acids or dipeptides such as **2–4** bearing functionality capable of reacting chemically with biological nucleophiles.^{14–17} Also known are nonpeptidic, small molecule hydrazides represented by LDN-27219 (**5**)¹⁸ and aryl aminoethyl ketones represented by **6**.¹⁹ Detailed mechanism of inhibition studies failed to conclusively identify the site of binding of **5**, and it was reported to bind “at the enzyme's GTP

Received: April 22, 2011

Published: January 6, 2012

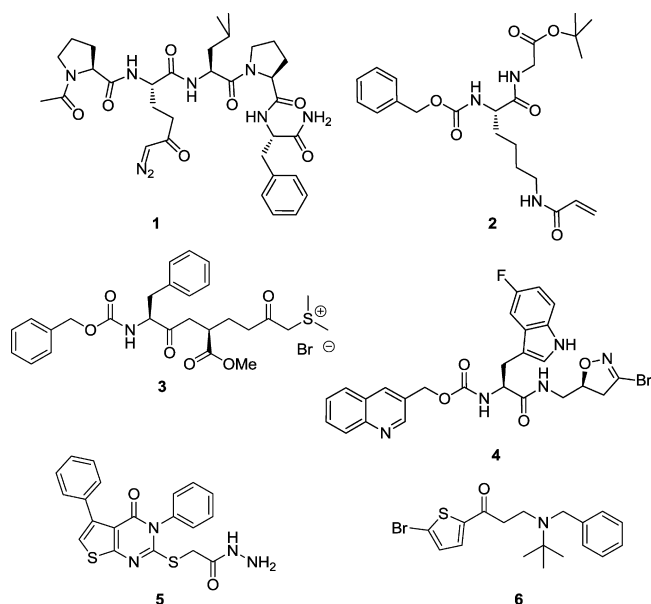


Figure 1. Known inhibitors of TG2.

site or a site that regulates binding of GTP".²⁰ The mechanism of inhibition of **6** has not been reported. Limited selectivity data are available for some of these compounds against at most one or two transglutaminase isoforms.

As mentioned, TG2 has been implicated in the pathology of HD, an autosomal dominant, progressive neurodegenerative disease that is characterized clinically by motor, cognitive, and behavioral deficits. TG2 expression and transglutaminase activity have been shown to be increased in the brains of HD patients and in HD mouse models. This enhanced activity has been correlated with impaired mitochondrial function and shown genetically to modify the progression of the pathogenic phenotype against the R6/1 and R6/2 HD mouse models.^{21–25} Specifically, genetic deletion of TG2 in the context of these models leads to improved phenotypes including a reduction in neuronal death, improvement of motor function, and prolonged survival. With the caveat in mind that genetic deletion of a protein may not have the same effect as inhibition of its activity, we sought to identify potent, selective TG2 inhibitors to recapitulate the results of genetic deletion experiments in proof of concept studies in animal models of HD.

Because the transamidation activity of TG2 is mediated by an active site cysteine, it was expected that a high throughput screening (HTS) strategy would identify electrophilic and otherwise reactive compounds in addition to amine-bearing compounds that could compete for the lysine-bearing substrate.^{26,27} While compounds bearing reactive functionality would be unsuitable starting points for a medicinal chemistry effort directed toward identifying a drug development candidate, these types of hits were deemed acceptable for our more modest goal of identifying an *in vivo* tool for target validation purposes, provided they possessed adequate chemical stability and selectivity. In particular, the selectivity profile across other transamidating and active-site cysteine-containing enzymes is an important factor in the development of TG2 inhibitors for both target validation and therapeutic applications. For example, inhibition of TG1 could result in ichthyosis while inhibition of factor XIIIa might be expected to result in compromised blood clot stabilization and increased bleeding.^{28–30} To interrogate general chemical reactivity, selectivity, and kinetics

of inhibition, specific assays that were previously described were used to triage hits resulting from the HTS.²⁷

RESULTS AND DISCUSSION

Hit Identification and Characterization. An HTS campaign to identify inhibitors of TG2 transamidation activity was run against the Evotec screening collection of 283K compounds. The screen resulted in 2473 primary hits displaying at least 28% inhibition at 10 μM compound concentration, for a hit rate of 0.9%. The HTS was run at the EC_{50} of Ca^{2+} activation for TG2 transamidation, as it was postulated that under these conditions TG2 would be present for inhibition in both the open and closed conformations. In principle, we hoped to identify hits that acted through either the cysteine containing transamidation site or the GTPase site. In practice, however, we did not identify any hits that were competitive with GTP for the closed form. Consistent with this, the X-ray structural data indicated that the guanosine nucleotide binding site is extremely small and unlikely to accommodate molecules of the size typified in the screening set. Furthermore, subsequent virtual screening efforts based on this structure were also unsuccessful in identifying hits that were competitive with GTP (data not shown). In addition to the HTS, virtual screening using the 2Q3Z open form structure and a fragment-based screen were applied to identify hits. After hit confirmation from fresh powder samples, four chemotypes represented by compounds **7a–d** emerged as potential starting points for medicinal chemistry (Figure 2). As an aside, all of the hits described re-

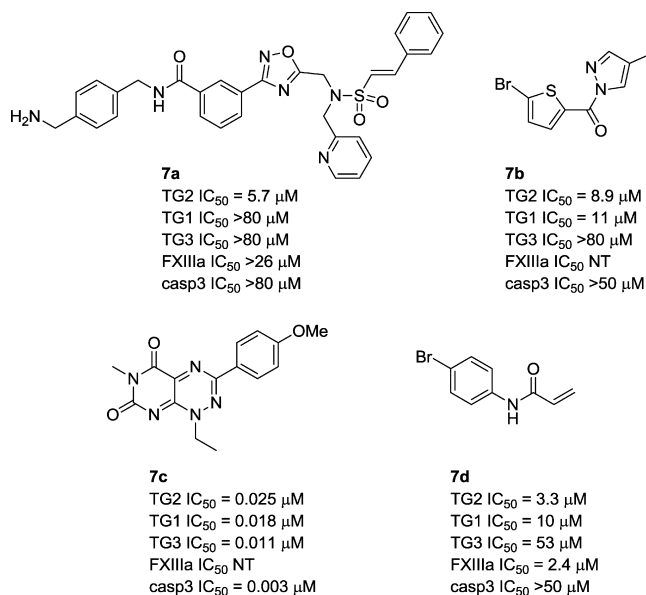


Figure 2. TG2 screening hits and selectivity profiles.

sulted from physical compound screening; our attempts at virtual screening did not yield additional hits.

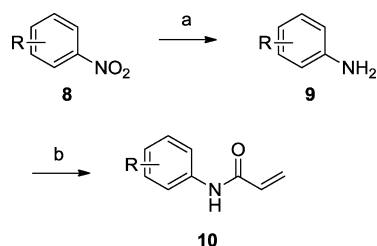
During hit profiling, **7a** was determined to have a TG2 IC_{50} of 5.7 μM . Through kinetics studies **7a** was found to have competitive properties toward the dansyllysine substrate (KxD) as indicated by a K_m increase with unchanged V_{max} (data not shown). This is consistent with a mode of inhibition whereby this compound acts as a pseudo-inhibitor or alternative acyl-acceptor substrate. While attracted by the selectivity of **7a** for TG2, the high molecular weight of this hit (MW = 594) was a significant concern. Its viability as a starting point for medicinal

chemistry optimization rested on being able to improve ligand efficiency. These attempts proved unsuccessful, as a loss of activity was observed upon paring back the molecular weight of the compound. In support of the kinetics studies, protection or removal of the benzylic amine resulted in a complete loss of activity. In addition, since TG2 can catalyze deamidation and transamidation reactions, the potency and efficacy of inhibiting TG2 subsequent to formation of the key thioester bound enzyme–substrate intermediate might not match the potency and efficacy resulting from inhibiting thioester formation. Because of this concern and the poor ligand efficiency, **7a** fell from consideration for further medicinal chemistry efforts. The chemotype exemplified by bromothiophene **7b** were amides that based upon visual inspection were suspected of having poor chemical stability. Compound **7b** had a TG2 IC_{50} of $8.7 \mu\text{M}$ and was inactive in TG3 and caspase 3 counterassays when tested at 80 and $50 \mu\text{M}$, respectively.²⁷ The chemotype fell from consideration when unacceptable chemical reactivity was confirmed, as **7b** reacted with methanol and readily formed a conjugate with glutathione (GSH).³¹ The pyrimidotriazine **7c** was representative of many others in the set of primary hits and had a TG2 IC_{50} of $0.025 \mu\text{M}$. While the activity of this compound was attractive, the chemotype is a known fluorophore³² and has been shown to participate in thiol capture processes.³³ These compounds were eliminated from further consideration once it was determined that **7c** had an IC_{50} of $0.003 \mu\text{M}$ in the caspase 3 counterassay and had potent activity versus other transglutaminase isoforms.

Finally, 4-bromophenylacrylamide **7d** was identified which, as shown in Figure 2, displayed weak activity against TG2 ($IC_{50} = 3.3 \mu\text{M}$) with an encouraging selectivity profile against the other transglutaminases and complete selectivity versus caspase 3 when tested at $50 \mu\text{M}$. Upon variation of the incubation time of **7d** in the transamidation assay, the compound displayed time dependent inhibition consistent with irreversible inhibition. In addition, **7d** appeared to have acceptable stability and did not react with methanol or readily conjugate GSH. Preliminary evidenced suggested that the site of inhibition was Cys277 (see Supporting Information). We report here the SAR study of this chemotype, including the mode of inhibition, computational models to help rationalize the SAR, transglutaminase selectivity, cell lysate TG2 data, and DMPK profiling results of selected compounds.

Synthesis of Inhibitors. General methods used for the synthesis of the phenylacrylamide and heteroarylacrylamide compounds are illustrated in Schemes 1–4. As shown in

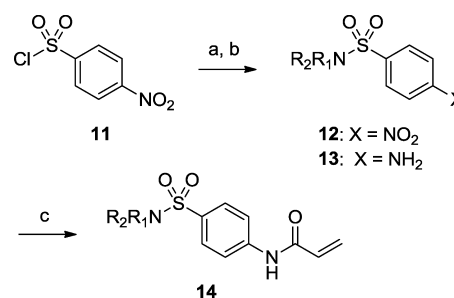
Scheme 1. General Synthesis of Simple Phenylacrylamides^a



^aReagents and conditions: (a) Fe, NH_4Cl (aq), EtOH/ H_2O (5:1), 80°C , 2 h; (b) acryloyl chloride, DIPEA, THF, 18 h.

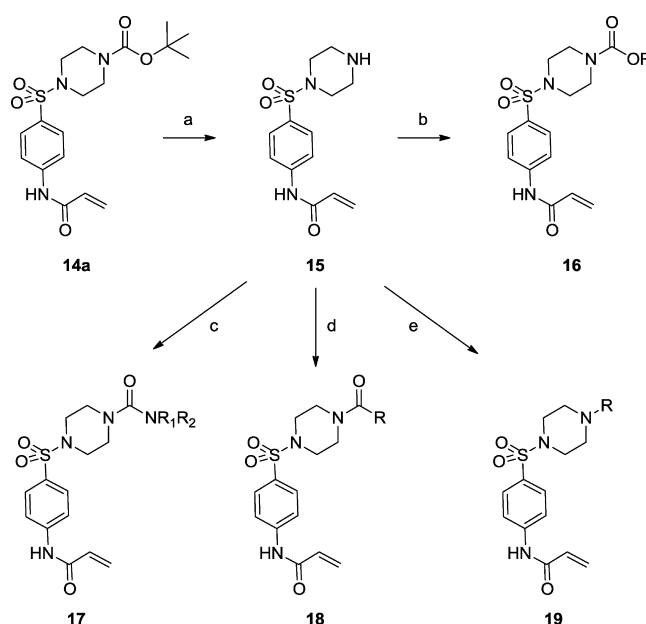
Scheme 1, commercially available nitrobenzenes **8** were reduced to the anilines **9** using reduced iron. Subsequent acylation

Scheme 2. General Synthesis of Sulfonamide-Bearing Phenylacrylamides^a



^aReagents and conditions: (a) DIPEA, THF, 2 h; (b) Fe, NH_4Cl (aq), EtOH/ H_2O (5:1), 80°C , 2 h; (c) acryloyl chloride, DIPEA, THF, 18 h.

Scheme 3. General Synthesis of Sulfonamidopiperazines^a

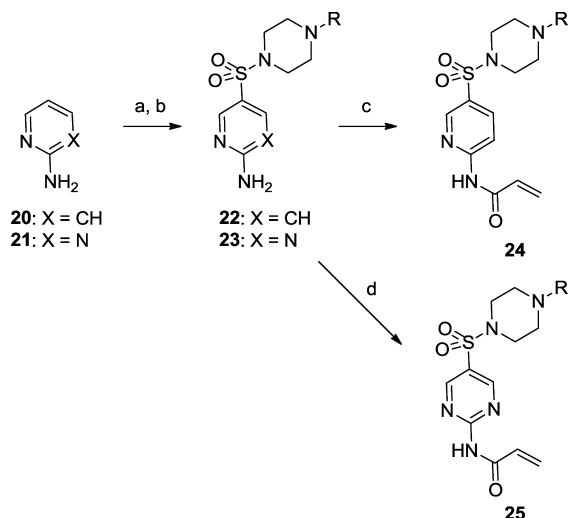


^aReagents and conditions: (a) 20% TFA/DCM, 4 h; (b) DIPEA, THF, RCO_2Cl , 2–10 h; (c) DIPEA, THF, $\text{R}_1\text{R}_2\text{NCOCl}$, 2–10 h; (d) DIPEA, THF, RCOCl , 2–10 h; (e) K_2CO_3 , DMF, RX, 50°C , 18 h.

using acryloyl chloride provided the acrylamides **10** in good yield.

Synthesis of phenylacrylamides bearing a sulfonamide moiety began by treating commercially available 4-nitrophenylsulfonyl chloride **11** with a diverse set of amines in the presence of diisopropylethylamine (DIPEA) in tetrahydrofuran (THF) to afford the sulfonamides **12** (Scheme 2). Subsequent reduction of the nitro group with iron gave the anilines **13**, which were then acylated using acryloyl chloride to provide the acrylamides **14** in good yield.

Synthesis of a wide range of substituted piperazines began with acid catalyzed deprotection of the *tert*-butoxycarbamate **14a** to afford piperazine **15** (Scheme 3). Base promoted acylation of **15** was achieved using a range of chloroformates, carbamoyl chlorides, and acid chlorides, resulting in carbamates **16a–ab**, ureas **17a–e**, and amides **18a–d**, respectively. Under slightly more forcing conditions, piperazine **15** could be alkylated using a range of alkyl halides to give alkyl or cycloalkyl substituted piperazines **19a,b**.

Scheme 4. General Synthesis of Heterocyclic Acrylamides^a

^aReagents and conditions: (a) ClSO₃H, SOCl₂, 150 °C, 2 h (X = CH) or 72 h (X = N); (b) DIPEA, THF, 2 h; (c) acryloyl chloride, DIPEA, DCM, -78 °C, 3 h; (d) NaH, acryloyl chloride, THF, 24 h.

Synthesis of analogues in which the phenylene group was replaced with a heterocycle (Scheme 4) began with chlorosulfonation of either 2-aminopyridine (**20**) or 2-aminopyrimidine (**21**) with chlorosulfonic acid in the presence of thionyl chloride. Base promoted sulfonamide formation then gave the substituted piperazine heterocyclic amines **22** and **23**. The pyridinyl derivatives **24** were prepared in good yield using a range of acylating agents and DIPEA in dichloromethane (DCM) at -78 °C; however, the pyrimidinyl derivatives **25** required more forcing conditions (NaH in THF at ambient temperature) to provide modest yields of the desired products.

Computational Models. While we were able to replicate the published 2Q3Z crystal structure with peptide **1**,¹⁴ we were unable to obtain X-ray quality crystals of inhibitor–TG2 complexes in the presence of any of our small molecule TG2 inhibitors despite significant efforts (data not shown). We attempted cocrystallization experiments with multiple compounds from our series using the hanging drop method. That compounds were bound to TG2 was confirmed using mass spectrometry. We suspect that the additional molecular contacts made by the peptide based inhibitors are necessary to stabilize the open form in a conformation favorable for crystallization. As a surrogate, design concepts were drawn by analyzing the interactions between the peptidic ligand **1** and TG2 found in the X-ray structure of the enzyme–inhibitor complex (Figure 3). As the structure of the peptidic ligand **1** bound in TG2 is a product of an irreversible reaction and there is no equilibrium between the bound and unbound state, the interactions found in the X-ray structure do not directly affect the affinity (reactivity) of **1** to TG2. However, we assumed that the covalently bound structure is a reasonable surrogate for the transition state or the prereaction complex, from which we obtained information on key nonbonding interactions. For studying interactions of this nature, molecular mechanics (MM) based potential functions are generally used. However, the accuracy of the MM method is often questionable, particularly where charge transfer and polarization are important for ligand binding. Moreover, numerous kinds of nonclassical intermolecular forces that may play an important role in inter- and intramolecular interactions

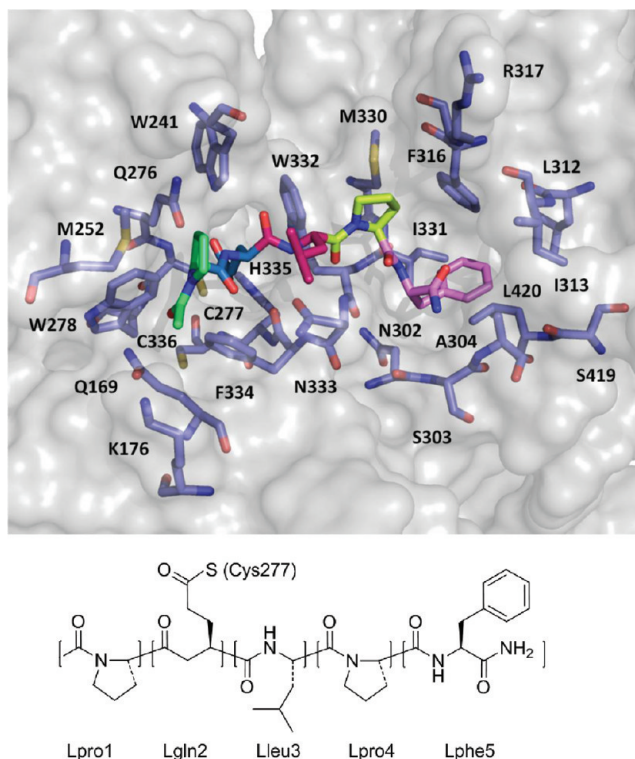


Figure 3. Structure of the peptide ligand **1** bound to TG2 and its fragmentation for FMO calculation (blue = nitrogen, red = oxygen, yellow = sulfur; TG2 is depicted in indigo, and the peptide ligand **1** is multicolored with Lpro1 in green, Lgln2 in blue, Llleu3 in purple, Lpro4 in yellow, and Lphe5 in pink).

are not parametrized in the MM potential functions. For this reason the use of ab initio quantum mechanical (QM) methods is highly desirable for a more accurate understanding of ligand–protein interactions. Until recently, the application of QM methods to rational structure-based drug design (SBDD) has been hampered by the extremely large computational resource required because of the scaling issues in application of the method to large biomolecular systems.

The fragment molecular orbital (FMO) method was proposed by Kitaura et al. to circumvent the scaling issue associated with the QM calculations of large molecular systems.^{34,35} The FMO method divides large molecular systems into numbers of fragments, and the molecular orbital calculations are performed on the fragments (monomer) and the fragment pairs (dimers). The total energy can be obtained as the summation of the monomer energies and the pair interaction energies (PIE). This method is well-suited for parallel computing and results in a dramatic decrease of computational time. Fragmentation of the protein molecule is usually done with one amino acid residue or ligand as the fragmentation unit. Detailed pairwise interaction information between the protein residues and the ligand is obtained as well as the total energy of the system.

Because of the large size of the TG2 protein, the complex that consisted of the residues within a 4 Å distance from the ligand became the basis for the calculation (70 fragments, 1208 atoms). The details of the procedures are described in the Experimental Section. The FMO calculation was performed at the MP2/6-31G** theory level, and the interaction energies between each fragmented section of the ligand and TG2 are summarized in Table 1. Detailed interaction profile diagrams

Table 1. Summary of the Theoretical Interaction Energies between Each Fragmented Section of Ligand 1 and TG2

fragment	interaction energy (kcal mol ⁻¹) ^a	contribution to the total interaction energy (%)	key interacting residues ^b
Lphe5	-64.3	38	Ile331 (HB), Trp332 (vdW), Asn333 (vdW), Ala304 (vdW)
Lpro4	-17.0	10	Trp332 (vdW), Asn333 (vdW), Phe334 (vdW)
Lleu3	-23.3	14	Asn333 (HB)
Lgln2	-48.1	29	Trp241, (HB), Gln276 (HB), Asp333 (HB), His335
Lpro1	-15.9	9	NA

^aThe interaction energies considered were nonbonding interactions only, and the covalent bonding energy between Lgln2 and Cys277 was excluded from the calculation. ^bHB = hydrogen bond. vdW = van der Waals interaction. NA = not applicable.

are also available in the Supporting Information. The interaction energy between covalently bonded fragments has no real physical meaning. Therefore, the interaction energy between Lgln2 and Cys277 was omitted from the table.

The FMO calculation revealed that a large part of theoretical nonbonding interactions comes from the Lphe5 and Lgln2 fragments (38% and 29% of the total, respectively). Lphe5 was found to be particularly important, providing a strong hydrogen bond to the backbone NH of Ile331 and also efficiently filling the space within the lipophilic region, which consists mainly of Phe316, Leu312, Ile331, and Leu420 (human TG2 numbering). Although the resulting energetic contribution to the binding for Lpro4 did not seem to be as significant, the distinct shape of Lpro4 was considered critical for placing the key Lphe5 residue into this lipophilic region. The N-terminal Lpro1 also seemed to have minimal contribution to the total interaction energy. The interaction energy profile of the peptidic ligand **1** was found to be in good agreement with the inhibitory activity data for truncated analogues of **1**. For example, removal of the C-terminal phenylalanine from **1** resulted in a total loss of TG2 activity, whereas the N-terminal proline could be removed with minimal loss of activity (data not shown).

In order to further enhance the selectivity profile for TG2 versus other related transglutaminases, homology modeling of the other transglutaminase isoforms was performed. Significant differences exist between the isoforms, particularly in the lipophilic region of the active sites of the enzymes which could be exploited to develop molecules with improved selectivity (Figure 4). In the **1**-TG2 complex structure the C-terminal phenylalanine residue of the peptidic ligand is placed in its highly lipophilic cavity.¹⁴ For the isoforms of TG2, TG1, TG3, and FXIIIa, major differences are found in this region at residue positions 312 and 420.^{29,36,37} The homology model of TG3 reveals that this isoform has a serine at position 312 and a histidine residue at position 420 that occupies the space in the middle of the cavity, rendering this pocket unsuitable for the binding of large lipophilic groups (Figure 4C). The selectivity profiles of the inhibitors presented in Table 3 are in agreement with this model. TG1 and FXIIIa have lipophilic pockets similar to that of TG2 in size. Docking of the pentapeptide ligand to the homology models of these two latter isoforms suggests that the C-terminal phenylalanine can be readily accommodated within their lipophilic regions. However, although they do not explicitly present the side chain functional groups within the pocket, TG1 and

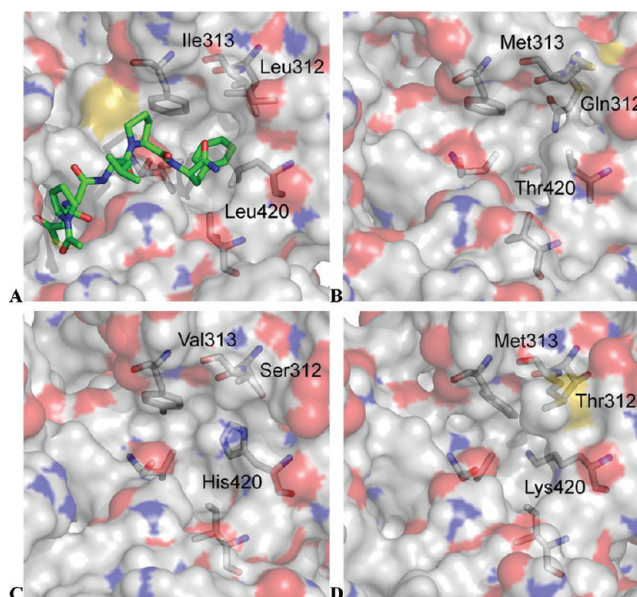


Figure 4. Homology models of the transglutaminase isoforms TG1, TG3, and FXIIIa highlighting residues lining the lipophilic pocket (green = peptide ligand **1**, blue = nitrogen, red = oxygen, yellow = sulfur, gray = carbon): (A) active site of TG2 in the open conformation, PDB code 2Q3Z¹⁴ (with peptide inhibitor **1** in green), showing the presence of Leu312 and Leu420; (B) homology model of the active site of FXIIIa showing the presence of Gln312 and Thr420 in the lipophilic pocket; (C) homology model of the active site of TG3 showing the presence of Ser312 and His420 in the lipophilic pocket; (D) homology model of the active site of TG1 showing Thr312 and Lys420.

FXIIIa have polar residues at the bottom of the pocket (Gln312, Thr420 for FXIIIa and Thr312, Lys420 for TG1 (parts B and D of Figure 4, respectively).

Simple Arylacrylamide SAR. Because of the time-dependent nature of irreversible inhibition, the IC₅₀ might not provide a reliable assessment of biochemical activity, since it is measured at a single time point. This was a concern especially for slower binding inhibitors; therefore, compounds were spot checked during the course of the SAR study to ensure that the 30 min compound incubation used to obtain the IC₅₀ values was adequate to show full inhibition of TG2. For many of the compounds irreversible inhibition constants (*K_i*) were measured from the monoexponential curves of the enzymatic reaction.³⁸ A typical example is shown for compound **7d** in Figure 5. Pseudo-first-order inactivation rate constants (*k_{obs}*) were calculated from these curves (Figure 5A). These values were then used to construct a plot of *k_{obs}* versus inhibitor concentration as shown in Figure 5B. Linear regression of the data from this plot yielded the inhibition constants *k_{cat}*, *k_{inact}*, and *K_i* from which *k_{inact}*/*K_i* was derived and reported in the tables. The graph in Figure 6 shows a log-log plot of the relationship between *k_{inact}*/*K_i* and IC₅₀ for all compounds upon which irreversible inhibition constants were measured, demonstrating a high correlation between these values. Similar high correlation was also observed between *k_{inact}*/*K_i* and IC₅₀ for TG1, TG3, and FXIIIa (available as Supporting Information), validating the use of the IC₅₀ for both the primary (TG2) and secondary assays in guiding medicinal chemistry.

An initial SAR survey around compound **7d** led to the series of analogues shown in Table 2. Replacement of the acrylamide with a vinylsulfonamide resulted in **10a** having 5-fold lower

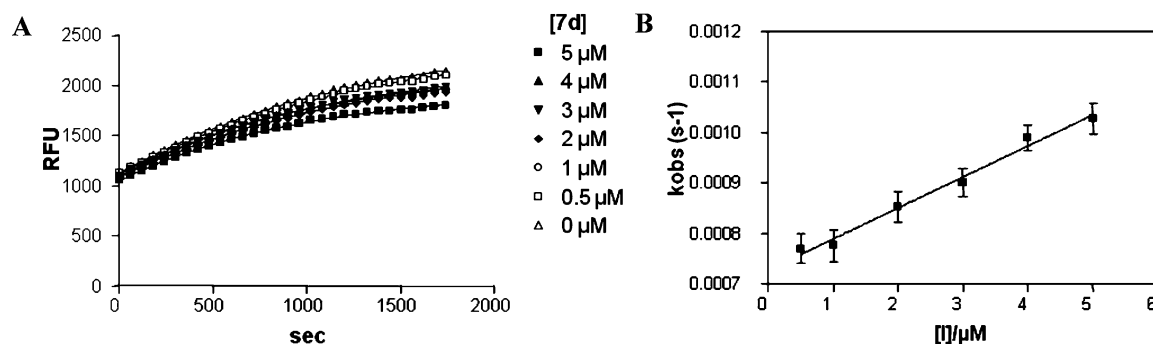


Figure 5. Determination of irreversible inhibition constants for **7d**: (A) exponential inactivation of TG2 by **7d** at varied concentration; a mono-exponential association equation (solid line) was used to fit k_{obs} ; (B) plot of k_{obs} versus inhibitor concentration.

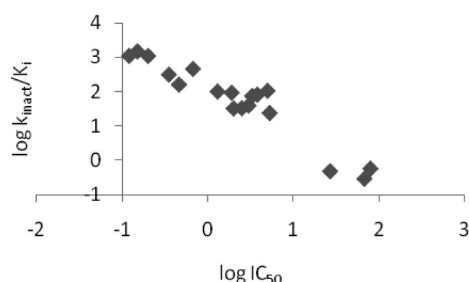


Figure 6. Correlation of TG2 inhibition $\log IC_{50}$ versus the irreversible inhibition $\log k_{\text{inact}}/K_i$ ($r^2 = 0.95$).

potency than **7d**. As expected, reduction of the acrylamide to the propionamide caused a complete loss of activity for **10b**, while inserting a methylene spacer into the aniline C–N bond in **10c** also resulted in a large decrease in activity. Comparison of the 2-bromo and 3-bromo analogues **10d** and **10e** with **7d** showed that 3-bromo and 4-bromo were equipotent while the 2-bromo analogue was inactive. In a comparison of substituents at the 4-position (**10f–o**), there was in general a strong correlation of TG2 potency with the electron withdrawing ability of the substituent.

Molecular docking was used to aid inhibitor design, prioritize compound targets for synthesis, and help in the understanding of binding interactions between our inhibitors and TG2. The open form of TG2 in complex with compound **1** (PDB code 2Q3Z) was prepared for docking. Given that our inhibitors covalently bind to the catalytic cysteine, Cys277, the covalent docking procedure provided by Gold was used for routine docking in which both protein and ligand contain the linking sulfur atom of Cys277. This required that the structures of the ligands be prepared as their corresponding thiol addition products with one open valence at sulfur. The docking procedure confirmed that the terminal vinylic carbon of the acrylamide moiety was indeed the site of reactivity with Cys277. In addition, docking of compound **10g** suggested hydrogen bonding interactions between the acrylamide CONH with the side chains of Trp241 and Gln276 (Figure 7A). In addition to these interactions, the model suggested that the sulfonyl might be engaged in a hydrogen bonding interaction with the side chain of Asn333. Furthermore, it was apparent that the sp^3 hybridization of the sulfonamide appeared capable of directing substituents toward the lipophilic region. Thus, significant activity and selectivity improvements might be achieved by extending the sulfonamide to better occupy this region and take advantage of this hydrophobic pocket and its potential for offering selectivity against other transglutaminases.

Extending the Sulfonamide into the Lipophilic Region. On the basis of examination of the binding mode proposed for our inhibitors, we began to investigate extending the sulfonamide in order to reach the lipophilic region. As shown in Table 3, many examples of this set showed significantly improved TG2 activity and selectivity compared to **10g**. All of the compounds showed improved selectivity against TG1 and FXIIIa and were inactive against TG3. The activity and selectivity of peptide **1** are shown for comparison. Given that transglutaminase isoform testing occurred over several days from the same DMSO stock solutions beginning with TG2 followed by other TG isoforms over the course of days, one could hypothesize that the observed selectivity was a result of compound degradation in the DMSO solution. To address this, we reassayed selected inhibitors from the same stocks against TG2 after the selectivity panel was completed and were able to confirm TG2 potency, thus verifying the previously observed selectivity.

Benzyl carbamate **16a** was one of the earliest potent compounds synthesized and displayed TG2 IC_{50} of $0.12 \mu\text{M}$ and an irreversible inhibition constant k_{inact}/K_i of $1087 \text{ M}^{-1} \text{ s}^{-1}$. When docked into TG2, **16a** appeared to conserve all interactions of **10g** while positioning the Cbz group for interaction with the lipophilic region (Figure 7B). The Boc-derivative **14a** was equipotent with **16a**, while piperazine **15**, which lacks a lipophilic substituent, was equipotent with **10g**. Of the aminopyrrolidines (**16b–e**), 3(*R*)-aminopyrrolidine **16b** was equipotent with **16a**, with the other isomers being 4- to 5-fold less potent. Of the remaining compounds from Table 3, only the diazabicyclooctane **16f** showed TG2 activity comparable to that of **16a**. Rendering the linker acyclic (**16g**), constraining the piperazine (**16h**), increasing the linker length by one to two atoms (**16i–l**), or increasing the ring size by 1 to the homopiperazine (**16m**) all resulted in decreased TG2 potency. Interestingly, the *m*-phenylacrylamide **16n** was only 3-fold less potent than **16a**.

The importance of the putative hydrogen bonding interactions between the acrylamide amide and Trp241/Gln276 is illustrated by the N-methylation of **14a** to afford acrylamide **26** and the isomer of **16a**, piperazine **27** (Figure 8). Compound **26** was approximately 40-fold less potent compared to **14a**. Similarly, compound **27** in which the piperazinyl and phenyl moieties of **16a** are transposed was approximately 25-fold less potent than **16a**. Taken together, these results suggest the importance of the acrylamide-Trp241/Gln276 interaction; however, confirmation of this and other aspects of the binding

Table 2. TG2 Activity of Simple Arylacrylamides^a

R	Cmpd No.	TG2 IC ₅₀ ± SD (μM)	TG2 k _{inact} /K _i (μM ⁻¹ s ⁻¹)
4-Br	7d	3.3 ± 2.0	74
---	10a	16	NT
---	10b	>80	NT
---	10c	43	NT
3-Br	10d	3.0 ± 0.0	39
2-Br	10e	>80	NT
4-F	10f	29	NT
4-SO ₂ N ₅	10g	1.9 ± 0.3	92
4-SO ₂ CH ₃	10h	5.0	105
4-NO ₂	10i	0.67	453
4-CF ₃	10j	3.8 ± 0.4	81
H	10k	43	NT
4-CH ₃	10l	45	NT
4-OC ₆ H ₅	10m	26	NT
4-OCH ₃	10n	58	NT
4-N ₅	10o	30	NT

^aValues accompanied by standard deviation were averaged from at least two independent experiments; they were otherwise obtained in a single determination. NT = not tested.

model would require additional experimentation, such as X-ray crystallography of an inhibitor–protein complex.

Defining the SAR of the Covalent Warhead. The SAR with respect to the acrylamide moiety was next investigated (Table 4). Because of the weak TG2 activity observed for most

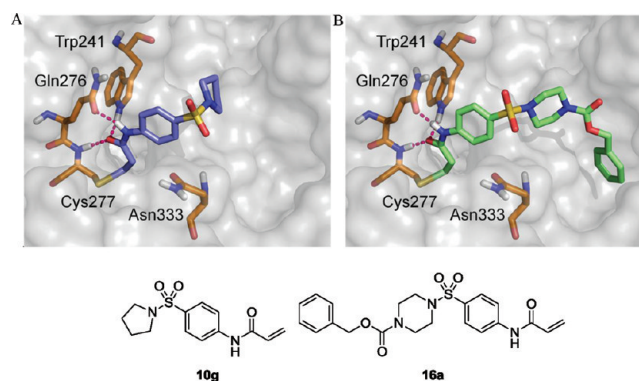
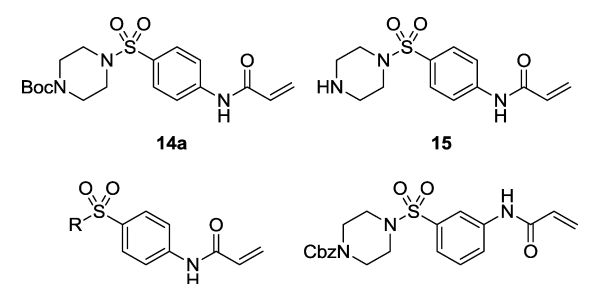


Figure 7. Binding model for interaction of 10g (in indigo, part A) and 16a (in green, part B) with TG2.

of these compounds, irreversible inhibition constants were determined for many of them, the results of which continued to reinforce the good correlation observed between the two inhibition constants and ensure that weak activity was not due to unfavorable kinetics of inhibition. Surprisingly, racemic epoxide 28b showed a 750-fold lower potency against TG2 relative to 28a. A series of acrylamides bearing substituents at the α - and/or β -positions was next explored (28c–k). Other than β -Z-chloroacrylamide 28j, none of these compounds showed comparable or improved TG2 potency relative to 14a. Somewhat surprisingly, a series comprised of ketones, esters, and nitriles (28l–q) were all determined to be completely inactive versus TG2. These results perhaps underscore fundamental differences in the topography of the catalytic tunnel proximal to Cys277 with the corresponding catalytic region in the cathepsins, which can accommodate and react with these warheads.³⁹ Activated nitriles are particularly good inhibitors of the cathepsins, which have a more open architecture in the region of the active site. In contrast, the catalytic tunnel of TG2 as exemplified in the 2Q3Z structure appears much narrower. In light of this, the micromolar TG2 potency of acetylene 28r, which would not be predicted as being a particularly good Michael acceptor, is noteworthy. Reversing the polarity of the Michael acceptor as in 28s and 28t also proved to be unrewarding. Only slightly better was tethering a diazoketone as in peptide 1; compounds 28u and 28v had TG2 potencies of 4 and 16 μ M, respectively.

An interesting finding was the 50-fold potency disparity between 28j and the β -E-chloro analogue 28k. This difference may be rationalized based on modeling the interactions in the catalytic region as shown in Figure 9. In preparing for such an analysis several assumptions were made: (1) the carbonyl oxygen of the acrylamide needs stabilization by one or more H-bond donor residues; (2) the carbonyl and double bond are required to be coplanar; (3) the acrylamide is required to be in the *s*-cis conformation, (4) the steric bulk of the chlorine atom has to be accommodated in the small catalytic cavity, (5) the incoming thiol needs to attack perpendicular to the plane of the acrylamide. With these assumptions in place β -chloroacrylamide fragments with (*S*)- and (*R*)-configurations were each covalently docked to TG2. In examination of the (*S*)-configuration adduct that would arise from *Z*-alkene 28j, it was noted that in the (*S*)-configuration the carbonyl oxygen is stabilized by Trp241 in the transition state and the carbonyl and (ex)double bond are nearly coplanar. By comparison, binding interactions between TG2 and the (*R*)-adduct that would result from *E*-alkene 28k were less energetically favored

Table 3. TG2 Activity and Transglutaminase Selectivity of Sulfonamides^a


R	Cmpd No.	TG2 IC ₅₀ ± SD (μM)	TG2 k _{inact} /K _i (μM ⁻¹ s ⁻¹)	TG1 IC ₅₀ (μM)	TG3 IC ₅₀ (μM)	FXIIIa IC ₅₀ (μM)
---	1	0.20 ± 0.14	1076	45	>80	>80
---	10g	1.9 ± 0.3	92	25	>80	0.77
---	14a	0.12 ± 0.00	NT	4.9	>80	0.43
---	15	1.3 ± 0.2	NT	45	>80	1.1
CbzN	16a	0.12 ± 0.05	1087	3.7	>80	0.42
CbzN	16b	0.096 ± 0.021	NT	3.6	NT	0.41
CbzHN	16c	0.52 ± 0.05	NT	14	>80	0.72
CbzN	16d	0.58 ± 0.03	NT	2.9	>80	0.50
CbzHN	16e	0.50 ± 0.14	NT	14	>80	0.96
CbzN	16f	0.14 ± 0.05	NT	9.5	>80	0.60
CH ₃	16g	1.5 ± 0.1	NT	8.1	>80	0.85
BocN	16h	0.30 ± 0.01	NT	14	NT	2.1
CbzHN	16i	0.21 ± 0.02	NT	2.9	>80	0.44
CbzN	16j	0.38 ± 0.02	NT	1.8	>80	0.52
CbzHN	16k	0.22 ± 0.02	NT	4.6	>80	0.31
CbzN	16l	0.45 ± 0.10	NT	2.7	>80	0.48
CbzN	16m	0.46 ± 0.01	159	4.6	>80	0.67
---	16n	0.35 ± 0.03	309	4.1	71	0.35

^aValues accompanied by standard deviation were averaged from at least two independent experiments; they were otherwise obtained in a single determination. NT = not tested.

and do not benefit from stabilization of the transition state by the protein.

SAR of the Phenylene Linker. In a comparison of peptide **1** with piperazine **16a**, it is immediately apparent that the *N*-acetylPro residue of the peptide inhibitor has no counterpart in **16a**. Furthermore, deletion of the Pro residue from **1** resulted in a nominal 3-fold loss in TG2 activity but more importantly significantly reduced transglutaminase selectivity (data not shown). As depicted in Figure 10, examination of the homology model suggests that FXIIIa is considerably more polar than TG2 in the region proximal to the *N*-acetylPro: Tyr169, Ser252, and Tyr334 in FXIIIa versus Gln169, Met252, and Phe334 in TG2. Substitution at the 2- or 3-position of the

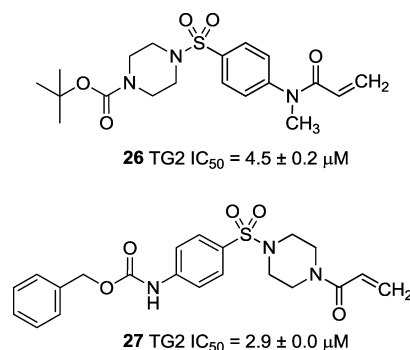


Figure 8. Inhibitors designed to interrogate specific putative hydrogen bonding interactions with Trp241/Gln276 of TG2.

phenyl moiety of **16a** was identified as a design strategy to potentially take advantage of these differences (Table 5). It was quickly determined that substitution at the 2-position was not well-tolerated (**29a** and **29b**). For the 3-position, methoxy (**29c**) or methyl (**29d**) resulted in an order of magnitude loss of potency relative to **14a**. Substitution with 3-trifluoromethyl (**29e**), 3-fluoro (**29f**), or 3-chloro (**29g**) was better tolerated with respect to TG2 activity; however, decreased selectivity against FXIIIa was observed. As highlights to this, **14a** and **16a** were 3- to 4-fold more active on TG2 than FXIIIa while **29e–g** were approximately 2- to 4-fold more active on FXIIIa than TG2.

Beyond Cbz: Filling the Lipophilic Region for Activity and Selectivity. For the lipophilic tail, replacement of the Cbz moiety with a variety of substituted benzyl carbamates resulted in compounds **16o–ab** (Table 6). Many of these showed comparable or improved TG2 potency when compared to **16a**. The 4-fluoro and the 2,3- and 3,5-difluorobenzyls **16o–q** all showed improved TG2 potency, with **16o** showing TG2 IC₅₀ of 0.046 μM. Ortho substituents, as in **16r–u** were well-tolerated but showed at best a 2-fold improvement in TG2 potency for **16u**. Of the 1- and 2-naphthylmethyl carbamates **16v** and **16w**, 1-naphthyl **16v** showed a slight improvement in TG2 potency while **16w** was approximately 2-fold less potent relative to **16a**. In comparing the 2-, 3-, and 4-phenoxybenzyl carbamates, the 3- and 4-derivatives **16x** and **16y** each showed 2-fold improvement in potency, while **16t** had potency comparable to that of **16a**. Moving away from the benzyl carbamate motif led to alkyl carbamates **16z–ab**. Unexpectedly, methyl carbamate **16z** was found to be equipotent with **16a**. Ethyl carbamate **16aa** improved on this potency by nearly 2-fold, and cyclopentyl carbamate **16ab** showed a further incremental improvement. These results may indicate that the sp²-hybridized aryl moieties of the benzyl type carbamates are not fully engaged with the lipophilic region and that sp³-hybridized groups might make stronger interactions. Amides **18a–c** were prepared to investigate the contribution of the carbamate linkage to TG2 activity and to reduce the number of rotatable bonds. Compared to **16a**, amide **18a** displayed a slight decrease in TG2 potency, whereas *trans*-2-phenylcyclopropylamide **18b**, which was prepared as the racemic mixture, was 2- to 3-fold more potent than **16a**. Cyclopropylamide **18c**, which lacks the pendant phenyl group, was equipotent with **16a**.

A series of lipophilic *N,N*-dialkylureas (**17a–e**) were next evaluated (Table 6). These compounds show improved TG2 potency compared to **16a**, with octahydroisoquinoline **17a** showing TG2 IC₅₀ of 0.020 μM and greater than 10-fold selectivity versus FXIIIa. Similar results were seen with the lipophilic

Table 4. TG2 Activity and Transglutaminase Selectivity of Acrylamide Replacements^a

28a-v

R ₁	R ₂	Cmpd No.	TG2 IC ₅₀ ± SD (μM)	TG2 k _{inact} /K _i (μM ⁻¹ s ⁻¹)	TG1 IC ₅₀ (μM)	FXIIIa IC ₅₀ (μM)	R ₁	R ₂	Cmpd No.	TG2 IC ₅₀ ± SD (μM)	TG2 k _{inact} /K _i (μM ⁻¹ s ⁻¹)	TG1 IC ₅₀ (μM)	FXIIIa IC ₅₀ (μM)
Boc		14a	0.12 ± 0.00	NT	4.9	0.43	Boc		28j	0.14 ± 0.02	1465	8.8	0.87
Cbz		16a	0.12 ± 0.05	1087	3.7	0.42	Boc		28k	6.8	5.3	NT	NT
		28a	0.032 ± 0.01	NT	5.6	0.28	Boc		28l	>80	NT	NT	NT
		28b	28 ± 1	0.48	NT	NT	Boc		28m	>80	NT	NT	NT
Boc		28c	2.3 ± 0.8	32	>80	8.9	Boc		28n	>80	80	NT	NT
Boc		28d	>80	NT	>80	>80	Boc		28o	>80	NT	NT	NT
Boc		28e	2.8 ± 0.4	33	>80	>80	Boc		28p	>80	NT	NT	NT
Boc		28f	2.8 ± 1.3	NT	>80	27	Boc		28q	>80	NT	>80	>80
Boc		28g	>80	NT	>80	>80	Boc		28r	1.4 ± 0.1	1.3	>80	6.7
Boc		28h	>10	NT	NT	NT	Cbz		28s	>80	NT	NT	NT
Boc		28i	>10	NT	NT	NT	Cbz		28t	91 ± 32	0.29	8.9	6.8
Boc		28i	>10	NT	NT	NT	Cbz		28u	4.0 ± 0.6	NT	6.4	46
Boc		28i	>10	NT	NT	NT	Cbz		28v	16 ± 1.0	NT	NT	NT

^aValues accompanied by standard deviation were averaged from at least two independent experiments; they were otherwise obtained in a single determination. NT = not tested.

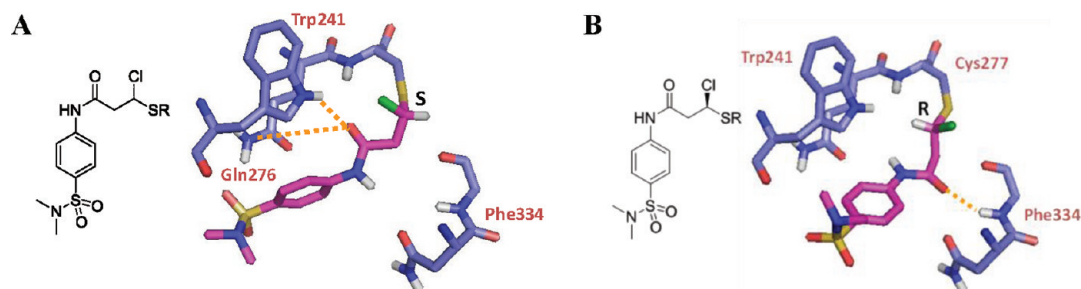


Figure 9. Models for the binding of β -chloroacrylamides **28j** and **28k** (magenta) with TG2 (indigo): (A) covalent adduct of (S)-chloride fragment and TG2 showing hydrogen bonding interactions of carbonyl with Trp241 and Gln276; (B) covalent adduct of (R)-chloride fragment and TG2 showing lack of stabilization from Trp241 and Cys277.

amides **28a** and **18d**, with the adamantyl derivative **18d** showing a TG2 IC₅₀ of 0.010 μM and 18-fold selectivity versus FXIIIa. With large lipophilic groups as are present in **18d**, ligand efficiency becomes a concern relative to compounds such

as **17c** and **28a**; however, further transglutaminase profiling revealed that **18d** had superior selectivity across all isoforms. Adamantylamide **18d** was 340-fold selective for TG2 versus TG1 and >8000-fold selective for TG2 versus TG3, while it had a

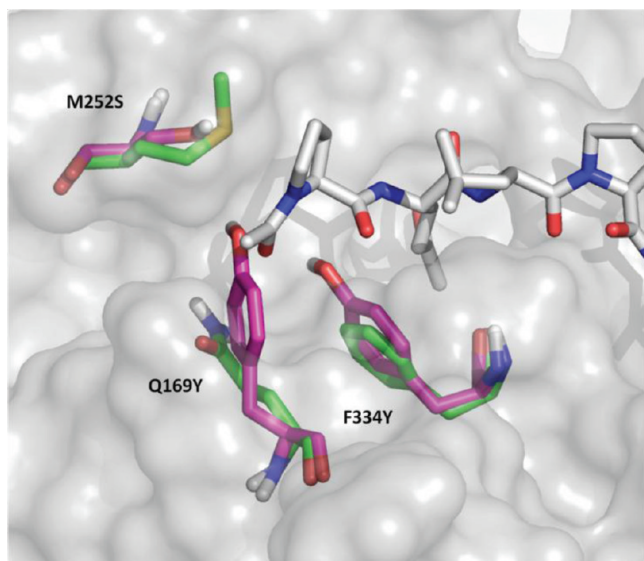


Figure 10. Homology model of FXIIIa (magenta) overlaid on the 2Q3Z TG2 structure (green) with peptide ligand 1 (gray).

TG6 IC₅₀ of 0.84 μ M (84-fold selectivity). In addition, when tested against mouse TG2, **18d** showed an IC₅₀ of 0.016 μ M. That no significant species difference was demonstrated for inhibition of the mouse and human isoforms is important for potential in vivo efficacy studies, given that our HD models are mouse models. If inhibition were significantly weaker in the mouse, higher tissue exposure levels would be required to affect pharmacodynamic and efficacy readouts.

A limited number of heterocyclic replacements intended to probe the contribution of the carbonyl group of the terminal lipophilic acyl moiety to transglutaminase activity were also investigated (Table 7). Pyridin-2-yl analogues **14b–f** showed improved potency versus **16a**, with 3-methylpyridin-2-yl **14c** having TG2 IC₅₀ of 0.025 μ M and 14-fold selectivity against FXIIIa. The requirement of the carbonyl or a carbonyl mimetic for potent inhibition of TG2 and selectivity over FXIIIa was underscored by comparison of unsubstituted phenyl **14g** and 2-trifluoromethylphenyl **14h** with pyridines **14b** and **14e**, respectively, which were 3- to 4-fold more potent against TG2. The significance of the carbonyl was further underscored by

alkyl-substituted analogues **19a** and **19b**. These compounds lack the terminal carbonyl but still bear a pendent phenyl substituent that could interact with the lipophilic region. These were 3- to 4-fold less potent against TG2 than **16a**, suggesting the importance of a lipophilic group attached to a carbonyl moiety or carbonyl mimetic for a productive interaction with the lipophilic pocket.

Replacement of the Phenylene Moiety with Pyridine and Pyrimidine. As a final chapter of the SAR investigation, replacement of the phenylene moiety with 2-pyridin-5-yl and 2-pyrimidin-5-yl heterocycles was investigated (Table 8). Overall, the pyrimidines **24a–d** and pyrimidines **25a–c** were approximately equipotent for TG2 as their phenylene counterparts **14a**, **16a**, **18c**, and **18d**. Strikingly, selectivity versus FXIIIa improved across the board with these changes, going from a maximum of 18-fold selectivity for **18d** to 145- and 175-fold for **24d** and **25c**, respectively. Rationalizing these selectivity findings using our FXIIIa homology model would be pure speculation, as the residues that are expected to stabilize the binding interactions, Trp241 and Gln276, are conserved between TG2 and FXIIIa. While encouraged by the improved selectivity, concern was mounting that increased electronegativity of the acrylamide might render it unacceptably reactive toward other biological nucleophiles. To investigate, the half-lives of three respective compounds, **14a** (phenylene), **24a** (2-pyridin-5-yl), and **25a** (2-pyrimidin-5-yl), were determined in the presence of 5 mM GSH as a prototypical biological nucleophile.³¹ The rate of disappearance of compound **14a** with glutathione was relatively low as indicated by an observed half-life of >24 h. By comparison **24a** and **25a** reacted much more rapidly, in line with the increased electronegativity of the heterocycle, showing half-lives for the disappearance of parent of 1 and 0.5 h, respectively. Although compounds like **24a** and **25a** demonstrated that a high degree of selectivity for inhibition of TG2 was possible, their reactivity in the presence of glutathione severely restricted their utility.

Cell Lysate Activity of TG2 Inhibitors. We had previously developed a cellular assay measuring transamidation based on incorporation of radioactive putrescine in HEK cells stably expressing TG2 (HEK-TG2).²⁷ Our inability to show potent (IC₅₀ < 1 μ M) inhibition of transamidation in this cell line with highly potent irreversible inhibitors from numerous chemical classes,²⁷ including those from the present study, was cause for

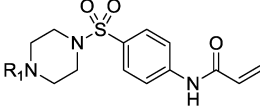
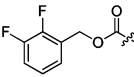
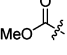
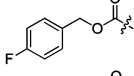
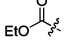
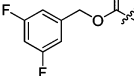
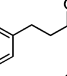
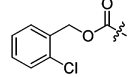
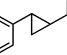
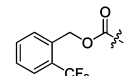
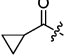
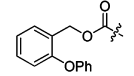
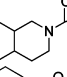
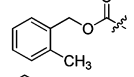
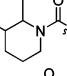
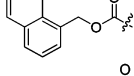
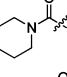
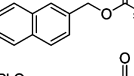
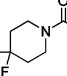
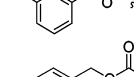
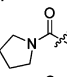
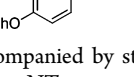
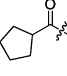
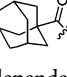
Table 5. Effect of Phenyl Substituents on Transglutaminase Activity^a

29

R ₁	R ₂	compd	TG2 IC ₅₀ ± SD (μ M)	TG1 IC ₅₀ (μ M)	TG3 IC ₅₀ (μ M)	FXIIIa IC ₅₀ (μ M)
Boc	H	14a	0.12 ± 0.00	4.9	>80	0.43
Cbz	H	16a	0.12 ± 0.05	3.7	>80	0.42
Cbz	2-N(CH ₃)CH ₂ CH(CH ₃) ₂	29a	76 ± 21	14	>80	>80
Cbz	2-F	29b	13 ± 4	20	>80	16
Boc	3-OCH ₃	29c	2.5 ± 0.1	19	>80	0.74
Boc	3-CH ₃	29d	0.91 ± 0.12	6.5	>80	0.21
Cbz	3-CF ₃	29e	0.18 ± 0.00	1.4	>80	0.039
Boc	3-F	29f	0.19	2.4	>80	0.051
Boc	3-Cl	29g	0.11 ± 0.06	0.95	69	0.066

^aValues accompanied by standard deviation were averaged from at least two independent experiments; they were otherwise obtained in a single determination.

Table 6. TG2 Activity and Selectivity of Selected Carbamates, Ureas, and Amides^a

R ₁	Cmpd No.	TG2 IC ₅₀ ± SD (μM)	Amides ^a			R ₁	Cmpd No.	TG2 IC ₅₀ ± SD (μM)	TG1 IC ₅₀ (μM)	TG3 IC ₅₀ (μM)	FXIIIa IC ₅₀ (μM)
			TG1 IC ₅₀ (μM)	TG3 IC ₅₀ (μM)	FXIIIa IC ₅₀ (μM)						
Cbz	16a	0.12 ± 0.05	3.7	>80	0.42		16z	0.11 ± 0.01	6.9	>80	0.31
	16o	0.046 ± 0.01	6.7	290	0.32		16aa	0.072 ± 0.026	5.0	110	0.18
	16p	0.054 ± 0.013	4.1	NT	0.33		16ab	0.044 ± 0.001	2.5	>80	0.24
	16q	0.070 ± 0.014	9.8	>80	0.50		18a	0.16 ± 0.02	10	NT	0.76
	16r	0.094 ± 0.044	6.1	>80	0.25		18b	0.034 ± 0.001	3.1	140	0.20
	16s	0.11 ± 0.01	8.3	>80	0.34		18c	0.11 ± 0.07	6.0	110	0.31
	16t	0.13 ± 0.00	10	>80	0.63		17a	0.020 ± 0.001	7.2	>80	0.28
	16u	0.070 ± 0.005	5.1	270	0.23		17b	0.026 ± 0.009	2.6	>80	0.33
	16v	0.082 ± 0.035	6.8	NT	0.38		17c	0.037 ± 0.000	4.1	>80	0.30
	16w	0.22 ± 0.13	76	>80	0.72		17d	0.041 ± 0.001	5.4	>80	0.31
	16x	0.054 ± 0.006	12	>80	0.67		17e	0.057 ± 0.001	5.4	>80	0.57
	16y	0.060 ± 0.005	7.7	>80	0.47		28a	0.032 ± 0.011	5.2	420	0.24
							18d	0.010 ± 0.004	3.4	>80	0.18

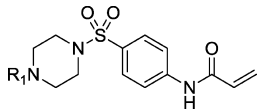
^aValues accompanied by standard deviation were averaged from at least two independent experiments; they were otherwise obtained in a single determination. NT = not tested.

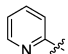
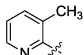
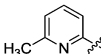
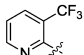
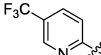
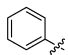
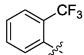
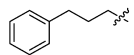
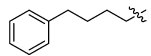
serious concern (data not shown). Additionally, establishing a potency rank ordering from the assay was made impossible, since the IC₅₀ values obtained were all in the range of 5–20 μM regardless of biochemical potency. In unsuccessful attempts to address this we investigated variables such as Ca²⁺ concentration, substrate, and compound incubation times. In addition to our HEK-TG2 cellular assay, also without success, we (1) employed a striatal cell line expressing mutant huntingtin as a “stressor”, (2) attempted to exploit the finding that TG2 inhibition results in protection from 3-nitropropionic acid mediated toxicity,⁴⁰ (3) employed an assay in SH-SY5Y cells using endogenously expressed TG2,⁴¹ and (4) attempted to measure the effect of TG2 activity on formation of γ-Glu-ε-Lys (GGEL).⁴² Intractable technical issues were noted with several of these alternatives.

Unable to identify potent activity in a whole cell assay, we took a step back and focused on developing a cell lysate model from our HEK-TG2 cells as a surrogate. As shown in Table 9, markedly improved potency was observed in cell lysates when

compared to the whole cell assay, compounds displayed a reasonable translation of biochemical potency to lysate potency, and the correlation allowed them to be rank ordered. Notably, the assay required 10 mM calcium ion concentration to observe good translation. Reducing the calcium ion concentration by 10-fold begins to negatively affect potency (data not shown). These results diminish concerns that compound-centric effects such as nonspecific binding to cellular proteins or poor solubility might be the root cause of weak activity in the whole cell assay and show that the compounds have submicromolar potency in a more complex assay system. While the translation and correlation between biochemical and lysate were reasonable, the physiological relevance of this assay is low; using it as a model to help predict the exposure necessary for in vivo efficacy would be inadvisable.

DMPK Profiling. Evaluation of druggability characteristics continued with mouse plasma stability, Caco2 permeability, and mouse liver microsomal profiling of selected compounds (Table 10). In general, the compounds showed reasonable

Table 7. TG2 Activity and Selectivity of Selected Aryl, Heteroaryl, and Alkyl Substituted Piperazines^a


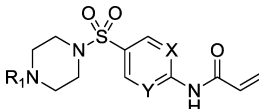
R ₁	Cmpd No.	TG2 IC ₅₀ ± SD (μM)	TG1 IC ₅₀ (μM)	TG3 IC ₅₀ (μM)	FXIIIa IC ₅₀ (μM)
Cbz	16a	0.12 ± 0.05	3.7	>80	0.42
	14b	0.055 ± 0.040	4.5	>80	0.50
	14c	0.025 ± 0.003	1.7	72	0.34
	14d	0.035 ± 0.000	4.2	56	0.22
	14e	0.052	5.9	>80	0.25
	14f	0.076 ± 0.021	18	>80	0.57
	14g	0.18 ± 0.02	6.1	>80	0.37
	14h	0.19 ± 0.01	57	>80	1.4
	19a	0.38 ± 0.03	15	>80	1.2
	19b	0.31 ± 0.05	22	>80	0.98

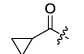
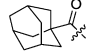
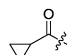
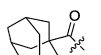
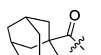
^aValues accompanied by standard deviation were averaged from at least two independent experiments; they were otherwise obtained in a single determination.

protein binding, low solubility, and low to moderate Caco2 permeability. From this short survey the phenylacrylamides **16n**, **15**, **18c**, **18d**, and **28a** had plasma half-lives of more than 2 h. The pyridines and pyrimidine (**24a**, **24c**, and **25a**) had plasma half-lives on the order of 30 min or less. While we cannot be certain of the cause of the shorter plasma half-lives of these compounds, shorter half-lives could have been predicted from their half-lives in the presence of 5 mM glutathione. Evidence in support of the acrylamide amide linkage as the site of metabolic instability was then obtained by testing the plasma stability of the aniline analogue **30** of cyclopropylamide **18c**. Aniline **30** showed no indication of metabolism over 24 h and appeared stable indefinitely in mouse plasma. This putative metabolite was determined to be inactive, as expected, when tested against TG2 at 80 μM. Compounds with reasonable plasma stability were progressed to mouse liver microsomal stability studies. Unfortunately, the results of these tests suggested that with the exception of **15**, all compounds were predicted to be rapidly cleared in vivo.

CONCLUSIONS

Evidence for direct covalent binding of screening hit **7d** at Cys277 of TG2 was obtained through inhibition studies with wild type and mutant forms of TG2. Using the published open-form X-ray crystal structure and with the aid of various computational models, we improved on the TG2 potency of **7d** by over 2 orders of magnitude while improving selectivity for other transglutaminase isoforms. Notable in this regard is **18d**, which

Table 8. Transglutaminase Activity of Pyridinylacrylamides and Pyrimidinylacrylamides^a


R ₁	X	Y	Cmpd No.	TG2 IC ₅₀ ± SD (μM)	TG1 IC ₅₀ (μM)	TG3 IC ₅₀ (μM)	FXIIIa IC ₅₀ (μM)
Boc	CH	CH	14a	0.12 ± 0.00	4.9	>80	0.43
Cbz	CH	CH	16a	0.12 ± 0.05	3.7	>80	0.42
	CH	CH	18c	0.11 ± 0.07	6.0	110	0.34
	CH	CH	18d	0.010 ± 0.004	3.4	>80	0.18
Boc	CH	N	24a	0.097 ± 0.046	3.8	>80	1.6
Cbz	CH	N	24b	0.078 ± 0.015	6.4	>80	1.3
	CH	N	24c	0.18 ± 0.09	3.4	>80	1.5
	CH	N	24d	0.015 ± 0.002	5.6	>80	2.2
Boc	N	N	25a	0.026 ± 0.011	1.8	NT	3.3
Cbz	N	N	25b	0.069 ± 0.016	5.1	NT	>80
	N	N	25c	0.014 ± 0.000	3.0	>80	2.5

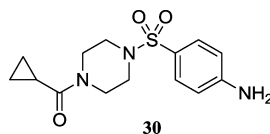
^aValues accompanied by standard deviation were averaged from at least two independent experiments; they were otherwise obtained in a single determination. NT = not tested.

Table 9. HEK-TG2 Cellular Lysate Activity^a

compd	TG2 IC ₅₀ (μM)	HEK-TG2 lysate IC ₅₀ (μM)	(HEK-TG2 lysate IC ₅₀)/(TG2 IC ₅₀)
26	4.5	32	7
10g	1.9	20.3	11
16m	0.46	3.2	7
16k	0.22	5.0	23
14a	0.12	0.62	5
14f	0.076	1.8	24
16q	0.070	3.0	43
16o	0.046	1.6	35
16aa	0.044	1.1	25
17d	0.041	0.81	20
17c	0.037	0.36	20
18b	0.034	1.2	35
28a	0.032	1.2	38
17b	0.026	0.45	17
14c	0.025	0.99	40
18d	0.010	0.77	77

^aValues accompanied by standard deviation were averaged from at least two independent experiments; they were otherwise obtained in a single determination.

had TG2 IC₅₀ of 10 nM and had 18, 84, 340, and >8000-fold selectivity against FXIIIa, TG6, TG1, and TG3, respectively. We further demonstrated that the compounds were stable in DMSO solution over the course of the selectivity evaluation, establishing that the observed selectivity was not an artifact of compound handling. To establish the relevance of compound IC₅₀ values for what are time-dependent inhibitors, a correlation

Table 10. DMPK Profile of Selected Inhibitors^a

compd	TG2 IC ₅₀ (μ M)	aq sol. (mg/mL)	Hu PPB ^b (%) unbound	PSA (\AA^2)	cLogP pH 7	Caco2 P_{app} (A-B) (nm s^{-1})	Caco2 P_{app} (B-A) (nm s^{-1})	mouse plasma $T_{1/2}$ (min)	mLM Cl_{int} ($\text{mL min}^{-1} \text{kg}^{-1}$)	mLM Cl_{int} ($\text{L h}^{-1} \text{kg}^{-1}$)
16n	0.072	0.01	2	96	3.9	NT	NT	126	2465	148
15	1.3	1.04	4	79	1.0	0	9	162	<50.8	<3.0
18c	0.11	0.05	11	87	1.2	65	115	209	119.9 \pm 68.8	7.2 \pm 4.1
18d	0.010	0.01	2	87	3.2	102	193	248	3203	192
28a	0.032	0.05	7	87	1.62	136	97	305	228.7	13.7
24a	0.097	0.04	NT	108	2.1	NT	NT	31.5	NT	NT
24c	0.18	0.25	96	99	0.26	11	6	33.5	NT	NT
25a	0.026	0.07	NT	108	2.1	NT	NT	14.3	NT	NT
30	>80	1.8	NT	84	0.71	NT	NT	>240	NT	NT

^aValues accompanied by standard deviation were averaged from at least two independent experiments; they were otherwise obtained in a single determination. ^bHuman plasma protein binding. NT = not tested.

was established between these values and the irreversible inhibition constants for several transglutaminase isoforms, with the finding that the IC₅₀ values are an accurate means to rank-order compound potency and selectivity.

In a cellular lysate assay a reasonable translation of biochemical activity to lysate potency was achieved and IC₅₀ < 1 μ M was observed for several compounds; however, this assay required a nonphysiologically high Ca²⁺ concentration. Additionally, DMPK profiling showed that the compounds have relatively poor solubility, poor to moderate permeability, and poor plasma stability, this last deficit being attributed to the labile acrylamide amide linkage. The phenylacrylamides displayed low reactivity in the presence of GSH, belying their acrylamide functionality.

Our inability to potently inhibit TG2 transamidation in whole cells using irreversible inhibitors has caused us to re-evaluate our effort. Efficacy end points in HD mouse models require 6 months or more of dosing. To manage risk in running such trials and to facilitate interpretation of results, it is imperative that compounds possess cellular activity and pharmacokinetic exposure levels in brain to cover, preferentially, some multiple of the cellular activity. This is to facilitate the modulation of pharmacodynamic markers needed to demonstrate in vivo target engagement. Given the weak cellular potency and poor plasma stability, it is unlikely that any of the inhibitors described would have adequate brain exposure to test our hypothesis. For this to occur, a better understanding of intracellular TG2 biology is likely needed, and perhaps only then can a physiologically meaningful transamidation-dependent cellular assay readout be validated. Such an assay is needed to facilitate compound selection for DMPK and in vivo studies. Since our current understanding of the biology is limiting in HD, we are continuing in our efforts to deepen this understanding while working to address the plasma stability issue. We will report our findings in due course. While these studies are ongoing, the current inhibitors may represent attractive agents for studies of TG2's role in cancer or celiac disease.

EXPERIMENTAL SECTION

Cloning, Expression, and Purification of Transglutaminases.

The full length (Met-1 to Ala-687) human TG2 PCR product was subcloned into the pET28a vector (Novagen) using the *Nde* I and *Hind* III restriction sites for expression in *E. coli*, incorporating an

N-terminal His-tag, generating the plasmid pET28a:hTG2. Mutagenesis of TG2 to generate the C285A point mutation was performed using a Quikchange kit (Stratagene). Complementary primers that include sequences flanking the site of the mutation (C285A_sense, CGCCCGCTGGCCGCCACAGTGCTGAGG; C285A_antisense, CCTCAGCACTGTGGCGGCCACGGCGGCG) were used in a mutagenesis reaction according to the manufacturer's instructions, using pET28a:hTG2 as template DNA, yielding the plasmid pET28a: TG2_C285A.

The constructs were transformed into *E. coli* Rosetta 2 (DE3) cells, and cells were grown overnight at 37 °C in 6 L of 2xYT medium containing 50 μ g/mL kanamycin. The cells were grown to OD₆₀₀ = 0.6 before addition of 100 μ M isopropyl- β -D-thiogalactopyranoside to induce expression at 20 °C overnight. The cells were harvested by centrifugation, flash frozen in liquid nitrogen, thawed at 37 °C, and resuspended in 90 mL of lysis buffer (50 mM potassium phosphate, pH 8.0, 300 mM NaCl, and 1 EDTA-free protease inhibitor tablet (Roche)) plus 4 μ L of 250 U/ μ L benzonase (Merck) at 4 °C. Lysis was achieved using 5 \times 30 s bursts of sonication on ice. The lysate was then centrifuged at 28000g and the supernatant recovered. The sample was loaded onto a column of 5 mL of TALON resin at 2 mL/min and eluted with 50 mM potassium phosphate, pH 8.0, 150 mM imidazole. Fractions were collected and loaded onto a 1 mL anion exchange column at 4 mL/min in 20 mM Tris, pH 7.2, 1 mM DTT, and 1 mM EDTA and eluted using a 1 M NaCl gradient. Selected fractions were loaded onto a Superdex 200, 26/60 gel filtration column pre-equilibrated in buffer (20 mM Tris, pH 7.2, 150 mM NaCl, 1 mM DTT, and 1 mM EDTA) at 2.4 mL/min. The pure fractions were verified by SDS-PAGE and pooled. Complex formation with **7d** was done as previously described.¹⁴ Briefly, 50 molar excess of CHDI-00201241 was incubated with 5 mg of pure TG2 in incubation buffer (20 mM Tris-HCl, pH 7.2, 1 mM DTT, 1 mM EDTA, 150 mM NaCl, 10 mM CaCl₂) at room temperature for 30 min and then at 4 °C overnight. Fractions were loaded onto a second 1 mL anion exchange column at 4 mL/min in 20 mM Tris, pH 7.2, 1 mM DTT, and 1 mM EDTA and eluted using a 1 M NaCl gradient. Selected fractions were pooled.

The full length mouse TG2 (Met-1 to Ala-686) PCR product was subcloned into the vector pETIJ-HV (Evotec in-house vector) using the *Eco*RI and *Not* I restriction sites for expression in *E. coli* incorporating an N-terminal His-tag. The construct was transformed into *E. coli* Rosetta 2 (DE3) cells, and cells were grown overnight at 37 °C in 6 L of 2xYT medium containing 50 μ g/mL kanamycin. The cells were grown to OD₆₀₀ = 0.6 before addition of 500 μ M isopropyl- β -D-thiogalactopyranoside to induce expression at 25 °C overnight. The cells were harvested by centrifugation, flash frozen in liquid nitrogen, thawed at 37 °C, and resuspended in 80 mL of lysis buffer (50 mM potassium phosphate, pH 8.0, 300 mM NaCl, and 1 non-EDTA

protease inhibitor tablet (Roche)) plus 4 μL of 250 U/ μL benzonase (Merck) at 4 °C. Lysis was achieved by five steps of 30 s sonication on ice. The lysate was centrifuged at 16 500 rpm for 60 min using a Beckman Avanti 30 centrifuge and an F0850 rotor and the supernatant recovered. The sample was loaded onto a 5 mL TALON column at 2 mL/min and eluted with 50 mM potassium phosphate, pH 8.0, 150 mM imidazole. Fractions were collected and loaded onto a 1 mL anion exchange column at 4 mL/min in 20 mM Tris, pH 7.2, 1 mM DTT, and 1 mM EDTA and eluted using a 1 M NaCl gradient. Selected fractions were loaded onto a Superdex 200, 26/60 gel filtration column pre-equilibrated in buffer (50 mM potassium phosphate, pH 8.0, 300 mM NaCl) at 2.0 mL/min. The pure fractions were analyzed using SDS-PAGE and pooled.

Additionally, human TG1, human TG3, human TG6, and human factor XIIIa were purchased from Zedira (Darmstadt, Germany).

Transamidation Inhibition Assays for Recombinant TG and TG2 HEK Cell Lysates. The fluorescent transamidation assay was performed as described.²⁷ In summary, 8 μM N,N-dimethylated casein (NMC) and 16 μM dansyl-labeled amine nucleophile (KxD) were used as substrates in 25 mM Hepes, pH 7.4, 250 mM NaCl, 2 mM MgCl_2 , 10 mM CaCl_2 , 0.2 mM DTT, and 0.05% Pluronic F-127 at 37 °C. A kinetic measurement was recorded (Safire or Ultra, Tecan; excitation, 350 nm; emission, 535 nm), and the reaction velocity derived from a linear fit was used as a measure for enzyme activity. All data points were normalized between 0% and 100% inhibition using the appropriate positive (full inhibition) and negative (no inhibition) controls. IC_{50} values were determined using an automated in-house data evaluation software package by means of a hyperbolic binding model with a variable Hill slope. Assay conditions were similar for recombinant TG isoforms TG2 (human and mouse), TG1, and TG6 apart from CaCl_2 concentrations, which were adjusted at half-maximal transamidation activity (0.5 mM for hTG2 and TG6; 0.2 mM for mTG2; 0.05 mM for TG1), and enzyme concentrations (20 nM hTG2 and TG6, 5 nM mTG2, 10 nM TG1). Factor XIII was activated using 0.1 $\mu\text{g}/\mu\text{L}$ thrombin (Sigma) in 35 mM Tris, pH 8.0, for 20 min at 30 °C, and the transamidation reaction was performed with 20 nM factor XIIIa in 50 mM Tris, pH 8.0, 1.25 mM CaCl_2 , 0.05% Pluronic F-127, 0.2 mM DTT. TG3 was activated with 0.02 $\mu\text{g}/\mu\text{L}$ thrombin under the same conditions as factor XIII, and assay conditions were 10 nM TG3 in 50 mM Hepes, pH 8.0, 20 mM CaCl_2 , 0.2 mM DTT, 0.05% Pluronic F-127.

For the lysate assay, HEK cells engineered to express human TG2 were cultured as previously described.²⁷ Cellular lysates were prepared by washing cultured cells twice with ice-cold PBS and harvesting them with a rubber policeman. The cells were then pelleted by centrifugation and lysed in 10 mM Tris-HCl, pH 7.5, 10 mM CaCl_2 , 1 mM EDTA, 1 mM PMSF with protease inhibitors (Roche protease inhibitor cocktail) followed by sonication using a Branson Sonifier 450 with 50 pulses (duty cycle 20, output control 6). The protein content was determined using the Bradford method, and 1.5 $\mu\text{g}/\mu\text{L}$ total protein was used in the fluorescent transamidation assay as described above.

MALDI ToF MS Analysis. Mass spectrometry analyses were performed using a Voyager-DE PRO BioSpectrometry workstation (matrix assisted laser desorption ionization time-of-flight mass spectrometer, PerSeptive Biosystems). Intact apoprotein and protein complexes with assumed covalent binders were measured following a sample workup procedure. An amount of 2 μL of the protein solution (1 $\mu\text{g}/\mu\text{L}$ protein in 20 mM Tris buffer, pH 7.2, 1 mM DTT, 1 mM EDTA, 150 mM NaCl) was placed on a nitrocellulose membrane filter (Millipore, 9004-70-O) and dialyzed against 100 mL of deionized water. After 30 min 1 μL of the sample was taken and mixed with 1 μL of sinapinic acid solution (hydroxycinnamic acid, supernatant of a 10 mg/mL solution in 70% acetonitrile, 30% proteomics grade water, and 0.1% TFA) used as a matrix. Resulting samples were placed on a MALDI target plate and allowed to cocrystallize through evaporation at room temperature. Measurements were performed in linear detection mode in the mass range of 10 000 to 100 000 Da. Data analysis was performed using Data Explorer, version 4.0.0, data analysis software (PerSeptive Biosystems). For analysis of the potentially modified amino acid residues a tryptic digestion of the apoprotein with the

protein inhibitor complexes was performed. An amount of 100 μL of each sample (1 $\mu\text{g}/\mu\text{L}$ protein in 20 mM Tris buffer, pH 7.2, 1 mM DTT, 1 mM EDTA, 150 mM NaCl) was acidified with 1 μL of 100 mM HCl, and 5 μL of a 1 mg/mL mass spectrometry grade trypsin solution (Sigma) was added. Following an overnight incubation at 37 °C the reaction was terminated by addition of 100 μL of acetonitrile. Samples were subsequently evaporated under reduced pressure and redissolved in 10 μL of water. To remove remaining buffer salts interfering with the sample ionization, all samples were desalted using ZipTip $\mu\text{-C18}$ desalting tips (Millipore). Final MALDI samples were prepared by mixing 1 μL of the desalted digest with 1 μL of α -cyano-4-hydroxycinnamic acid (supernatant of a 10 mg/mL solution in 70% acetonitrile, 30% proteomics grade water, and 0.1% TFA). Spectra were recorded in linear detection mode in the mass range of 500–5000 Da. For data analysis expected peptide fragments were compared with experimentally determined m/z values.

Molecular Docking Procedures. The X-ray structure data of TG2 with peptide ligand 1 covalently bound (PDB code 2Q3Z) were used for docking. The structure was prepared by removing all water molecules and the peptide ligand. Hydrogen atoms were added where needed, and the protonation state of charged residues was adjusted to reflect their state at pH7 using the Protonate 3D tool implemented in the MOE molecular modeling package (Chemical Computing Group Inc.). Amino acid residues within 13 Å of the sulfur atom of Cys277 were defined as the binding site. The docking was accomplished using the covalent docking option of the GOLD docking software (version 4.0 or 4.1).⁴³ A covalent link for use with individual ligands was used in this work wherein both the protein and the ligand incorporate the linking sulfur atom of Cys277. This required that the structures of the ligands be prepared as their corresponding thiol addition products with one open valence at the sulfur. Other settings were set at the default values. The bound structure of peptide ligand 1 to TG2 was reproduced with satisfactory accuracy (rmsd of $C\alpha$ of 0.68 Å).

Computational Method for FMO Calculation. All the molecular modeling work necessary for preparation of the input structures for the FMO calculations was carried out in the MOE molecular modeling package. TG2–peptide ligand 1 complex structure was prepared based on the published X-ray data (PDB code 2Q3Z). A truncated partial structure of the TG2–peptidic ligand 1 complex was prepared by selecting the amino acid residues within 4 Å from 1. The new C-terminals created by truncation were modeled as N-methylamides, and acetyl groups were added to the N-terminals. Hydrogen atoms were added, and the protonation state of the acidic and basic amino acid residues were adjusted at pH 7 using the Protonate 3D tool within MOE. The positions of the hydrogen atoms in the complex were optimized using the MMFF94x force field in the presence of the Born continuous water model while fixing the coordinates of the heavy atoms. The protein was fragmented using a one-fragment-per-residue fragmentation scheme, and the peptide ligand was fragmented similarly into five sections as shown in Figure 3. The FMO calculations in this work were performed using GAMESS software (April 2008 version)⁴⁴ at the MP2/6-31G** theory level. The calculations were run on PC clusters consisting of 24–40 CPU cores. The input files were prepared using Facio software^{45,46} after preprocessing of the structure in MOE.

Homology Model Construction. The sequences of human TG1 (P22735), TG3 (Q08188), and FXIII (P00488) were retrieved from the Swiss-Protein Database. All of the molecular modeling studies were carried out using the MOE software. The structure of TG2 deposited in the protein data bank (PDB code 2Q3Z) was used as the structure template for homology model construction. Ten models were constructed for each transglutaminase isoform, and the models with the lowest Coulomb and generalized Born⁴⁷ interaction energies were further optimized using force field energy minimization followed by short molecular dynamics (MD) simulations (simulated annealing). The coordinates of the α -carbons of the amino acids were fixed during the MD simulations.

General Synthetic Procedures. Commercially available reagents and solvents (HPLC grade) were used without further purification. ¹H NMR spectra were recorded on a Bruker DRX 500 MHz spectrometer

or Bruker DPX 250 MHz spectrometer in deuterated solvents, and ^{13}C NMR spectra were recorded on a Bruker DPX 250 MHz spectrometer equipped with a B-VT 3300 variable temperature controller unit (high temperature only) and a four nucleus (QNP) switchable probe for observation of ^1H , ^{13}C , ^{19}F , ^{31}P with ^2H lock in deuterated solvents. Chemical shifts (δ) are in parts per million. Thin-layer chromatography (TLC) analysis was performed with Kieselgel 60 F₂₅₄ (Merck) plates and visualized using UV light.

Analytical HPLC–MS was performed on Shimadzu LCMS-2010EV systems using reverse phase Atlantis dC18 columns (3 μm , 2.1 mm \times 50 mm), gradient 5–100% B (A = water/0.1% formic acid, B = acetonitrile/0.1% formic acid) over 3 min, injection volume of 3 μL , flow of 1.0 mL/min. UV spectra were recorded at 215 nm using a Waters 2788 dual wavelength UV detector. Mass spectra were obtained over the range m/z 150–850 at a sampling rate of 2 scans per second using Waters LCT or analytical HPLC–MS on Shimadzu LCMS-2010EV systems using reverse phase Water Atlantis dC18 columns (3 μm , 2.1 mm \times 100 mm), gradient 5–100% B (A = water/0.1% formic acid, B = acetonitrile/0.1% formic acid) over 7 min, injection volume of 3 μL , flow of 0.6 mL/min. UV spectra were recorded at 215 nm using a Waters 2996 photodiode array. Data were integrated and reported using Shimadzu PsiPort software. Accurate mass measurement was carried out using a Waters Micromass LCT Premier orthogonal acceleration time-of-flight mass spectrometer 4 GHz TDC with LockSpray enable. All compounds display purity of >95% as determined by this method, unless stated otherwise.

N-(4-Bromophenyl)acrylamide (7d). 4-Bromoaniline (0.3 g, 1.74 mmol) was dissolved in THF (5 mL). To this was added diisopropylethylamine (0.5 mL, 5.2 mmol) in one portion followed by the dropwise addition of acryloyl chloride (0.19 mL, 1.91 mmol), and the mixture was stirred at room temperature under a nitrogen atmosphere for 3 h. The THF was removed under vacuum, and the resulting crude material was diluted with DCM (20 mL) and washed sequentially with NaOH (1 M solution, 10 mL), HCl (1 M solution, 10 mL), and brine (10 mL) before being dried (MgSO₄), filtered, and concentrated to give the title compound (0.34 g, 90% yield) as a white powder. MS (ES⁺) m/z (M + 1) 228; HRMS (ES⁺) m/z 225.9859 (225.9868 calcd for C₉H₈BrNO, M + H); ^1H NMR (500 MHz, DMSO) 10.28 (s, 1H), 7.59–7.71 (m, 2H), 7.46–7.56 (m, 2H), 6.35–6.48 (m, 1H), 6.22–6.32 (m, 1H), 5.69–5.84 (m, 1H); ^{13}C NMR (126 MHz, DMSO-*d*₆) δ 163.2, 138.4, 131.6, 127.3, 121.2, 115.1.

Ethenesulfonic Acid (4-Bromophenyl)amide (10a). MS (ES⁺) m/z (M + 1) 263; δ_{H} (500 MHz, DMSO-*d*₆) 7.41–7.55 (2H, m), 7.03–7.14 (2H, m), 6.77 (dd, J = 16.39, 9.93 Hz, 1H), 5.97–6.17 (2H, m).

N-(4-Bromophenyl)propionamide (10b). MS (ES⁺) m/z (M + 1) 230; HRMS (ES⁺) m/z 228.0034 (228.0024 calcd for C₉H₁₀BrNO, M + H); ^1H NMR (500 MHz, DMSO) 9.98 (s, 1H) 7.58 (d, J = 9.92 Hz, 2H), 7.48 (d, J = 9.92 Hz, 2H), 2.28 (q, J = 6.2 Hz, 2H), 1.04 (t, J = 6.2 Hz, 3H); ^{13}C NMR (126 MHz, DMSO-*d*₆) δ 172.2, 138.7, 131.5, 120.9, 114.4, 29.5, 9.6.

N-(4-Bromobenzyl)acrylamide (10c). MS (ES⁺) m/z (M + 1) 241, 243; HRMS (ES⁺) m/z 240.0027 (240.0024 calcd for C₁₀H₁₀BrNO, M + H); ^1H NMR (500 MHz, DMSO) 7.79 (br s, 1H), 6.61–6.73 (m, 2H), 6.38 (d, J = 8.39 Hz, 2H), 5.37–5.49 (m, 1H), 5.22–5.33 (m, 1H), 4.79 (dd, J = 10.07, 2.14 Hz, 1H), 3.47 (d, J = 6.10 Hz, 2H); ^{13}C NMR (126 MHz, DMSO-*d*₆) δ 164.7, 138.8, 131.5, 131.2, 129.6, 125.6, 119.9, 41.5.

N-(3-Bromophenyl)acrylamide (10d). MS (ES⁺) m/z (M + 1) 227, 229; HRMS (ES⁺) m/z 225.9877 (225.9868 calcd for C₉H₈BrNO, M + H); ^1H NMR (500 MHz, DMSO) 10.31 (s, 1H), 8.05 (s, 1H), 7.62–7.52 (m, 1H), 7.30–7.22 (m, 2H), 6.48–6.24 (m, 2H), 5.83–5.78 (m, 1H); ^{13}C NMR (126 MHz, DMSO-*d*₆) δ 163.4, 140.6, 131.5, 130.8, 127.6, 126.1, 121.6, 118.1.

N-(2-Bromophenyl)acrylamide (10e). MS (ES⁺) m/z (M + 1) 227, 229; δ_{H} (500 MHz, DMSO-*d*₆) 8.84 (1H, br s), 6.75–6.87 (2H, m), 6.55 (td, J = 7.67, 1.45 Hz, 1H), 6.32 (td, J = 7.71, 1.68 Hz, 1H), 5.74 (dd, J = 17.01, 10.30 Hz, 1H), 5.43 (dd, J = 17.01, 1.91 Hz, 1H), 4.86–5.01 (1H, m).

N-(4-Fluorophenyl)acrylamide (10f). MS (ES⁺) m/z (M + 1) 166; HRMS (ES⁺) m/z 166.0675 (166.0668 calcd for C₉H₈FN₂O,

M + H); ^1H NMR (500 MHz, DMSO) 10.21 (s, 1H), 7.68–7.61 (m, 2H), 7.19–7.11 (m, 2H), 6.42–6.23 (m, 2H), 5.74–5.71 (m, 1H); ^{13}C NMR (126 MHz, DMSO-*d*₆) δ 163.1, 158.1 (d, J = 249 Hz), 135.4, 131.7, 127.0, 121.1, 115.4 (d, J = 22 Hz).

N-[4-(Pyrrolidine-1-sulfonyl)phenyl]acrylamide (10g). MS (ES⁺) m/z (M + 1) 281; HRMS (ES⁺) m/z 281.0950 (281.0960 calcd for C₁₃H₁₆N₂O₃S, M + H); ^1H NMR (500 MHz, DMSO) 10.56 (s, 1H), 7.84–7.96 (m, 2H), 7.77 (d, J = 8.67 Hz, 2H), 6.41–6.52 (m, 1H), 6.28–6.38 (m, 1H), 5.84 (d, J = 9.93 Hz, 1H), 3.12 (t, J = 6.62 Hz, 4H), 1.59–1.71 (m, 4H); ^{13}C NMR (126 MHz, DMSO-*d*₆) δ 163.7, 143.0, 131.4, 130.2, 128.6, 128.1, 119.2, 47.8, 24.7.

N-[4-Methanesulfonylphenyl]acrylamide (10h). MS (ES⁺) m/z (M + 1) 226; HRMS (ES⁺) m/z 226.0544 (226.0538 calcd for C₁₀H₁₁NO₃S, M + H); ^1H NMR (500 MHz, DMSO) 9.70 (br s, 1H), 6.89–7.08 (m, 4H), 5.49–5.65 (m, 1H), 5.35–5.46 (m, 1H), 4.94 (dd, J = 10.09, 1.89 Hz, 1H), 2.23–2.29 (m, 3 H); ^{13}C NMR (126 MHz, DMSO-*d*₆) δ 163.9, 143.7, 135.1, 131.5, 128.4, 119.3, 44.0.

N-[4-Nitrophenyl]acrylamide (10i). MS (ES⁺) m/z (M + 1) 193; HRMS (ES⁺) m/z 193.0622 (193.0613 calcd for C₉H₈N₂O₃, M + H); ^1H NMR (500 MHz, DMSO) 10.76 (s, 1H), 8.19–8.30 (m, 2H), 7.86–7.97 (m, 2H), 6.30–6.55 (m, 2H), 5.87 (dd, J = 10.09, 1.73 Hz, 1 H); ^{13}C NMR (126 MHz, DMSO-*d*₆) δ 163.9, 145.2, 142.4, 131.2, 128.6, 125.0, 119.1.

N-[4-Trifluoromethylphenyl]acrylamide (10j). MS (ES⁺) m/z (M + 1) 216; HRMS (ES⁺) m/z 216.0627 (216.0636 calcd for C₁₀H₈F₃NO, M + H); ^1H NMR (500 MHz, DMSO) 10.50 (s, 1H), 7.88 (d, J = 8.51 Hz, 2H), 7.70 (d, J = 8.51 Hz, 2H), 6.41–6.52 (m, 1H), 6.23–6.38 (m, 1H), 5.83 (dd, J = 10.09, 1.89 Hz, 1H); ^{13}C NMR (126 MHz, DMSO-*d*₆) δ 163.66, 142.59, 131.46, 127.94, 126.15, 125.46, 123.35, 119.26.

N-Phenylacrylamide (10k). MS (ES⁺) m/z (M + 1) 148; HRMS (ES⁺) m/z 148.0772 (148.0762 calcd for C₉H₉NO, M + H); ^1H NMR (500 MHz, DMSO) 10.13 (s, 1H), 7.68–7.63 (m, 2H), 7.32–7.29 (m, 2H), 7.08–7.04 (m, 1H), 6.42–6.23 (m, 2H), 5.81–5.78 (m, 1H); ^{13}C NMR (126 MHz, DMSO-*d*₆) δ 163.2, 139.0, 131.9, 128.8, 126.9, 123.5, 119.3.

N-[4-Toluy]acrylamide (10l). MS (ES⁺) m/z (M + 1) 162; HRMS (ES⁺) m/z 162.0923 (162.0919 calcd for C₁₀H₁₁NO, M + H); ^1H NMR (500 MHz, DMSO) 10.05 (s, 1H), 7.55 (d, J = 8.35 Hz, 2H), 7.06–7.17 (m, 2H), 6.42 (dd, J = 17.02, 10.09 Hz, 1H), 6.24 (dd, J = 17.02, 2.05 Hz, 1H), 5.67–5.79 (m, 1H), 2.21–2.31 (m, 3H); ^{13}C NMR (126 MHz, DMSO-*d*₆) δ 162.9, 136.5, 132.4, 132.0, 129.2, 126.6, 119.3, 20.5.

N-[4-Phenoxyphenyl]acrylamide (10m). MS (ES⁺) m/z (M + 1) 240; HRMS (ES⁺) m/z 240.1032 (240.1025 calcd for C₁₅H₁₃NO₂, M + H); ^1H NMR (500 MHz, DMSO) 10.56 (s, 1H), 7.68–7.64 (m, 2H), 7.33–7.31 (m, 2H), 7.11–7.08 (m, 1H), 7.01–6.95 (m, 4H), 6.52–6.28 (m, 2H), 5.72 (m, 1H).

N-[4-Methoxyphenyl]acrylamide (10n). MS (ES⁺) m/z (M + 1) 178; HRMS (ES⁺) m/z 178.0876 (178.0868 calcd for C₁₀H₁₁NO₂, M + H); ^1H NMR (500 MHz, DMSO) 10.02 (s, 1H), 8.07 (s, 1H), 7.34–7.57 (m, 4H), 6.40 (dd, J = 17.02, 10.09 Hz, 1H), 6.22 (dd, J = 17.02, 1.89 Hz, 1H), 5.64–5.79 (m, 1H), 3.33 (br s, 4H), 1.77–1.90 (m, 4H); ^{13}C NMR (126 MHz, DMSO-*d*₆) δ 162.7, 155.4, 132.2, 132.0, 126.3, 120.8, 113.9, 55.2.

4-[4-(2-Fluoroacryloylamino)benzenesulfonyl]piperazine-1-carboxylic Acid *tert*-Butyl Ester (28c). MS (ES⁺) m/z (M + 23) 436; HRMS (ES⁺) m/z 314.0973 (314.0975 calcd for C₁₈H₂₄FN₃O₅S, M + H, loss of *tert*-butyl); ^1H NMR (500 MHz, DMSO) 10.71 (s, 1H), 8.01 (d, J = 8.80 Hz, 2H), 7.72 (d, J = 8.80 Hz, 2H), 5.68–5.86 (m, 1H), 5.51 (dd, J = 15.59, 3.85 Hz, 1H), 2.83 (t, J = 4.68 Hz, 4H), 1.33 (s, 9H); ^{13}C NMR (126 MHz, DMSO-*d*₆) δ 157.4 (d, J = 192.5 Hz), 154.5, 153.4, 142.3, 129.7, 128.7, 120.5, 100.9 (d, J = 14.7 Hz), 79.3, 45.8, 27.9.

4-[4-(2-Methylacryloylamino)benzenesulfonyl]piperazine-1-carboxylic Acid *tert*-Butyl Ester (28d). MS (ES⁺) m/z (M + 23) 432; δ_{H} (500 MHz, DMSO-*d*₆) 10.24 (1H, s), 7.97 (d, J = 8.80 Hz, 2H), 7.69 (d, J = 8.62 Hz, 2H), 5.86 (1H, s), 5.61 (1H, s), 3.39 (4H, br s), 2.82 (t, J = 4.68 Hz, 4H), 1.96 (3H, s), 1.34 (9H, s).

4-(4-But-2-enoylamino)benzenesulfonyl]piperazine-1-carboxylic Acid *tert*-Butyl Ester (28f). MS (ES⁺) *m/z* (M + 23) 432; HRMS (ES⁺) *m/z* 310.1213 (310.1225 calcd for C₁₉H₂₇N₃O₅S, M + H, loss of *tert*-butyl); ¹H NMR (500 MHz, CDCl₃) 7.61–7.81 (m, 4H), 7.42 (s, 1H), 6.92–7.16 (m, 1H), 5.98 (dd, *J* = 15.13, 1.56 Hz, 1H), 3.51 (t, *J* = 4.77 Hz, 4H), 2.96 (br s, 4H), 1.96 (dd, *J* = 6.88, 1.38 Hz, 3H), 1.42 (s, 9H); ¹³C NMR (126 MHz, DMSO-*d*₆) δ 167.4, 153.4, 143.6, 140.0, 128.6, 128.5, 121.0, 119.7, 79.3, 45.8, 27.9, 18.6.

4-[4-(2-Methylbut-2-enoylamino)benzenesulfonyl]piperazine-1-carboxylic Acid *tert*-Butyl Ester (28g). MS (ES⁺) *m/z* (M + 23) 446; HRMS (ES⁺) *m/z* 324.1384 (324.1382 calcd for C₂₀H₂₉N₃O₅S, M + H, loss of *tert*-butyl); ¹H NMR (500 MHz, DMSO) 10.10 (s, 1H), 7.93 (d, *J* = 8.83 Hz, 2H), 7.64 (d, *J* = 8.83 Hz, 2H), 6.35–6.60 (m, 1H), 3.41–3.49 (m, 4H), 2.79 (t, *J* = 4.87 Hz, 4H), 1.70–1.86 (m, 6H), 1.28–1.43 (m, 9H); ¹³C NMR (126 MHz, DMSO-*d*₆) δ 168.3, 153.4, 143.9, 132.4, 131.6, 128.6, 128.1, 119.5, 79.3, 45.8, 27.9, 13.9, 12.5.

4-[4-(4,4,4-Trifluorobut-2-enoylamino)benzenesulfonyl]piperazine-1-carboxylic Acid *tert*-Butyl Ester (28h). MS (ES⁺) *m/z* (M + 23) 486; HRMS (ES⁺) *m/z* 364.0939 (364.0943 calcd for C₁₉H₂₄F₃N₃O₅S, M + H, loss of *tert*-butyl); ¹H NMR (500 MHz, DMSO) 11.00 (s, 1H), 7.91 (d, *J* = 8.62 Hz, 2H), 7.74 (d, *J* = 8.62 Hz, 2H), 6.86–7.09 (m, 2H), 3.40–3.45 (m, 4H), 2.84 (br s, 4H), 1.34 (s, 9H); ¹³C NMR (126 MHz, DMSO-*d*₆) δ 161.0, 153.4, 142.6, 132.7 (q, *J* = 6 Hz), 129.5, 129.0, 127.4 (q, *J* = 34 Hz), 123.0 (q, *J* = 270 Hz), 119.5, 79.4, 45.8, 43.0 (br), 42.0 (br), 27.9.

4-[4-(4,4,4-Trifluoro-3-methylbut-2-enoylamino)benzenesulfonyl]piperazine-1-carboxylic Acid *tert*-Butyl Ester (28i). MS (ES⁺) *m/z* (M + 23) 500; HRMS (ES⁺) *m/z* 378.1096 (378.1099 calcd for C₂₀H₂₆F₃N₃O₅S, M + H, loss of *tert*-butyl); ¹H NMR (500 MHz, DMSO) 7.89 (d, *J* = 8.62 Hz, 2H), 7.72 (d, *J* = 8.80 Hz, 2H), 6.72 (s, 1H), 3.40–3.50 (m, 4H), 2.83 (t, *J* = 4.77 Hz, 4H), 2.25 (s, 3H), 1.34 (s, 9H); ¹³C NMR (126 MHz, DMSO-*d*₆) δ 162.7, 153.4, 142.8, 129.1, 129.0, 125.1 (q, *J* = 6 Hz), 119.2, 79.3, 45.7, 27.9, 11.7.

4-[4-(Ethoxycarbonylmethylamino)benzenesulfonyl]piperazine-1-carboxylic Acid *tert*-Butyl Ester (28m). MS (ES⁺) *m/z* (M + 23) 450; δ_H (500 MHz, DMSO-*d*₆) 7.42 (d, *J* = 8.83 Hz, 2H), 7.02 (t, *J* = 6.23 Hz, 1H), 6.69 (d, *J* = 8.83 Hz, 2H), 4.13 (q, *J* = 7.09 Hz, 2H), 4.01 (d, *J* = 6.15 Hz, 2H), 3.39–3.42 (4H, m), 2.75 (t, *J* = 4.89 Hz, 4H), 1.35 (9H, s).

4-[4-(2-Cyanoacetyl)amino]benzenesulfonyl]piperazine-1-carboxylic Acid *tert*-Butyl Ester (28o). MS (ES⁺) *m/z* (M + 23) 431; HRMS (ES⁺) *m/z* 309.1033 (309.1021 calcd for C₁₈H₂₄N₄O₅S, M + H, loss of *tert*-butyl); ¹H NMR (250 MHz, DMSO) 10.74 (s, 1H), 7.60–7.86 (m, 4H), 3.97 (s, 2H), 3.38–3.46 (m, 4H), 2.73–2.87 (m, 4H), 1.32 (s, 9H); ¹³C NMR (126 MHz, DMSO-*d*₆) δ 162.0, 153.4, 142.7, 129.1, 129.0, 119.1, 115.6, 79.3, 45.7, 27.9, 27.1.

***N*-(4-Aminophenyl)acrylamide.** *N*-[4-Nitrophenyl]acrylamide (10i, 0.38 g, 1.98 mmol) was suspended in a 5:1 mixture of ethanol and water (10 mL). To this solution was added iron powder (0.22 g, 4.00 mmol) followed by saturated ammonium chloride solution (1 mL), and the mixture was heated to 80 °C for 3 h. After this time, the reaction mixture was cooled to room temperature and filtered through a pad of Celite. The Celite was washed with ethanol (10 mL) and ethyl acetate (50 mL), and the solution was concentrated under vacuum. The resulting residue was partitioned between DCM (50 mL) and water (20 mL). The organic layer was separated, dried with MgSO₄, filtered, and concentrated to afford the title compound (0.32 g, 99% yield) as a white solid. MS (ES⁺) *m/z* (M + H)⁺ 163. δ_H (500 MHz, DMSO-*d*₆) 9.73 (1H, s), 7.30 (d, *J* = 8.67 Hz, 2H), 6.47–6.58 (2H, m), 6.37 (dd, *J* = 17.02, 10.25 Hz, 1H), 6.16 (dd, *J* = 16.95, 1.81 Hz, 1H), 5.65 (dd, *J* = 10.09, 1.73 Hz, 1H), 4.90 (2H, br s).

Pyrrolidine-1-carboxylic Acid (4-Acryloylamino)phenylamide (10o). Triphosgene (0.05 g, 0.17 mmol) was added in one portion to a stirred solution of *N*-(4-aminophenyl)acrylamide (0.1 g, 0.57 mmol) and diisopropylethylamine (0.09 mL, 0.57 mmol) in THF (5 mL), and the resulting mixture was stirred at room temperature under a nitrogen atmosphere for 5 min. After this time pyrrolidine (0.04 mL, 0.57 mmol) was added in one portion and the resulting mixture was stirred at room temperature under a nitrogen atmosphere

for 18 h. After this time the reaction mixture was concentrated, and the residue was purified using flash column chromatography (elution, 1% methanol, 99% DCM) to give the title compound (0.06 g, 45% yield) as a white powder. MS (ES⁺) *m/z* (M + 1) 260; HRMS (ES⁺) *m/z* 260.1390 (260.1399 calcd for C₁₄H₁₇N₃O₂, M + H); ¹H NMR (500 MHz, DMSO) 10.02 (s, 1H), 8.07 (s, 1H), 7.37–7.56 (m, 4H), 6.40 (dd, *J* = 17.02, 10.09 Hz, 1H), 6.22 (dd, *J* = 17.02, 1.89 Hz, 1H), 5.64–5.81 (m, 1H), 3.28–3.35 (m, 4H), 1.75–1.93 (m, 4H); ¹³C NMR (126 MHz, DMSO-*d*₆) δ 162.7, 154.0, 136.4, 133.1, 132.0, 126.3, 120.0, 119.5, 45.7, 25.0.

4-[4-(3-(*Z*-Chloroacryloylamino)benzenesulfonyl]piperazine-1-carboxylic Acid *tert*-Butyl Ester (28j). 3-Chloroacrylic acid (0.12 g, 1.1 mmol) followed by pyridine (0.3 mL) was added sequentially portionwise to a stirred solution of 4-(4-aminobenzenesulfonyl)piperazine-1-carboxylic acid *tert*-butyl ester (0.1 g, 0.29 mmol) in THF/DMA (3:2, 5 mL) at room temperature. To this mixture was added EDC (0.29 g, 1.5 mmol) in one portion, and the mixture was stirred at room temperature under a nitrogen atmosphere for 1 h. After this time the mixture was diluted with ethyl acetate (50 mL) and washed with water (100 mL), saturated NaHCO₃ (100 mL), and HCl (100 mL, 2M). The organic layer was separated, dried (MgSO₄), filtered, and concentrated under vacuum and the resulting residue was purified using flash column chromatography (elution, 40% ethyl acetate, 60% heptane) to give the title compound (0.009 g, 5% yield) as a white solid. MS (ES⁺) *m/z* (M + 23) 452; δ_H (250 MHz, DMSO-*d*₆) 10.66 (1H, s), 7.88 (d, *J* = 8.68 Hz, 2H), 7.69 (d, *J* = 8.68 Hz, 2H), 7.00 (d, *J* = 8.07 Hz, 1H), 6.57 (d, *J* = 7.77 Hz, 1H), 3.40–3.57 (4H, m), 2.77–2.89 (5H, m), 1.33 (10H, s).

4-[4-(3-(*E*-Chloroacryloylamino)benzenesulfonyl]piperazine-1-carboxylic Acid *tert*-Butyl Ester (28k). MS (ES⁺) *m/z* (M + 23) 452, 453; δ_H (250 MHz, DMSO-*d*₆) 10.65 (1H, br s), 7.83–7.92 (2H, 2), 7.69 (d, *J* = 8.83 Hz, 2H), 7.47 (1H, s), 6.63 (d, *J* = 13.10 Hz, 1H), 2.72–2.96 (6H, m), 1.32 (11H, s).

4-[4-(2-Oxopropionylamino)benzenesulfonyl]piperazine-1-carboxylic Acid *tert*-Butyl Ester (28p). MS (ES⁺) *m/z* (M + 23) 434; δ_H (500 MHz, DMSO-*d*₆) 10.88 (1H, s), 8.09 (d, *J* = 8.80 Hz, 2H), 7.65–7.79 (3H, m), 3.44–3.50 (4H, m), 2.83 (t, *J* = 4.77 Hz, 4H), 2.44 (3H, s), 1.34 (9H, s).

4-[4-(3-Cyanomethylureido)benzenesulfonyl]piperazine-1-carboxylic Acid *tert*-Butyl Ester (28l). Phosgene (20% solution in toluene, 0.34 mL, 1.7 mmol) was added dropwise to a stirred solution of 4-(4-aminobenzenesulfonyl)piperazine-1-carboxylic acid *tert*-butyl ester (0.18 g, 5.3 mmol) and diisopropylethylamine (0.18 mL, 6.4 mmol) in THF (5 mL) at room temperature. To this mixture was added aminoacetonitrile (0.035 g, 6.4 mmol) in one portion, and the mixture was stirred at room temperature under a nitrogen atmosphere overnight. After this time the mixture was concentrated, diluted with DCM (20 mL), and washed with water (10 mL), saturated NaHCO₃ (10 mL), and HCl (10 mL, 2 M solution). The organic layer was separated, dried (MgSO₄), filtered, and concentrated under vacuum and the resulting residue was purified using flash column chromatography (elution, 70% DCM, 30% ethyl acetate) to give the title compound (0.045 g, 20% yield) as a white solid. MS (ES⁺) *m/z* (M + 23) 446; HRMS (ES⁺) *m/z* 424.1646 (424.1655 calcd for C₁₈H₂₃N₃O₅S, M + H); ¹H NMR (250 MHz, DMSO) 9.52 (s, 1H), 7.52–7.69 (m, 4H), 6.91 (t, *J* = 5.94 Hz, 1H), 4.13 (d, *J* = 5.79 Hz, 2H), 3.21–3.29 (m, 4H), 2.69–2.84 (m, 4H), 1.32 (s, 9H); ¹³C NMR (126 MHz, DMSO-*d*₆) δ 154.4, 153.4, 144.5, 128.9, 126.6, 118.3, 117.6, 79.2, 45.8, 28.4, 27.9.

4-(4-Nitrobenzenesulfonyl)piperazine-1-carboxylic Acid Benzyl Ester. Diisopropylethylamine (0.82 mL, 4.95 mmol) was added in one portion to a stirred solution of piperazine-1-carboxylic acid benzyl ester (1.0 g, 4.5 mmol) in DCM (10 mL) at room temperature. To this mixture was added 4-nitrophenylsulfonfyl chloride (1.1 g, 4.95 mmol) in one portion, and the mixture was stirred at room temperature under a nitrogen atmosphere for 1 h. After this time the solvent was removed under vacuum and the resulting residue was purified using flash column chromatography (elution, 70% heptane, 30% ethyl acetate) to give the title compound (1.82 g, 100% yield) as a white solid. *t*_R = 1.43 min; MS (ES⁺) *m/z* (M + Na⁺) 428.

4-(4-Cyanobenzenesulfonyl)piperazine-1-carboxylic Acid *tert*-Butyl Ester (28q). MS (ES⁺) *m/z* (M + 1) 252; HRMS (ES⁺) *m/z* 252.0800 (252.0807 calcd for C₁₆H₂₁N₃O₄S, M + H, loss of *tert*-butyl); ¹H NMR (500 MHz, DMSO) 8.14 (d, *J* = 8.25 Hz, 2H), 7.91 (d, *J* = 8.25 Hz, 2H), 3.39 (br s, 4H), 2.92 (t, *J* = 4.86 Hz, 4H), 1.35 (s, 9H); ¹³C NMR (126 MHz, DMSO-*d*₆) δ 153.3, 139.2, 133.7, 128.3, 117.7, 115.8, 79.4, 45.6, 27.9.

4-(4-Aminobenzenesulfonyl)piperazine-1-carboxylic Acid Benzyl Ester. 4-(4-Nitro-benzenesulfonyl)piperazine-1-carboxylic acid benzyl ester (1.82 g, 4.5 mmol) was suspended in a 5:1 mixture of ethanol and water (30 mL). To this solution was added iron powder (0.65 g, 11.7 mmol) followed by saturated ammonium chloride solution (1 mL), and the mixture was heated to 80 °C for 3 h. After this time, the reaction mixture was cooled to room temperature and filtered through a pad of Celite, the Celite was washed with ethanol (10 mL) and ethyl acetate (50 mL), and the solution was concentrated under vacuum. The resulting residue was partitioned between DCM (50 mL) and water (20 mL). The organic layer was separated, dried with MgSO₄, filtered, and concentrated to afford the title compound (1.5 g, 89% yield) as a white solid. *t*_R = 1.29 min; MS (ES⁺) *m/z* (M + H)⁺ 376.

4-(4-Acryloylamino-benzenesulfonyl)piperazine-1-carboxylic Acid Benzyl Ester (16a). 4-(4-Aminobenzenesulfonyl)piperazine-1-carboxylic acid benzyl ester (0.25 g, 0.67 mmol) was dissolved in THF (10 mL). To this was added diisopropylethylamine (0.33 mL, 1.9 mmol) in one portion followed by the dropwise addition of acryloyl chloride (0.06 mL, 0.74 mmol), and the mixture was stirred at room temperature under a nitrogen atmosphere for 3 h. The THF was removed under vacuum and the resulting crude material was purified using column chromatography (elution, 20% heptane, 80% ethyl acetate) to give the title compound (57 mg, 20% yield) as a white powder. MS (ES⁺) *m/z* (M + 1) 430; HRMS (ES⁺) *m/z* 430.1431 (430.1437 calcd for C₂₁H₂₃N₃O₅S, M + H); ¹H NMR (500 MHz, DMSO) 10.60 (s, 1H) 7.92 (d, *J* = 8.70 Hz, 2H), 7.70 (d, *J* = 8.85 Hz, 2H), 7.18–7.44 (m, 5H), 6.41–6.52 (m, 1H), 6.27–6.38 (m, 1H), 5.84 (dd, *J* = 10.07, 1.83 Hz, 1H), 5.02 (s, 2H), 3.48 (br s, 4H), 2.87 (br s, 4H); ¹³C NMR (126 MHz, DMSO-*d*₆) δ 163.8, 154.2, 143.4, 136.6, 131.4, 128.9, 128.6, 128.4, 128.2, 127.9, 127.6, 119.2, 66.5, 45.7, 42.8.

4-(4-Acryloylamino-benzenesulfonyl)piperazine-1-carboxylic Acid *tert*-Butyl Ester (14a). MS (ES⁺) *m/z* (M + 23) 418; HRMS (ES⁺) *m/z* 418.1400 (418.1413 calcd for C₁₈H₂₅N₃O₅SNa, M + Na); ¹H NMR (500 MHz, DMSO) 10.60 (br s, 1H), 7.92 (d, *J* = 8.67 Hz, 2H), 7.70 (d, *J* = 8.67 Hz, 2H), 6.27–6.54 (m, 2H), 5.84 (dd, *J* = 10.17, 1.50 Hz, 1H), 3.38–3.45 (m, 4H), 2.83 (t, *J* = 4.65 Hz, 4H), 1.36 (s, 9H); ¹³C NMR (126 MHz, DMSO-*d*₆) δ 163.7, 153.4, 143.3, 131.3, 128.9, 128.6, 128.1, 119.1, 79.3, 45.7, 43.0, 41.9, 27.9.

3-(4-Acryloylamino-benzenesulfonylamino)-(S)-pyrrolidine-1-carboxylic Acid Benzyl Ester (16b). MS (ES⁺) *m/z* (M + 1) 430; HRMS (ES⁺) *m/z* 430.1441 (430.1437 calcd for C₂₁H₂₃N₃O₅S, M + H); ¹H NMR (500 MHz, DMSO) 10.54 (s, 1H), 7.92 (d, *J* = 8.65 Hz, 1H), 7.85 (d, *J* = 8.65 Hz, 2H), 7.76 (d, *J* = 8.65 Hz, 2H), 7.39–7.26 (m, 5H), 6.50–6.27 (m, 2H), 5.83 (d, *J* = 1.52 Hz, 2H), 5.02 (d, *J* = 1.52 Hz, 2H), 3.71–3.62 (m, 1H), 3.34 (obscured, 2H), 3.28–3.21 (m, 1H), 3.11–3.04 (m, 1H), 1.91–1.84 (m, 1H), 1.72–1.61 (m, 1H); ¹³C NMR (126 MHz, DMSO-*d*₆) δ 163.7, 153.8, 142.6, 137.0, 134.9, 131.4, 119.2, 119.1, 65.8, 52.3, 51.5, 51.3, 50.8, 44.0, 43.5, 31.3, 30.5.

3-(4-Acryloylamino-benzenesulfonylamino)-(S)-pyrrolidine-1-carboxylic Acid Benzyl Ester (16c). MS *m/z* (M + 1) 430; HRMS (ES⁺) *m/z* 430.1449 (430.1437 calcd for C₂₁H₂₃N₃O₅S, M + H); ¹H NMR (500 MHz, DMSO) 9.72 (s, 1H), 7.08 (d, *J* = 8.54 Hz, 2H), 6.92 (d, *J* = 8.39 Hz, 2H), 6.44–6.58 (m, 6H), 5.57–5.70 (m, 1H), 5.42–5.54 (m, 1H), 5.00 (dd, *J* = 10.15, 1.60 Hz, 1H), 3.94–4.25 (m, 2H), 3.02 (sxt, *J* = 5.92 Hz, 1H), 2.27–2.46 (m, 3H), 2.19 (dd, *J* = 10.15, 4.65 Hz, 1H), 1.02–1.10 (m, 1H), 0.76–0.89 (m, 1H), 0.38–0.51 (m, 1H); ¹³C NMR (126 MHz, DMSO-*d*₆) δ 163.9, 155.8, 143.3, 137.0, 131.6, 130.1, 128.8, 128.5, 128.3, 128.1 (two peaks), 119.3, 65.6, 53.0, 50.3, 46.4, 30.4.

3-(4-Acryloylamino-benzenesulfonylamino)-(R)-pyrrolidine-1-carboxylic Acid Benzyl Ester (16d). MS (ES⁺) *m/z* (M + 23) 430; HRMS (ES⁺) *m/z* 430.1435 (430.1437 calcd for C₂₁H₂₃N₃O₅S,

M + H); ¹H NMR (500 MHz, DMSO) 10.54 (s, 1H), 7.84–8.00 (m, 3H), 7.78 (d, *J* = 8.70 Hz, 2H), 7.22–7.42 (m, 5H) 6.40–6.52 (m, 1H), 6.23–6.37 (m, 1H), 5.83 (d, *J* = 10.07 Hz, 1H), 5.02 (d, *J* = 11.44 Hz, 2H), 3.66 (d, *J* = 3.66 Hz, 1H), 3.19–3.27 (m, 1H), 3.00–3.15 (m, 1H), 1.83–1.97 (m, 1H), 1.62–1.79 (m, 1H).

3-(4-Acryloylamino-benzenesulfonylamino)-(R)-pyrrolidine-1-carboxylic Acid Benzyl Ester (16e). MS (ES⁺) *m/z* (M + 23) 430; HRMS (ES⁺) *m/z* 430.1434 (430.1437 calcd for C₂₁H₂₃N₃O₅S, M + H); ¹H NMR (500 MHz, DMSO) 9.73 (br s, 1H), 7.09 (d, *J* = 8.62 Hz, 2H), 6.93 (d, *J* = 8.44 Hz, 2H), 6.36–6.64 (m, 7H), 5.43–5.70 (m, 2H), 5.01 (dd, *J* = 10.18, 1.56 Hz, 1H), 3.98–4.27 (m, 2H), 3.03 (sxt, *J* = 5.94 Hz, 1H), 2.11–2.47 (m, 4H), 1.09 (dq, *J* = 13.18, 6.79 Hz, 1H), 0.83 (dq, *J* = 12.56, 6.20 Hz, 1H); ¹³C NMR (126 MHz, DMSO-*d*₆) δ 163.7, 155.6, 143.1, 136.8, 131.4, 129.9, 128.6, 128.4, 128.1, 127.9, 119.1, 65.4, 52.9, 50.1, 46.2, 30.2.

5-(4-Acryloylamino-benzenesulfonyl)hexahydropyrrolo[3,4-*c*]pyrrole-2-carboxylic Acid Benzyl Ester (16f). MS (ES⁺) *m/z* (M + 1) 456; HRMS (ES⁺) *m/z* 456.1585 (456.1593 calcd for C₂₃H₂₅N₃O₅S, M + H); ¹H NMR (250 MHz, DMSO) 9.74 (s, 1 H), 7.02–7.15 (m, 2 H), 6.87–6.98 (m, 2 H), 6.37–6.61 (m, 5 H), 5.40–5.71 (m, 2 H), 4.92–5.07 (m, 1 H), 4.06–4.25 (m, 2 H), 2.59 (d, *J* = 7.01 Hz, 2 H), 2.43 (d, *J* = 7.31 Hz, 2 H), 2.16 (d, *J* = 8.68 Hz, 4 H), 1.85–2.03 (m, 2 H); ¹³C NMR (126 MHz, DMSO-*d*₆) δ 163.7, 153.7, 143.2, 137.0, 131.4, 129.3, 128.8, 128.4, 128.1, 127.8, 127.4, 119.1, 65.8, 52.0, 50.0, 49.4, 41.6, 40.7.

{2-[(4-Acryloylamino-benzenesulfonyl)methylamino]ethyl}-methylcarbamic Acid Benzyl Ester (16g). MS (ES⁺) *m/z* (M + 1) 432; δ_H (500 MHz, CDCl₃) 7.72–7.56 (5H, m), 7.31–7.18 (5H, m), 6.44–6.15 (2H, m), 5.77–5.72 (1H, m), 5.06 (2H, s), 3.45–3.36 (2H, m), 3.16–3.03 (2H, m), 2.94–2.91 (3H, m), 2.74 (3H, s), 2.55 (2H, s).

5-(4-Acryloylamino-benzenesulfonyl)-2,5-diazabicyclo-[2.2.1]heptane-2-carboxylic Acid *tert*-Butyl Ester (16h). MS (ES⁺) *m/z* (M + 23) 430; δ_H (500 MHz, CDCl₃) 7.86–7.77 (4H, m), 7.58 (1H, s), 6.51–6.25 (2H, m), 5.86 (d, *J* = 10.2 Hz, 1H), 4.47 (2H, s), 3.51–3.13 (4H, m), 1.74–1.66 (1H, m), 1.46–1.24 (1H, m).

N-[4-(4-Pyridin-2-yl)piperazine-1-sulfonyl]phenylacrylamide (14b). MS (ES⁺) *m/z* (M + 1) 373; HRMS (ES⁺) *m/z* 373.1351 (373.1334 calcd for C₁₈H₂₀N₄O₃S, M + H); ¹H NMR (500 MHz, CDCl₃) 8.15 (dd, *J* = 4.58, 1.47 Hz, 1H), 7.69–7.81 (m, 4H), 7.44–7.58 (m, 2H), 6.58–6.69 (m, 2H), 6.50 (d, *J* = 16.87 Hz, 1H), 6.27 (dd, *J* = 16.87, 10.27 Hz, 1H), 5.86 (d, *J* = 10.27 Hz, 1H), 3.60–3.71 (m, 4H), 3.08–3.17 (m, 4H); ¹³C NMR (126 MHz, DMSO-*d*₆) δ 163.7, 158.3, 147.5, 143.3, 137.7, 131.4, 128.9, 128.6, 128.2, 119.2, 113.6, 107.5, 45.6, 44.0.

N-[4-[4-(3-Methylpyridin-2-yl)piperazine-1-sulfonyl]phenyl]-acrylamide (14c). MS (ES⁺) *m/z* (M + 1) 387; HRMS (ES⁺) *m/z* 387.1480 (387.1491 calcd for C₁₉H₂₂N₄O₃S, M + H); ¹H NMR (500 MHz, CDCl₃) 8.11–8.16 (m, 1H), 7.73–7.85 (m, 4H), 7.58 (s, 1H), 7.40 (d, *J* = 6.97 Hz, 1H), 6.88 (dd, *J* = 7.15, 4.95 Hz, 1H), 6.51 (dd, *J* = 16.87, 0.92 Hz, 1H), 6.29 (dd, *J* = 16.87, 10.27 Hz, 1H), 5.80–5.93 (m, 1H), 3.11–3.33 (m, 8H), 2.19 (s, 3H); ¹³C NMR (126 MHz, DMSO-*d*₆) δ 163.8, 160.4, 145.0, 143.3, 139.4, 131.4, 129.0, 128.8, 128.2, 124.4, 119.2, 118.4, 48.5, 46.0, 17.7.

N-[4-[4-(6-Methylpyridin-2-yl)piperazine-1-sulfonyl]phenyl]-acrylamide (14d). MS (ES⁺) *m/z* (M + 1) 387; HRMS (ES⁺) *m/z* 387.1494 (387.1491 calcd for C₁₉H₂₂N₄O₃S, M + H); ¹H NMR (500 MHz, CDCl₃) 7.69–7.82 (m, 4H), 7.60 (s, 1H), 7.37 (dd, *J* = 8.22, 7.46 Hz, 1H), 6.44–6.55 (m, 2H), 6.39 (d, *J* = 8.38 Hz, 1H), 6.20–6.34 (m, 1H), 5.85 (dd, *J* = 10.13, 1.29 Hz, 1H), 3.58–3.69 (m, 4H), 3.06–3.16 (m, 4H), 2.37 (s, 3H); ¹³C NMR (126 MHz, DMSO-*d*₆) δ 163.7, 157.8, 155.8, 143.3, 138.0, 131.4, 128.9, 128.6, 128.2, 119.2, 112.7, 104.2, 45.6, 43.9, 24.2.

N-[4-[4-(3-Trifluoromethylpyridin-2-yl)piperazine-1-sulfonyl]phenyl]acrylamide (14e). MS (ES⁺) *m/z* (M + 1) 441; HRMS (ES⁺) *m/z* 441.1220 (441.1208 calcd for C₁₉H₁₉F₃N₄O₃S, M + H); ¹H NMR (500 MHz, CDCl₃) 8.38–8.48 (m, 1H), 7.71–7.90 (m, 5H), 7.48 (s, 1H), 7.04 (dd, *J* = 7.70, 4.77 Hz, 1H), 6.51 (d, *J* = 16.69 Hz, 1H), 6.28 (dd, *J* = 16.87, 10.27 Hz, 1H), 5.87 (d, *J* = 10.64 Hz, 1H), 3.31–3.41 (m, 4H), 3.11–3.24 (m, 4H); ¹³C NMR (126 MHz, DMSO-*d*₆) δ 163.8, 158.8, 151.7, 143.4, 137.7 (q, *J* = 5 Hz), 131.4,

129.0, 128.7, 128.2, 123.8 (q, $J = 273$ Hz), 119.2, 118.7, 116.1 (q, $J = 31$ Hz), 49.9, 45.9.

N-[4-[4-(6-Trifluoromethylpyridin-3-yl)piperazine-1-sulfonyl]phenyl]acrylamide (14f). MS (ES^+) m/z ($M + 1$) 441; δ_H (500 MHz, MeOD) 8.33 (1H, s), 7.91 (d, $J = 8.85$ Hz, 2H), 7.68–7.81 (m, 3H), 6.88 (d, $J = 9.16$ Hz, 1H), 6.34–6.52 (2H, m), 5.83 (dd, $J = 8.62, 3.13$ Hz, 1H), 3.70–3.83 (4H, m), 3.05–3.14 (4H, m).

N-[4-(4-Phenylpiperazine-1-sulfonyl)phenyl]acrylamide (14g). MS (ES^+) m/z ($M + 1$) 372; HRMS (ES^+) m/z 372.1377 (372.1382 calcd for $C_{19}H_{21}N_3O_3S$, $M + H$); 1H NMR (500 MHz, DMSO) 10.59 (s, 1H), 7.94 (d, $J = 8.70$ Hz, 2H), 7.75 (d, $J = 8.70$ Hz, 2H), 7.20 (t, $J = 7.93$ Hz, 2H), 6.90 (d, $J = 8.09$ Hz, 2H), 6.80 (t, $J = 7.25$ Hz, 1H), 6.40–6.51 (m, 1H), 6.25–6.35 (m, 1H), 5.84 (dd, $J = 10.07, 1.68$ Hz, 1H), 3.16–3.25 (m, 4H), 2.95–3.05 (m, 4H); ^{13}C NMR (126 MHz, DMSO- d_6) δ 163.7, 150.4, 143.4, 131.4, 129.0, 128.5, 128.2, 119.7, 119.2, 116.2, 47.9, 45.8.

N-[4-[4-(2-Trifluoromethylphenyl)piperazine-1-sulfonyl]phenyl]acrylamide (14h). MS (ES^+) m/z ($M + 1$) 440; HRMS (ES^+) m/z 440.1273 (440.1256 calcd for $C_{20}H_{20}F_3N_3O_3S$, $M + H$); 1H NMR (500 MHz, DMSO) 7.72–7.90 (m, 4H), 7.47–7.65 (m, 3H), 7.35 (d, $J = 7.89$ Hz, 1H), 7.21–7.30 (m, 3H), 6.52 (d, $J = 16.87$ Hz, 1H), 6.30 (dd, $J = 16.87, 10.27$ Hz, 1H), 5.88 (d, $J = 10.27$ Hz, 1H), 3.17 (br s, 4H), 3.01 (t, $J = 4.77$ Hz, 4H).

N-[4-[4-(3-Phenylpropyl)piperazine-1-sulfonyl]phenyl]acrylamide (19a). MS (ES^+) m/z ($M + 1$) 415; HRMS (ES^+) m/z 414.1844 (414.1851 calcd for $C_{22}H_{27}N_3O_3S$, $M + H$); 1H NMR (500 MHz, DMSO) 10.59 (s, 1H), 7.93 (d, $J = 8.70$ Hz, 2H), 7.70 (d, $J = 8.70$ Hz, 2H), 7.05–7.30 (m, 5H), 6.41–6.53 (m, 1H), 6.26–6.37 (m, 1H), 5.84 (dd, $J = 10.15, 1.60$ Hz, 1H), 2.86 (br s, 4H), 2.53–2.56 (m, 2H), 2.35–2.46 (m, 4H), 2.26 (t, $J = 7.10$ Hz, 2H), 1.65 (quin, $J = 7.36$ Hz, 2H); ^{13}C NMR (126 MHz, DMSO- d_6) δ 163.7, 143.3, 142.0, 131.4, 128.9, 128.6, 128.3, 128.2, 125.6, 119.1, 56.5, 51.6, 45.9, 32.7, 28.0.

N-[4-[4-(4-Phenylbutyl)piperazine-1-sulfonyl]phenyl]acrylamide (19b). MS (ES^+) m/z ($M + 1$) 428; δ_H (250 MHz, DMSO- d_6) 9.75 (1H, s), 7.09 (d, $J = 8.68$ Hz, 2H), 6.86 (d, $J = 8.83$ Hz, 2H), 6.22–6.47 (5H, m), 5.39–5.76 (2H, m), 4.88–5.08 (1H, m), 1.93–2.09 (4H, m), 1.33–1.58 (6H, m), 0.32–0.75 (5H, m).

4-[4-Acryloylamino-3-(isobutylmethylamino)benzenesulfonyl]piperazine-1-carboxylic Acid Benzyl Ester (29a). MS (ES^+) m/z ($M + 1$) 515; HRMS (ES^+) m/z 515.2345 (515.2328 calcd for $C_{26}H_{34}N_4O_5S$, $M + H$); 1H NMR (500 MHz, DMSO) 9.32 (s, 1H), 7.56 (d, $J = 8.80$ Hz, 1H), 7.25–7.41 (m, 5H), 7.00 (dd, $J = 8.99, 2.93$ Hz, 1H), 6.89 (d, $J = 2.93$ Hz, 1H), 6.49 (dd, $J = 17.06, 10.27$ Hz, 1H), 6.21 (dd, $J = 17.06, 1.47$ Hz, 1H), 5.74 (d, $J = 10.09$ Hz, 1H), 5.04 (s, 2H), 3.41 (br s, 4H), 3.17 (d, $J = 7.15$ Hz, 2H), 2.85–3.02 (m, 8H), 1.98 (dq, $J = 13.58, 6.83, 6.83, 6.83$ Hz, 1H), 0.79–0.95 (m, 7H); ^{13}C NMR (126 MHz, DMSO- d_6) δ 163.7, 154.1, 146.7, 136.6, 131.9, 129.2, 128.9, 128.4, 127.9, 127.6, 126.8, 122.8, 116.4, 110.7, 66.5, 59.4, 45.1, 42.9 (br), 26.8, 20.1.

4-[4-(Acryloylmethyl-amino)benzenesulfonyl]piperazine-1-carboxylic Acid *tert*-Butyl Ester (26). Sodium hydride (0.050 g, 26 mmol) was added in one portion to a stirred solution of 4-(4-acryloylamino)benzenesulfonyl]piperazine-1-carboxylic acid *tert*-butyl ester (14a, 0.1 g, 0.25 mmol) in THF (1 mL). The mixture was stirred at room temperature for 5 min before methyl iodide (0.05 g, 0.25 mmol) was added in one portion, and stirring continued for 1 h. After this time, the reaction mixture was concentrated under vacuum and the resulting residue purified using preparative HPLC to give the title compound (6.6 mg, 7% yield) as a white solid. MS (ES^+) m/z ($M + 23$) 432; δ_H (500 MHz, MeOD) 7.69–7.82 (2H, m), 7.33–7.50 (2H, m), 6.01–6.27 (2H, m), 5.50–5.61 (1H, m), 3.41 (4H, br s), 3.29 (3H, s), 2.90 (t, $J = 5.04$ Hz, 4H), 1.31 (9H, s).

N-[4-(Piperazine-1-sulfonyl)phenyl]acrylamide (15). Trifluoroacetic acid (3 mL) was added in one portion to a solution of 4-(4-acryloylamino)benzenesulfonyl]piperazine-1-carboxylic acid *tert*-butyl ester (3, 1.23 g, 3.11 mmol) in DCM (6 mL). The resulting mixture was stirred at room temperature for 2 h under a nitrogen atmosphere, after which time, the mixture was concentrated under vacuum to give the title compound (0.9 g, 98% yield) as an orange foam which was used without further purification. MS (ES^+) m/z ($M + 1$) 296; δ_H

(500 MHz, DMSO- d_6) 10.66 (1H, s), 8.62 (1H, br s), 7.96 (d, $J = 8.67$ Hz, 2H), 7.76 (d, $J = 8.67$ Hz, 2H), 6.41–6.54 (1H, m), 6.28–6.39 (1H, m), 5.86 (dd, $J = 10.17, 1.50$ Hz, 1H), 3.15–3.25 (4H, m), 3.08 (4H, br s).

4-Benzyloxycarbonylaminopiperidine-1-carboxylic Acid *tert*-Butyl Ester. Diisopropylethylamine (0.9 mL, 5.5 mmol) was added in one portion to a stirred solution of 4-aminopiperidine-1-carboxylic acid *tert*-butyl ester (1.0 g, 5.0 mmol) in THF (10 mL) at room temperature. To this mixture was added benzyl chloroformate (0.78 mL, 5.5 mmol) dropwise, and the mixture was stirred at room temperature under a nitrogen atmosphere for 18 h. After this time the mixture was diluted with ethyl acetate (50 mL) and washed with water (100 mL), saturated $NaHCO_3$ (100 mL), and HCl (100 mL, 2M). The organic layer was separated, dried ($MgSO_4$), filtered, and concentrated under vacuum. The resulting residue was purified using flash column chromatography (elution, 50% heptane, 50% ethyl acetate) to give the title compound (1.2 g, 73% yield) as a colorless oil. MS (ES^+) m/z ($M + 23$) 357.

Piperidin-4-ylcarbamic Acid Benzyl Ester. HCl (10 mL, 4 M solution in dioxane) was added in one portion to a stirred solution of 4-benzyloxycarbonylaminopiperidine-1-carboxylic acid *tert*-butyl ester (1.2 g, 3.6 mmol) in dioxane (5 mL), and the suspension was stirred at room temperature under a nitrogen atmosphere for 3 h. After this time the mixture was concentrated under vacuum and the resulting solid was collected by filtration, washed with TBME (3 \times 100 mL), and dried under vacuum to give the title compound (0.74 g, 88% yield) as a white solid. MS (ES^+) m/z ($M + 1$) 236.

[1-(4-Nitrobenzenesulfonyl)piperidin-4-yl]carbamic Acid Benzyl Ester. Diisopropylethylamine (1.04 mL, 7.0 mmol) was added in one portion to a stirred solution of piperidin-4-yl-carbamic acid benzyl ester (0.74 g, 3.1 mmol) in THF (10 mL) at room temperature. To this mixture was added 4-nitrophenylsulfonyl chloride (0.77 g, 3.5 mmol) in one portion, and the mixture was stirred at room temperature under a nitrogen atmosphere for 1 h. After this time the solvent was removed under vacuum and the resulting residue was partitioned between ethyl acetate (50 mL) and HCl (50 mL, 1 M solution). The organic layer was separated and washed with brine (50 mL) before being dried ($MgSO_4$), filtered, and concentrated under vacuum. The resulting white solid was suspended in heptane, collected by filtration, and washed with water (50 mL), heptane (50 mL), and TBME (50 mL) before being dried under vacuum to afford the title compound (1.3 g, 100% yield) as a white solid. MS (ES^+) m/z ($M + 1$) 420.

[1-(4-Aminobenzenesulfonyl)piperidin-4-yl]carbamic Acid Benzyl Ester. [1-(4-Nitrobenzenesulfonyl)piperidin-4-yl]carbamic acid benzyl ester (1.3 g, 3.5 mmol) was suspended in a 5:1 mixture of ethanol and water (30 mL). To this solution was added iron powder (0.48 g, 9.1 mmol) followed by saturated ammonium chloride solution (1 mL), and the mixture was heated to 80 $^{\circ}C$ for 3 h. After this time, the reaction mixture was cooled to room temperature and filtered through a pad of Celite, the Celite was washed with ethanol (10 mL) and ethyl acetate (50 mL), and the solution was concentrated under vacuum. The resulting residue was partitioned between DCM (50 mL) and water (20 mL). The organic layer was separated, dried with $MgSO_4$, filtered, and concentrated to afford the title compound (1.25 g, 99% yield) as a brown solid. MS (ES^+) m/z ($M + 1$) 390.

[1-(4-Acryloylamino)benzenesulfonyl]piperidin-4-yl]carbamic Acid Benzyl Ester (16k). [1-(4-Aminobenzenesulfonyl)piperidin-4-yl]carbamic acid benzyl ester (1.29 g, 3.3 mmol) was dissolved in DCM (20 mL). To this was added diisopropylethylamine (1.64 mL, 9.9 mmol) in one portion followed by the dropwise addition of acryloyl chloride (0.3 mL, 3.6 mmol), and the mixture was stirred at room temperature under a nitrogen atmosphere for 18 h. The THF was removed under vacuum and the resulting crude material was purified using preparative HPLC to give the title compound (10.4 mg, 1% yield) as a white powder. MS (ES^+) m/z ($M + 1$) 444; δ_H (250 MHz, DMSO- d_6) 10.56 (1H, s), 7.89 (d, $J = 8.83$ Hz, 2H), 7.68 (d, $J = 8.68$ Hz, 2H), 7.20–7.42 (m, 6H, m), 6.19–6.56 (2H, m), 5.74–5.90 (1H, m), 4.96 (2H, s), 3.40–3.50 (2H, m), 2.40 (2H, br s), 1.78 (d, $J = 9.59$ Hz, 2H), 1.26–1.53 (2H, m).

[1-(4-Acryloylamino-benzenesulfonyl)piperidin-4-ylmethyl]-carbamoyl Acid Benzyl Ester (16i). MS (ES^+) m/z ($M + 1$) 458; δ_H (500 MHz, DMSO- d_6) 10.57 (1H, s), 7.90 (d, $J = 8.70$ Hz, 2H), 7.69 (d, $J = 8.70$ Hz, 2H), 7.22–7.40 (6H, m), 6.41–6.53 (1H, m), 6.22–6.38 (1H, m), 5.84 (dd, $J = 10.07$, 1.68 Hz, 1H), 4.96–5.02 (2H, m), 3.59 (d, $J = 11.60$ Hz, 2H), 2.86 (t, $J = 6.26$ Hz, 2H), 2.18 (t, $J = 11.06$ Hz, 2H), 1.67 (d, $J = 11.75$ Hz, 2H), 1.33 (d, $J = 10.68$ Hz, 1H), 1.05–1.20 (2H, m).

4-[(4-Acryloylamino-benzenesulfonylamino)methyl]-piperidine-1-carboxylic Acid Benzyl Ester (16j). MS (ES^+) m/z ($M + 1$) 458; HRMS (ES^+) m/z 458.1738 (458.1750 calcd for $C_{23}H_{27}N_3O_5S$, $M + H$); 1H NMR (500 MHz, DMSO) 9.66 (s, 1H), 6.86–7.05 (m, 4H), 6.71 (t, $J = 6.18$ Hz, 1H), 6.40–6.58 (m, 6H), 5.54–5.68 (m, 1H), 5.40–5.50 (m, 1H), 4.98 (dd, $J = 10.07$, 1.83 Hz, 1H), 4.20 (s, 2H), 3.11 (d, $J = 13.28$ Hz, 2H), 1.70–2.02 (m, 4H), 0.59–0.83 (m, 3H), 0.11 (qd, $J = 12.21$, 4.27 Hz, 2H); ^{13}C NMR (126 MHz, DMSO- d_6) δ 163.8, 154.5, 142.5, 137.2, 135.0, 131.6, 128.6, 128.1, 128.0, 127.8, 127.7, 119.3, 66.2, 47.9, 43.5, 35.8, 29.1.

4-(4-Acryloylamino-benzenesulfonyl)[1,4]diazepane-1-carboxylic Acid Benzyl Ester (16m). MS (ES^+) m/z ($M + 1$) 444; δ_H (500 MHz, DMSO- d_6) 10.55 (1H, s), 7.83–7.93 (2H, m), 7.75 (dd, $J = 8.47$, 4.65 Hz, 2H), 7.26–7.40 (5H, m), 6.23–6.51 (2H, m), 5.72–5.86 (2H, m), 4.94–5.11 (2H, m), 3.51 (dt, $J = 11.71$, 5.82 Hz, 2H), 3.41 (d, $J = 8.39$ Hz, 3H), 1.67–1.78 (2H, m).

4-(3-Acryloylamino-benzenesulfonyl)piperazine-1-carboxylic Acid Benzyl Ester (16n). MS (ES^+) m/z ($M + 1$) 430; HRMS (ES^+) m/z 430.1432 (430.1437 calcd for $C_{21}H_{23}N_3O_5S$, $M + H$); 1H NMR (500 MHz, DMSO) 10.55 (s, 1H), 8.15 (s, 1H), 7.94 (d, $J = 8.25$ Hz, 1H), 7.61 (t, $J = 7.98$ Hz, 1H), 7.42 (d, $J = 7.70$ Hz, 1H), 7.25–7.35 (m, 5H), 6.27–6.48 (m, 2H), 5.83 (dd, $J = 10.09$, 1.65 Hz, 1H), 5.02 (s, 2H), 3.49 (br s, 4H), 2.90 (br s, 4H); ^{13}C NMR (126 MHz, DMSO- d_6) δ 163.6, 154.2, 139.9, 136.6, 135.2, 131.4, 130.1, 128.4, 127.9, 127.6, 123.6, 122.2, 117.7, 66.5, 45.7, 42.8.

4-(4-Nitrobenzenesulfonylamino)piperidine-1-carboxylic Acid *tert*-Butyl Ester. 4-Nitrophenylsulfonyl chloride (1.1 g, 5.4 mmol) was added in one portion to a stirred solution of 4-aminopiperidine-1-carboxylic acid *tert*-butyl ester (1.0 g, 4.9 mmol) and diisopropylethylamine (1.3 mL, 7.3 mmol) in THF (10 mL). The resulting mixture was stirred at room temperature under a nitrogen atmosphere for 1 h, after which time the solvent was removed under vacuum to give the title compound (1.92 g, 100% yield) as an orange solid which was used without further purification. MS (ES^+) m/z ($M + 23$) 408.

4-Nitro-*N*-piperidin-4-ylbenzenesulfonamide. HCl (20 mL, 4 M solution in dioxane) was added in one portion to a stirred solution of 4-(4-nitrobenzenesulfonylamino)piperidine-1-carboxylic acid *tert*-butyl ester (1.92 g, 4.9 mmol) in dioxane (5 mL), and the suspension was stirred at room temperature under a nitrogen atmosphere for 3 h. After this time the mixture was concentrated under vacuum and the resulting solid was collected by filtration, washed with TBME (3×100 mL), and dried under vacuum to give the title compound (1.4 g, 100% yield) as a white solid. MS (ES^+) m/z ($M + 1$) 286.

4-(4-Nitrobenzenesulfonylamino)piperidine-1-carboxylic Acid Benzyl Ester. Benzyl chloroformate (0.7 mL, 4.9 mmol) was added dropwise to a cool (0 °C) solution of 4-nitro-*N*-piperidin-4-ylbenzenesulfonamide (1.4 g, 4.9 mmol) and diisopropylethylamine (1.6 mL, 9.8 mmol) in THF (10 mL). The resulting mixture was warmed to room temperature and stirred under a nitrogen atmosphere for 18 h. After this time, the mixture was diluted with ethyl acetate (50 mL) and washed with water (50 mL). The organic layer was separated, dried ($MgSO_4$), filtered, and concentrated under vacuum. The resulting residue was purified using flash column chromatography (elution, 50% heptane, 50% ethyl acetate) to give the title compound (0.98 g, 48% yield) as a white solid. MS (ES^+) m/z ($M + 1$) 420.

4-(4-Aminobenzenesulfonylamino)piperidine-1-carboxylic Acid Benzyl Ester. 4-(4-Nitrobenzenesulfonylamino)piperidine-1-carboxylic acid benzyl ester (0.98 g, 2.4 mmol) was suspended in a 5:1 mixture of ethanol and water (30 mL). To this solution was added iron powder (0.34 g, 6.1 mmol) followed by saturated ammonium chloride solution (1 mL), and the mixture was heated to 80 °C for 3 h. After this time, the reaction mixture was cooled to room temperature and

filtered through a pad of Celite. The Celite was washed with ethanol (10 mL) and ethyl acetate (50 mL), and the solution was concentrated under vacuum. The resulting residue was partitioned between DCM (50 mL) and water (20 mL). The organic layer was separated, dried with $MgSO_4$, filtered, and concentrated to afford the title compound (1 g, 100% yield) as a brown solid. MS (ES^+) m/z ($M + 1$) 390.

4-(4-Acryloylamino-benzenesulfonylamino)piperidine-1-carboxylic Acid Benzyl Ester (16l). 4-(4-Aminobenzenesulfonylamino)piperidine-1-carboxylic acid benzyl ester (1 g, 2.4 mmol) was dissolved in THF (10 mL). To this was added diisopropylethylamine (1.27 mL, 7.2 mmol) in one portion followed by the dropwise addition of acryloyl chloride (0.2 mL, 2.6 mmol), and the mixture was stirred at room temperature under a nitrogen atmosphere for 3 h. The THF was removed under vacuum and the resulting crude material was purified using column chromatography (elution, 40% heptane, 60% ethyl acetate) to give the title compound (89 mg, 8% yield) as a white powder. MS (ES^+) m/z ($M + 1$) 444; HRMS (ES^+) m/z 444.1603 (444.1593 calcd for $C_{22}H_{25}N_3O_5S$, $M + H$); 1H NMR (500 MHz, DMSO) 10.58 (s, 1H), 7.70–7.95 (m, 5H), 7.28–7.47 (m, 5H), 6.30–6.58 (m, 2H), 5.84–5.97 (m, 1H), 5.10 (s, 2H), 3.84 (d, $J = 13.43$ Hz, 2H), 3.13–3.26 (m, 1H), 2.95 (d, $J = 7.17$ Hz, 2H), 1.63 (dd, $J = 12.89$, 3.13 Hz, 2H), 1.17–1.39 (m, 2H); ^{13}C NMR (126 MHz, DMSO- d_6) δ 163.6, 154.3, 142.4, 136.9, 136.1, 131.4, 128.4, 128.0, 127.8, 127.5, 119.1, 66.1, 49.7, 42.0, 32.0.

***N*-[4-(4-Cyclopentanecarbonylpiperazine-1-sulfonyl)phenyl]acrylamide (28a).** Diisopropylethylamine (0.24 mL, 1.36 mmol) was added in one portion to a stirred solution of *N*-[4-(piperazine-1-sulfonyl)phenyl]acrylamide (15, 0.1 g, 0.34 mmol) in THF (5 mL). The mixture was stirred at room temperature for 5 min before cyclopentanecarbonyl chloride (0.06 g, 0.44 mmol) was added dropwise, and the resulting mixture was stirred at room temperature under a nitrogen atmosphere for 18 h. The crude reaction mixture was concentrated under vacuum and the residue was purified using preparative HPLC to give the title compound (0.012 g, 11% yield) as a white powder. MS (ES^+) m/z ($M + 1$) 392; HRMS (ES^+) m/z 392.1649 (392.1644 calcd for $C_{19}H_{25}N_3O_4S$, $M + H$); 1H NMR (500 MHz, DMSO) 10.61 (s, 1H), 7.92 (d, $J = 8.80$ Hz, 2H), 7.70 (d, $J = 8.80$ Hz, 2H), 6.40–6.54 (m, 1H), 6.27–6.36 (m, 1H), 5.84 (dd, $J = 10.09$, 1.83 Hz, 1H), 3.51–3.66 (m, 4H), 2.78–2.96 (m, 4H), 1.64–1.79 (m, 2H), 1.37–1.61 (m, 7H); ^{13}C NMR (126 MHz, DMSO- d_6) δ 173.5, 163.7, 143.4, 131.4, 128.9, 128.6, 128.2, 119.2, 46.2 (br), 45.8 (br), 44.1 (br), 40.4 (br), 39.9, 29.5, 25.6.

4-(4-Acryloylamino-benzenesulfonyl)piperazine-1-carboxylic Acid Methyl Ester (16z). MS (ES^+) m/z ($M + 23$) 354; HRMS (ES^+) m/z 354.1126 (354.1124 calcd for $C_{15}H_{19}N_3O_5S$, $M + H$); 1H NMR (500 MHz, DMSO) 10.57 (s, 1H), 7.91 (d, $J = 8.83$ Hz, 2H), 7.69 (d, $J = 8.67$ Hz, 2H), 6.41–6.51 (m, 1H), 6.27–6.38 (m, 1H), 5.83 (dd, $J = 10.17$, 1.65 Hz, 1H), 3.54 (s, 3H), 3.43 (t, $J = 4.65$ Hz, 4H), 2.85 (t, $J = 4.73$ Hz, 4H); ^{13}C NMR (126 MHz, DMSO- d_6) δ 163.8, 154.8, 143.4, 131.4, 128.9, 128.7, 128.2, 119.2, 52.5, 45.6, 42.6 (br).

4-(4-Acryloylamino-benzenesulfonyl)piperazine-1-carboxylic Acid Ethyl Ester (16aa). MS (ES^+) m/z ($M + 23$) 368; HRMS (ES^+) m/z 368.1294 (368.1280 calcd for $C_{16}H_{21}N_3O_5S$, $M + H$); 1H NMR (500 MHz, DMSO) 10.58 (s, 1H), 7.91 (d, $J = 8.83$ Hz, 2H), 7.69 (d, $J = 8.83$ Hz, 2H), 6.41–6.50 (m, 1H), 6.28–6.37 (m, 1H), 5.83 (dd, $J = 10.09$, 1.73 Hz, 1H), 3.98 (q, $J = 7.09$ Hz, 2H), 3.43 (br s, 4H), 2.85 (t, $J = 4.81$ Hz, 4H), 1.03–1.18 (m, 3H); ^{13}C NMR (126 MHz, DMSO- d_6) δ 163.7, 154.3, 143.4, 131.4, 128.9, 128.6, 128.2, 119.2, 61.0, 45.7, 42.6 (br), 14.5.

4-(4-Acryloylamino-benzenesulfonyl)piperazine-1-carboxylic Acid Cyclopentyl Ester (16ab). MS (ES^+) m/z ($M + 23$) 408; HRMS (ES^+) m/z 408.1604 (408.1593 calcd for $C_{19}H_{25}N_3O_5S$, $M + H$); 1H NMR (500 MHz, DMSO) 10.58 (s, 1H), 7.91 (d, $J = 8.67$ Hz, 2H), 7.69 (d, $J = 8.83$ Hz, 2H), 6.42–6.50 (m, 1H), 6.27–6.36 (m, 1H), 5.77–5.88 (m, 1H), 4.91 (dt, $J = 5.60$, 3.03 Hz, 1H), 3.41 (t, $J = 4.89$ Hz, 4H), 2.84 (t, $J = 4.49$ Hz, 4H), 1.68–1.78 (m, 2H), 1.43–1.63 (m, 6H); ^{13}C NMR (126 MHz, DMSO- d_6) δ 163.7, 154.1, 143.4, 131.4, 128.9, 128.6, 128.2, 119.2, 77.5, 45.7, 42.5 (br), 32.3, 23.1.

N-[4-[4-(3-Phenylpropionyl)piperazine-1-sulfonyl]phenyl]acrylamide (18a). MS (ES⁺) *m/z* (M + 23) 428; HRMS (ES⁺) *m/z* 428.1628 (428.1644 calcd for C₂₂H₂₅N₃O₄S, M + H); ¹H NMR (500 MHz, DMSO) 10.64 (s, 1H), 7.93 (d, *J* = 8.70 Hz, 2H), 7.68 (d, *J* = 8.70 Hz, 2H), 7.01–7.22 (m, 5H), 6.42–6.53 (m, 1H), 6.26–6.38 (m, 1H), 5.85 (d, *J* = 11.29 Hz, 1H), 3.45–3.61 (m, 4H), 2.66–2.87 (m, 6H), 2.56 (t, *J* = 7.71 Hz, 2H); ¹³C NMR (126 MHz, DMSO-*d*₆) δ 170.17, 163.93, 143.57, 141.30, 131.52, 129.06, 128.71, 128.55, 128.41, 128.30, 125.99, 119.39, 46.08, 45.98, 44.33, 33.78, 30.87.

N-[4-[4-(2-Phenylcyclopropanecarbonyl)piperazine-1-sulfonyl]phenyl]acrylamide (18b). MS (ES⁺) *m/z* (M + 23) 440; δ_H (500 MHz, DMSO-*d*₆) 10.58 (1H, s), 7.91 (d, *J* = 8.67 Hz, 2H), 7.64–7.76 (2H, m), 7.04–7.31 (5H, m), 6.40–6.52 (1H, m), 6.24–6.35 (1H, m), 5.83 (dd, *J* = 10.09, 1.73 Hz, 1H), 3.46–3.84 (4H, m), 2.73–3.02 (4H, m), 2.24 (t, *J* = 6.70 Hz, 2H), 1.28–1.36 (1H, m), 1.15 (td, *J* = 7.21, 3.86 Hz, 1H).

N-[4-(4-Cyclopropanecarbonylpiperazine-1-sulfonyl)phenyl]acrylamide (18c). MS (ES⁺) *m/z* (M + 23) 364; HRMS (ES⁺) *m/z* 364.1336 (364.1331 calcd for C₁₇H₂₁N₃O₄S, M + H); ¹H NMR (500 MHz, DMSO) 10.60 (s, 1H), 7.92 (d, *J* = 8.83 Hz, 2H), 7.71 (d, *J* = 8.83 Hz, 2H), 6.42–6.52 (m, 1H), 6.21–6.36 (m, 1H), 5.84 (dd, *J* = 10.17, 1.81 Hz, 1H), 3.47–3.85 (m, 4H), 2.72–3.02 (m, 4H), 1.81–1.96 (m, 1H), 0.59–0.71 (m, 4H); ¹³C NMR (126 MHz, DMSO-*d*₆) δ 171.1, 163.7, 143.4, 131.4, 128.9, 128.6, 128.2, 119.2, 46.3 (br), 45.8 (br), 44.1 (br), 40.7 (br), 10.2, 7.1.

N-[4-[4-(Pyrrolidine-1-carbonyl)piperazine-1-sulfonyl]phenyl]acrylamide (17e). MS (ES⁺) *m/z* (M + 1) 393; δ_H (500 MHz, DMSO-*d*₆) 10.58 (1H, s), 7.92 (d, *J* = 8.83 Hz, 2H), 7.70 (d, *J* = 8.83 Hz, 2H), 6.40–6.52 (1H, m), 6.23–6.37 (1H, m), 5.83 (dd, *J* = 10.09, 1.73 Hz, 1H), 3.11–3.27 (8H, m), 2.79–2.96 (4H, m), 1.60–1.75 (4H, m).

N-[4-(4-Adamantane-1-carbonyl)piperazine-1-sulfonyl]phenyl]acrylamide (18d). MS (ES⁺) *m/z* (M + 1) 458; HRMS (ES⁺) *m/z* 458.2121 (458.2114 calcd for C₂₄H₃₁N₃O₄S, M + H); ¹H NMR (500 MHz, DMSO) 10.57 (s, 1H), 7.89 (d, *J* = 8.67 Hz, 2H), 7.67 (d, *J* = 8.83 Hz, 2H), 6.38–6.48 (m, 1H), 6.21–6.34 (m, 1H), 5.81 (dd, *J* = 10.09, 1.73 Hz, 1H), 3.63 (br s, 4H), 2.81 (t, *J* = 4.33 Hz, 4H), 1.47–1.95 (m, 14H); ¹³C NMR (126 MHz, DMSO-*d*₆) δ 174.6, 163.8, 143.4, 131.4, 128.9, 128.5, 128.2, 119.2, 46.2, 43.9 (br), 40.9, 38.3, 35.9, 27.8.

4-[4-(1-Oxobut-2-nylamino)benzenesulfonyl]piperazine-1-carboxylic Acid *tert*-Butyl Ester (28r). But-2-ynoic acid (0.19 g, 2.36 mmol) followed by pyridine (0.6 mL) was added sequentially portionwise to a stirred solution of 4-(4-aminobenzenesulfonyl)piperazine-1-carboxylic acid *tert*-butyl ester (0.2 g, 0.59 mmol) in THF/DMA (3:2, 5 mL) at room temperature. To this mixture was added EDC (0.6 g, 3.1 mmol) in one portion, and the mixture was stirred at room temperature under a nitrogen atmosphere for 1 h. After this time the mixture was diluted with ethyl acetate (50 mL) and washed with water (100 mL), saturated NaHCO₃ (100 mL), and HCl (100 mL, 2M). The organic layer was separated, dried (MgSO₄), filtered, and concentrated under vacuum and the resulting residue was purified using flash column chromatography (elution, 20% ethyl acetate, 80% DCM) to give the title compound (0.05 g, 19% yield) as a white solid. MS (ES⁺) *m/z* (M + 23) 430; δ_H (250 MHz, DMSO-*d*₆) 11.07 (1H, s), 7.76–7.89 (2H, m), 7.66 (d, *J* = 8.68 Hz, 2H), 2.79 (t, *J* = 4.64 Hz, 4H), 1.94–2.16 (3H, m), 1.32 (9H, s).

4-(4-But-2-enoylamino)benzenesulfonyl]piperazine-1-carboxylic Acid *tert*-Butyl Ester (28e). Lindlar's catalyst (0.005 g, 0.001 mmol) was added in one portion to a stirred solution of 4-[4-(1-oxobut-2-nylamino)benzenesulfonyl]piperazine-1-carboxylic acid *tert*-butyl ester (0.05 g, 0.11 mmol) in methanol (5 mL) at room temperature. The resulting mixture was then stirred at room temperature under a hydrogen atmosphere for 2 h. After this time, the reaction mixture was filtered through Celite and concentrated under vacuum to give the title compound (0.02 g, 40% yield) as a white solid. MS (ES⁺) *m/z* (M + 23) 432; HRMS (ES⁺) *m/z* 310.1232 (310.1225 calcd for C₁₉H₂₇N₃O₅S, M + H, loss of *tert*-butyl); ¹H NMR (500 MHz, DMSO) 10.44 (s, 1H), 7.89 (d, *J* = 8.62 Hz, 2H), 7.67 (d, *J* = 8.62 Hz, 2H), 6.31 (dq, *J* = 11.42, 7.26 Hz, 1H), 6.04 (dd, *J* = 11.37, 1.65 Hz, 1H), 3.39 (br s, 3H), 2.82 (t, *J* = 4.68 Hz, 4H), 2.13 (dd, *J* = 7.15, 1.47 Hz, 3H),

1.34 (s, 10H); ¹³C NMR (126 MHz, DMSO-*d*₆) δ 165.0, 153.4, 143.7, 142.6, 128.8, 128.1, 123.3, 118.8, 79.3, 45.8, 27.9, 15.0.

4-Nitro-2-trifluoromethylbenzenesulfonyl Chloride. Sodium nitrite (1.8 g, 26 mmol) was added portionwise to a stirred solution of 4-nitro-2-trifluoromethylphenylamine (5.0 g, 24 mmol) in acetic acid (37 mL) and HCl (concentrated, 7.5 mL) while maintaining the temperature below 15 °C. This solution was then added dropwise to a stirred solution of saturated sulfur dioxide, copper(II) chloride (0.6 g, 4.5 mmol), and water (7.5 mL) in acetic acid (24 mL) at 5 °C. The reaction mixture was allowed to warm to room temperature and poured over ice–water and stirred for a further 15 min. The resulting precipitate was collected by filtration, washed with water, and dried overnight in a vacuum oven to give the title compound (3.5 g, 71% yield) as a yellow solid which was used without further purification.

4-(4-Nitro-2-trifluoromethylbenzenesulfonyl)piperazine-1-carboxylic Acid Benzyl Ester. Diisopropylethylamine (1.2 mL, 7.0 mmol) was added in one portion to a stirred solution of piperazine-1-carboxylic acid benzyl ester (0.76 g, 3.5 mmol) in DCM (15 mL) at room temperature. To this mixture was added 4-nitro-2-trifluoromethylbenzenesulfonyl chloride (1.0 g, 3.5 mmol) in one portion, and the mixture was stirred at room temperature under a nitrogen atmosphere for 1 h. After this time, the mixture was diluted with DCM (20 mL) and washed with HCl (1 M, 20 mL) and NaOH (1 M, 20 mL). The organic layer was separated, dried (MgSO₄), filtered, and concentrated under vacuum to give the title compound (1.43 g, 87% yield) as a purple solid. MS (ES⁺) *m/z* (M + 23) 496; δ_H (500 MHz, DMSO-*d*₆) 8.65–8.60 (2H, m), 8.31–8.33 (1H, m), 7.38–7.29 (5H, m), 5.07 (2H, m), 3.56–3.46 (4H, m), 3.30–3.25 (4H, m).

4-(4-Amino-2-trifluoromethylbenzenesulfonyl)piperazine-1-carboxylic Acid Benzyl Ester. 4-(4-Nitro-2-trifluoromethylbenzenesulfonyl)piperazine-1-carboxylic acid benzyl ester (0.5 g, 1.0 mmol) was suspended in a 5:1 mixture of ethanol and water (20 mL). To this solution was added iron powder (0.16 g, 2.6 mmol) followed by saturated ammonium chloride solution (1 mL), and the mixture was heated to 80 °C for 3 h. After this time, the reaction mixture was cooled to room temperature and filtered through a pad of Celite, the Celite was washed with ethanol (10 mL) and ethyl acetate (50 mL), and the solution was concentrated under vacuum. The resulting residue was partitioned between DCM (50 mL) and water (20 mL). The organic layer was separated, dried with MgSO₄, filtered, and concentrated to afford the title compound (0.44 g, 94% yield) as a yellow solid. MS (ES⁺) *m/z* (M + 1) 444.

4-(4-Acryloylamino-2-trifluoromethylbenzenesulfonyl)piperazine-1-carboxylic Acid Benzyl Ester (29e). 4-(4-Amino-2-trifluoromethylbenzenesulfonyl)piperazine-1-carboxylic acid benzyl ester (0.44 g, 0.11 mmol) was dissolved in THF (15 mL). To this solution was added diisopropylethylamine (0.52 mL, 0.33 mmol) in one portion followed by the dropwise addition of acryloyl chloride (0.09 mL, 0.11 mmol), and the mixture was stirred at room temperature under a nitrogen atmosphere for 3 h. The THF was removed under vacuum and the resulting crude material was purified using preparative HPLC to give the title compound (70 mg, 14% yield) as a white solid. MS (ES⁺) *m/z* (M + 23) 520; δ_H (250 MHz, DMSO-*d*₆) 10.31 (1H, s), 7.57–7.78 (4H, m), 7.27–7.50 (5H, m), 6.69 (dd, *J* = 16.75, 10.36 Hz, 1H), 6.03 (dd, *J* = 16.75, 2.28 Hz, 1H), 5.63 (dd, *J* = 10.51, 2.28 Hz, 1H), 5.17 (2H, s), 3.59 (4H, br s), 2.84 (t, *J* = 4.72 Hz, 4H).

4-(4-Acryloylamino-3-fluorobenzenesulfonyl)piperazine-1-carboxylic Acid Benzyl Ester (29b). MS (ES⁺) *m/z* (M + 1) 448; HRMS (ES⁺) *m/z* 448.1349 (448.1342 calcd for C₂₁H₂₂FN₃O₅S, M + H); ¹H NMR (250 MHz, DMSO) 9.63 (s, 1H), 7.87–8.04 (m, 1H), 7.54–7.68 (m, 2H), 7.24–7.42 (m, 5H), 6.42–6.60 (m, 1H), 6.15–6.31 (m, 1H), 5.73–5.88 (m, 1H), 5.02 (s, 2H), 3.41 (br s, 4H), 2.97 (t, *J* = 4.95 Hz, 4H); ¹³C NMR (126 MHz, DMSO-*d*₆) δ 163.8, 158.3 (d, *J* = 248 Hz), 154.1, 136.5, 132.1 (d, *J* = 3 Hz), 131.4, 129.6 (d, *J* = 8 Hz), 129.4 (d, *J* = 6 Hz), 128.4, 128.0, 127.9, 127.6, 121.3 (d, *J* = 23 Hz), 116.4 (d, *J* = 27 Hz), 66.5, 45.1, 42.9 (br).

4-(4-Acryloylamino-2-methoxybenzenesulfonyl)piperazine-1-carboxylic Acid *tert*-Butyl Ester (29c). MS (ES⁺) *m/z* (M + 23) 448; HRMS (ES⁺) *m/z* 326.1170 (326.1175 calcd for C₁₉H₂₇N₃O₆S,

M + H, loss of *tert*-butyl); ^1H NMR (500 MHz, DMSO) 10.54 (s, 1H), 7.62–7.72 (m, 2H), 7.28–7.38 (m, 1H), 6.39–6.53 (m, 1H), 6.27–6.35 (m, 1H), 5.79–5.86 (m, 1H), 3.86 (s, 3H), 3.38–3.44 (m, 4H), 2.95–3.13 (m, 4H), 1.37 (s, 9H); ^{13}C NMR (126 MHz, DMSO- d_6) δ 163.8, 157.4, 153.6, 145.0, 131.9, 131.4, 128.2, 119.3, 110.4, 103.0, 79.3, 55.8, 45.5, 28.0.

4-(4-Acryloylamino-2-methylbenzenesulfonyl)piperazine-1-carboxylic Acid *tert*-Butyl Ester (29d). MS (ES^+) m/z ($M + 23$) 432; δ_{H} (500 MHz, DMSO- d_6) 10.49 (1H, s), 7.61–7.82 (3H, m), 6.41–6.51 (1H, m), 6.25–6.36 (1H, m), 5.83 (dd, $J = 10.09$, 1.65 Hz, 1H), 3.38 (4H, br s), 2.93–3.02 (4H, m), 2.54 (3H, s), 1.37 (9H, s).

4-(4-Acryloylamino-2-fluorobenzenesulfonyl)piperazine-1-carboxylic Acid *tert*-Butyl Ester (29f). MS (ES^+) m/z ($M + 23$) 436; HRMS (ES^+) m/z 310.1228 (310.1225 calcd for $\text{C}_{19}\text{H}_{27}\text{N}_3\text{O}_5\text{S}$, $M + \text{H}$, loss of *tert*-butyl); ^1H NMR (250 MHz, DMSO) 7.80 (dd, $J = 12.94$, 1.98 Hz, 1H), 7.66 (t, $J = 8.38$ Hz, 1H), 7.38 (dd, $J = 8.76$, 1.90 Hz, 1H), 6.21–6.40 (m, 2H), 5.74 (dd, $J = 6.24$, 5.63 Hz, 1H), 3.31–3.48 (m, 5H), 3.01 (t, $J = 4.72$ Hz, 4H), 1.24–1.37 (m, 9H); ^{13}C NMR (126 MHz, DMSO- d_6) δ 163.7, 153.5, 143.1, 138.6, 131.4, 131.3, 128.8, 128.1, 122.4, 116.4, 79.3, 45.0, 28.0, 20.7.

4-(4-Acryloylamino-2-chlorobenzenesulfonyl)piperazine-1-carboxylic Acid *tert*-Butyl Ester (29g). MS (ES^+) m/z ($M + 1$) 423; δ_{H} (250 MHz, DMSO- d_6) 10.68 (1H, s), 8.07 (d, $J = 2.13$ Hz, 1H), 7.90 (d, $J = 8.83$ Hz, 1H), 7.70 (dd, $J = 8.76$, 2.06 Hz, 1H), 6.24–6.53 (2H, m), 5.74–5.96 (1H, m), 3.33–3.42 (4H, m), 3.02–3.18 (4H, m), 1.36 (9H, s).

4-(4-Acryloylamino-2-chlorobenzenesulfonyl)piperazine-1-carboxylic Acid 2,3-Difluorobenzyl Ester (16o). Phosgene (0.5 mL, 20% solution in toluene) was added in one portion to a stirred solution of 2,3-difluorobenzyl alcohol (0.2 g, 1.36 mmol) in THF (2 mL), and the resulting mixture was stirred at room temperature under a nitrogen atmosphere for 3 h. After this time the reaction mixture was concentrated under vacuum and the resulting residue was diluted with DMF (2 mL) and added dropwise to a stirred solution of *N*-[4-(piperazine-1-sulfonyl)phenyl]acrylamide (15, 0.2 g, 0.68 mmol) and diisopropylethylamine (0.35 mL, 2.04 mmol) in DMF (4 mL). The resulting mixture was stirred at room temperature under a nitrogen atmosphere for 18 h. After this time the reaction mixture was concentrated under vacuum and the residue was purified using preparative HPLC to give the title compound (0.029 g, 12% yield) as a white powder. MS (ES^+) m/z ($M + 1$) 466; δ_{H} (500 MHz, DMSO- d_6) 10.58 (1H, s), 7.92 (d, $J = 8.35$ Hz, 2H), 7.70 (d, $J = 8.20$ Hz, 2H), 7.35–7.45 (1H, m), 7.14–7.27 (2H, m), 6.43–6.53 (1H, m), 6.30–6.40 (1H, m), 5.85 (d, $J = 10.09$ Hz, 1H), 5.11 (2H, s), 3.47 (4H, br s), 2.87 (4H, br s).

4-(4-Acryloylamino-2-chlorobenzenesulfonyl)piperazine-1-carboxylic Acid 4-Fluorobenzyl Ester (16p). MS (ES^+) m/z ($M + 1$) 448; δ_{H} (500 MHz, DMSO- d_6) 10.61 (1H, br s), 7.93 (d, $J = 8.32$ Hz, 2H), 7.69 (d, $J = 8.32$ Hz, 2H), 7.38–7.31 (2H, m), 7.16–7.11 (2H, m), 6.50–6.27 (2H, m), 5.83 (d, $J = 10.12$ Hz, 1H), 4.98 (2H, s), 3.51–3.42 (4H, m), 2.89–2.81 (4H, m).

4-(4-Acryloylamino-2-chlorobenzenesulfonyl)piperazine-1-carboxylic Acid 3,5-Difluorobenzyl Ester (16q). MS (ES^+) m/z ($M + 1$) 466; HRMS (ES^+) m/z 466.1233 (466.1248 calcd for $\text{C}_{21}\text{H}_{21}\text{F}_2\text{N}_3\text{O}_5\text{S}$, $M + \text{H}$); ^1H NMR (500 MHz, DMSO) 10.57 (s, 1H), 7.91 (d, $J = 8.83$ Hz, 2H), 7.70 (d, $J = 8.67$ Hz, 2H), 7.12–7.19 (m, 1H), 7.05 (d, $J = 6.46$ Hz, 2H), 6.41–6.51 (m, 1H), 6.27–6.38 (m, 1H), 5.83 (dd, $J = 10.17$, 1.66 Hz, 1H), 5.03 (s, 2H), 3.49 (br s, 4H), 2.89 (t, $J = 4.81$ Hz, 4H); ^{13}C NMR (126 MHz, DMSO- d_6) δ 163.7, 162.3 (dd, $J = 247$, 14 Hz), 153.8, 143.4, 141.2 (t, $J = 10$ Hz), 131.4, 128.9, 128.6, 128.2, 119.2, 110.4 (dd, $J = 20$, 6 Hz), 103.2 (t, $J = 26$ Hz), 65.1, 45.6, 42.7 (br).

4-(4-Acryloylamino-2-chlorobenzenesulfonyl)piperazine-1-carboxylic Acid 2-Chlorobenzyl Ester (16r). MS (ES^+) m/z ($M + 1$) 464; HRMS (ES^+) m/z 464.1058 (464.1047 calcd for $\text{C}_{21}\text{H}_{22}\text{ClN}_3\text{O}_5\text{S}$, $M + \text{H}$); ^1H NMR (500 MHz, DMSO) 10.60 (br s, 1H), 7.91 (d, $J = 8.67$ Hz, 2H), 7.69 (d, $J = 8.67$ Hz, 2H), 7.27–7.50 (m, 3H), 6.41–6.51 (m, 1H), 6.26–6.37 (m, 1H), 5.80–5.89 (m, 1H), 5.09 (s, 2H), 3.48 (br s, 3H), 2.87 (d, $J = 4.26$ Hz, 3H); ^{13}C NMR (126 MHz, DMSO- d_6) δ 163.7, 153.9, 143.4, 133.9, 132.9, 132.4, 131.3, 129.9, 129.9, 129.3, 128.9, 128.5, 128.2, 127.3, 119.2, 64.0, 45.6, 42.8.

4-(4-Acryloylamino-2-chlorobenzenesulfonyl)piperazine-1-carboxylic Acid 2-Trifluoromethylbenzyl Ester (16s). MS (ES^+) m/z ($M + 1$) 498; HRMS (ES^+) m/z 498.1298 (498.1311 calcd for $\text{C}_{22}\text{H}_{22}\text{F}_3\text{N}_3\text{O}_5\text{S}$, $M + \text{H}$); ^1H NMR (500 MHz, DMSO) 10.60 (br s, 1H), 7.91 (d, $J = 8.83$ Hz, 1H), 7.48–7.79 (m, 4H), 6.40–6.53 (m, 1H), 6.26–6.37 (m, 1H), 5.78–5.92 (m, 1H), 5.18 (s, 2H), 3.48 (br s, 4H), 2.87 (br s, 4H); ^{13}C NMR (126 MHz, DMSO- d_6) δ 162.6, 152.6, 142.3, 133.3, 131.7, 130.2, 128.9, 127.7, 127.5, 127.4, 127.1, 125.4 (q, $J = 30$ Hz), 124.9 (q, $J = 6$ Hz), 123.0 (q, $J = 274$ Hz), 118.0, 62.0, 44.5, 41.6 (br).

***N*-[4-[2-(2-Phenoxyphenyl)acetyl]piperazine-1-sulfonyl]phenylacrylamide (16t).** MS (ES^+) m/z ($M + 1$) 506; HRMS (ES^+) m/z 506.1755 (506.1750 calcd for $\text{C}_{27}\text{H}_{27}\text{N}_3\text{O}_5\text{S}$, $M + \text{H}$); ^1H NMR (500 MHz, DMSO) 10.62 (s, 1H), 7.93 (d, $J = 8.83$ Hz, 2H), 7.66 (d, $J = 8.83$ Hz, 2H), 7.15–7.31 (m, 4H), 6.91–7.08 (m, 2H), 6.72–6.85 (m, 3H), 6.43–6.55 (m, 1H), 6.25–6.39 (m, 1H), 5.77–5.92 (m, 1H), 3.43–3.66 (m, 6H), 2.74 (t, $J = 4.73$ Hz, 3H); ^{13}C NMR (126 MHz, DMSO- d_6) δ 168.4, 163.8, 156.9, 154.2, 143.4, 131.9, 131.4, 129.7, 128.9, 128.5, 128.3, 127.5, 123.6, 122.9, 119.2, 118.8, 117.8, 45.8, 45.7, 44.5, 40.5, 33.6.

4-(4-Acryloylamino-2-chlorobenzenesulfonyl)piperazine-1-carboxylic Acid 2-Methylbenzyl Ester (16u). MS (ES^+) m/z ($M + 1$) 444; HRMS (ES^+) m/z 444.1597 (444.1593 calcd for $\text{C}_{22}\text{H}_{25}\text{N}_3\text{O}_5\text{S}$, $M + \text{H}$); ^1H NMR (500 MHz, DMSO) 10.58 (s, 1H), 7.91 (d, $J = 8.67$ Hz, 2H), 7.68 (d, $J = 8.83$ Hz, 2H), 7.00–7.29 (m, 4H), 6.40–6.50 (m, 1H), 6.26–6.37 (m, 1H), 5.83 (dd, $J = 10.17$, 1.66 Hz, 1H), 5.02 (s, 2H), 3.46 (br s, 4H), 2.80–2.95 (m, 4H), 2.22 (s, 3H); ^{13}C NMR (126 MHz, DMSO- d_6) δ 163.8, 154.1, 143.4, 136.4, 134.4, 131.4, 130.1, 128.9, 128.6, 128.6, 128.2, 128.1, 125.8, 119.2, 65.1, 45.7, 42.7, 18.4.

4-(4-Acryloylamino-2-chlorobenzenesulfonyl)piperazine-1-carboxylic Acid Naphthalen-1-ylmethyl Ester (16v). MS (ES^+) m/z ($M + 23$) 502; δ_{H} (500 MHz, DMSO- d_6) 10.61 (1H, br s), 7.80–7.99 (5H, m), 7.67 (d, $J = 8.67$ Hz, 2H), 7.29–7.59 (4H, m), 6.42–6.53 (1H, m), 6.27–6.39 (1H, m), 5.85 (dd, $J = 10.09$, 1.73 Hz, 1H), 5.48 (2H, s), 3.45 (4H, br s), 2.69–2.96 (4H, m).

4-(4-Acryloylamino-2-chlorobenzenesulfonyl)piperazine-1-carboxylic Acid Naphthalen-2-ylmethyl Ester (16w). MS (ES^+) m/z ($M + 23$) 502; HRMS (ES^+) m/z 480.1577 (480.1593 calcd for $\text{C}_{25}\text{H}_{25}\text{N}_3\text{O}_5\text{S}$, $M + \text{H}$); ^1H NMR (500 MHz, DMSO) 10.61 (br s, 1H), 7.64–7.97 (m, 11H), 7.38–7.59 (m, 4H), 6.26–6.53 (m, 2H), 5.80–5.91 (m, 1H), 5.19 (s, 2H), 3.51 (br s, 4H), 2.89 (t, $J = 4.89$ Hz, 4H); ^{13}C NMR (126 MHz, DMSO- d_6) δ 163.8, 154.2, 143.4, 134.2, 132.7, 132.5, 131.4, 128.9, 128.6, 128.2, 128.1, 127.8, 127.6, 126.4, 126.3, 126.2, 125.6, 119.7, 66.6, 45.7, 42.8.

***N*-[4-[2-(3-Phenoxyphenyl)acetyl]piperazine-1-sulfonyl]phenylacrylamide (16x).** MS (ES^+) m/z ($M + 1$) 506; δ_{H} (500 MHz, DMSO- d_6) 10.59 (1H, s), 7.91 (d, $J = 8.67$ Hz, 2H), 7.67 (d, $J = 8.83$ Hz, 2H), 7.35 (t, $J = 7.88$ Hz, 2H), 7.22 (t, $J = 7.88$ Hz, 1H), 7.11 (t, $J = 7.33$ Hz, 1H), 6.75–7.01 (5H, m), 6.26–6.51 (2H, m), 5.83 (dd, $J = 10.09$, 1.73 Hz, 1H), 3.65 (2H, s), 3.53 (d, $J = 3.78$ Hz, 4H), 2.72–2.90 (4H, m).

***N*-[4-[2-(4-Phenoxyphenyl)acetyl]piperazine-1-sulfonyl]phenylacrylamide (16y).** MS (ES^+) m/z ($M + 1$) 506; δ_{H} (500 MHz, DMSO- d_6) 10.59 (1H, s), 7.91 (d, $J = 8.67$ Hz, 2H), 7.69 (d, $J = 8.83$ Hz, 2H), 7.36 (t, $J = 7.88$ Hz, 2H), 7.06–7.20 (3H, m), 6.79–7.00 (4H, m), 6.40–6.50 (1H, m), 6.25–6.37 (1H, m), 5.83 (dd, $J = 10.17$, 1.81 Hz, 1H), 3.50–3.68 (6H, m), 2.75–2.88 (4H, m).

***N*-[4-[4-(Octahydroisoquinoline-2-carbonyl)piperazine-1-sulfonyl]phenyl]acrylamide (17a).** MS (ES^+) m/z ($M + 1$) 461; δ_{H} (500 MHz, DMSO- d_6) 10.59 (1H, s), 7.92 (d, $J = 8.83$ Hz, 2H), 7.70 (d, $J = 8.83$ Hz, 2H), 6.39–6.53 (1H, m), 6.25–6.36 (1H, m), 5.71–5.89 (1H, m), 3.06–3.28 (5H, m), 2.72–2.95 (6H, m), 1.05–1.80 (12H, m).

***N*-[4-[4-(Octahydroquinoline-1-carbonyl)piperazine-1-sulfonyl]phenyl]acrylamide (17b).** MS (ES^+) m/z ($M + 1$) 461; HRMS (ES^+) m/z 461.2210 (461.2223 calcd for $\text{C}_{23}\text{H}_{32}\text{N}_4\text{O}_4\text{S}$, $M + \text{H}$); ^1H NMR (500 MHz, DMSO) 10.59 (s, 1H), 7.92 (d, $J = 8.67$ Hz, 2H), 7.70 (d, $J = 8.67$ Hz, 2H), 6.41–6.52 (m, 1H), 6.25–6.37 (m, 1H), 5.83 (dd, $J = 10.17$, 1.66 Hz, 1H), 3.59 (d, $J = 12.14$ Hz, 1H), 3.04–3.28 (m, 5H), 2.74–2.93 (m, 5H), 1.06–1.81 (m, 13H); ^{13}C

NMR (126 MHz, DMSO-*d*₆) δ 163.7, 162.7, 143.4, 131.4, 128.9, 128.7, 128.2, 119.2, 54.7, 46.1, 45.6, 41.3, 34.6, 31.0, 25.5, 25.4, 23.6, 23.3, 19.9.

N-{4-[4-(Piperidine-1-carbonyl)piperazine-1-sulfonyl]phenyl}acrylamide (17c). MS (ES⁺) *m/z* (M + 1) 407; HRMS (ES⁺) *m/z* 407.1746 (407.1753 calcd for C₁₉H₂₆N₄O₄S, M + H); ¹H NMR (500 MHz, DMSO) 10.58 (s, 1H), 7.92 (d, *J* = 8.83 Hz, 2H), 7.70 (d, *J* = 8.67 Hz, 2H), 6.44–6.52 (m, 1H), 6.27–6.37 (m, 1H), 5.78–5.88 (m, 1H), 3.16 (t, *J* = 4.81 Hz, 4H), 2.98–3.08 (m, 4H), 2.86 (d, *J* = 4.26 Hz, 4H), 1.33–1.56 (m, 6H); ¹³C NMR (126 MHz, DMSO-*d*₆) δ 163.7, 162.8, 143.4, 131.4, 128.9, 128.6, 128.2, 119.2, 47.0, 45.8, 45.6, 25.2, 24.1.

N-{4-[4-(4,4-Difluoropiperidine-1-carbonyl)piperazine-1-sulfonyl]phenyl}acrylamide (17d). MS (ES⁺) *m/z* (M + 1) 443; HRMS (ES⁺) *m/z* 443.1564 (443.1565 calcd for C₁₉H₂₄F₂N₄O₄S, M + H); ¹H NMR (500 MHz, DMSO) 10.66 (s, 1H), 7.98 (d, *J* = 8.80 Hz, 2H), 7.77 (d, *J* = 8.80 Hz, 2H), 6.47–6.56 (m, 1H), 6.34–6.44 (m, 1H), 5.90 (dd, *J* = 10.18, 1.74 Hz, 1H), 3.21–3.33 (m, 8H), 2.93 (d, *J* = 4.40 Hz, 4H), 1.89–2.03 (m, 4H).

6-Aminopyridine-3-sulfonyl Chloride. 2-Aminopyridine (3.0 g, 32.0 mmol) was added portionwise to neat chlorosulfonic acid (18.0 mL, 270.0 mmol) at 0 °C. Upon complete addition the mixture was heated to reflux for 2 h, after which time the hot mixture was poured onto ice (600 mL) and the solution carefully neutralized by the portionwise addition of solid NaHCO₃. The resulting mixture was extracted with ethyl acetate (3 × 200 mL), and the organic layer was separated, dried (MgSO₄), filtered, and concentrated under vacuum. The resulting solid was recrystallized from heptane/diethyl ether to afford the title compound (2.23 g, 36% yield) as a white solid. δ_{H} (250 MHz, CDCl₃) 8.63 (1H, s), 7.91–7.85 (1H, m), 6.50–6.47 (1H, m), 5.24 (2H, br s).

4-(6-Aminopyridine-3-sulfonyl)piperazine-1-carboxylic Acid *tert*-Butyl Ester. Diisopropylethylamine (0.4 mL, 2.4 mmol) was added in one portion to a stirred solution of piperazine-1-carboxylic acid *tert*-butyl ester (0.41 g, 2.2 mmol) in THF (10 mL) at room temperature. To this mixture was added 6-aminopyridine-3-sulfonyl chloride (0.5 g, 2.4 mmol) in one portion, and the mixture was stirred at room temperature under a nitrogen atmosphere for 1 h. After this time, the resulting solid was collected by filtration, washed with ether, and dried under vacuum to afford the title compound (0.49 g, 86% yield) as a white solid. MS (ES⁺) *m/z* (M + 1) 261.

4-(6-Acryloylaminopyridine-3-sulfonyl)piperazine-1-carboxylic Acid *tert*-Butyl Ester (24a). 4-(6-Aminopyridine-3-sulfonyl)piperazine-1-carboxylic acid *tert*-butyl ester (0.67 g, 0.51 mmol) was dissolved in DCM (5 mL). To this solution was added diisopropylethylamine (0.17 mL, 1.0 mmol) in one portion, and the resulting mixture was cooled to –78 °C, followed by the dropwise addition of acryloyl chloride (0.05 mL, 0.61 mmol), and the mixture was stirred at room temperature under a nitrogen atmosphere for 3 h. The reaction mixture was then diluted with DCM (20 mL), and the organic layer was washed sequentially with water (20 mL) and brine (20 mL) before being dried (MgSO₄), filtered, and concentrated under vacuum. The resulting residue was purified using flash column chromatography (elution: 20% heptane, 80% ethyl acetate) to give the title compound (0.1 g, 45% yield) as a white solid. MS (ES⁺) *m/z* (M + 1) 397; HRMS (ES⁺) *m/z* 397.1541 (397.1546 calcd for C₁₇H₂₄N₄O₅S, M + H); ¹H NMR (500 MHz, DMSO) 11.28 (s, 1H), 8.65 (d, *J* = 2.21 Hz, 1H), 8.41 (d, *J* = 8.83 Hz, 1H), 8.15 (dd, *J* = 8.91, 2.44 Hz, 1H), 6.65 (dd, *J* = 17.02, 10.09 Hz, 1H), 6.38 (dd, *J* = 16.95, 1.66 Hz, 1H), 5.78–5.94 (m, 1H), 3.41 (br s, 4H), 2.92 (t, *J* = 4.89 Hz, 4H), 1.35 (s, 9H); ¹³C NMR (126 MHz, DMSO-*d*₆) δ 164.3, 155.3, 153.4, 147.5, 138.3, 131.0, 129.2, 126.3, 113.3, 79.3, 45.6, 27.9.

4-(6-Acryloylaminopyridine-3-sulfonyl)piperazine-1-carboxylic Acid Benzyl Ester (24b). MS (ES⁺) *m/z* (M + 1) 431; δ_{H} (500 MHz, CDCl₃) 8.56 (d, *J* = 2.02 Hz, 1H), 8.41 (d, *J* = 8.80 Hz, 1H), 8.12 (1H, s), 7.95 (dd, *J* = 8.80, 2.38 Hz, 1H), 7.20–7.31 (5H, m), 6.39–6.52 (1H, m), 6.12–6.31 (1H, m), 5.79–5.90 (1H, m), 4.95–5.07 (2H, m), 3.55 (t, *J* = 4.86 Hz, 4H), 2.96 (4H, br s).

N-[5-(4-Cyclopropanecarbonyl)piperazine-1-sulfonyl]pyridin-2-yl]acrylamide (24c). MS (ES⁺) *m/z* (M + 1) 365; HRMS (ES⁺) *m/z* 365.1284 (365.1284 calcd for C₁₆H₂₀N₄O₄S, M + H); ¹H

NMR (500 MHz, MeOD) 8.68 (d, *J* = 2.52 Hz, 1H), 8.46 (d, *J* = 8.83 Hz, 1H), 8.13 (dd, *J* = 8.83, 2.52 Hz, 1H), 6.31–6.65 (m, 2H), 5.86 (dd, *J* = 9.77, 2.05 Hz, 1H), 3.86 (br s, 2H), 3.63–3.75 (m, 2H), 2.99–3.19 (m, 4H), 1.82–1.97 (m, 1H), 0.66–0.88 (m, 4H); ¹³C NMR (126 MHz, DMSO-*d*₆) δ 171.1, 164.3, 155.3, 147.5, 138.3, 131.0, 129.2, 126.3, 113.3, 46.0, 45.6, 44.1, 40.7, 10.3, 7.1.

N-[5-(4-(Adamantane-1-carbonyl)piperazine-1-sulfonyl]pyridin-2-yl]acrylamide (24d). MS (ES⁺) *m/z* (M + 1) 459; δ_{H} (500 MHz, DMSO-*d*₆) 11.28 (1H, s), 8.64 (d, *J* = 2.21 Hz, 1H), 8.41 (d, *J* = 8.98 Hz, 1H), 8.14 (dd, *J* = 8.91, 2.44 Hz, 1H), 6.64 (dd, *J* = 17.02, 10.25 Hz, 1H), 6.37 (dd, *J* = 17.02, 1.42 Hz, 1H), 5.86 (dd, *J* = 10.17, 1.50 Hz, 1H), 3.68 (4H, br s), 2.92 (d, *J* = 4.26 Hz, 4H), 1.92 (3H, br s), 1.80 (6H, br s), 1.56–1.70 (6H, m).

2-Aminopyrimidine-5-sulfonyl Chloride. 2-Aminopyrimidine (3.0 g, 32.0 mmol) was added portionwise to neat chlorosulfonic acid (18.0 mL, 270.0 mmol) at 0 °C. Upon complete addition, thionyl chloride (10.0 mL, 137.0 mmol) was added and the mixture was heated to 150 °C for 92 h. After this time the hot mixture was poured dropwise onto ice (600 mL) and the resulting mixture was extracted with ethyl acetate (3 × 200 mL). The organic layer was separated, dried (MgSO₄), filtered, and concentrated under vacuum. The resulting solid was recrystallized from heptane/diethyl ether to afford the title compound (1.5 g, 25% yield) as a white solid. δ_{H} (500 MHz, CDCl₃) 8.72 (2H, s), 5.79 (2H, br s).

4-(2-Aminopyrimidine-5-sulfonyl)piperazine-1-carboxylic Acid *tert*-Butyl Ester. Diisopropylethylamine (0.9 mL, 5.4 mmol) was added in one portion to a stirred solution of piperazine-1-carboxylic acid *tert*-butyl ester (0.45 g, 2.4 mmol) in DCM (10 mL) at room temperature. To this mixture was added 2-aminopyrimidine-5-sulfonyl chloride (0.4 g, 2.4 mmol) in one portion, and the mixture was stirred at room temperature under a nitrogen atmosphere for 1 h. After this time, the resulting solid was collected by filtration, washed with ether, and dried under vacuum to afford the title compound (0.44 g, 56% yield) as a white solid. *m/z* (ES⁺) (M + 1) 357.

4-(2-Acryloylaminopyrimidine-5-sulfonyl)piperazine-1-carboxylic Acid *tert*-Butyl Ester (25a). Sodium hydride (0.058 g, 1.46 mmol) was added in one portion to a stirred solution of 4-(2-aminopyrimidine-5-sulfonyl)piperazine-1-carboxylic acid *tert*-butyl ester (0.250 g, 0.73 mmol) in THF (5 mL), and the mixture stirred for 5 min. After this time, acryloyl chloride (0.145 g, 1.60 mmol) was added dropwise and the reaction mixture was stirred at room temperature overnight before being diluted with ethyl acetate (50 mL) and washed sequentially with water (20 mL) and brine (20 mL) before being dried (MgSO₄), filtered, and concentrated under vacuum. The resulting residue was purified using preparative HPLC to give the title compound (0.002 g, 1% yield) as an off white solid. MS (ES⁺) *m/z* (M + 23) 420; δ_{H} (500 MHz, DMSO-*d*₆) 11.41 (1H, br s), 8.85–9.01 (2H, m), 6.71 (dd, *J* = 17.10, 10.17 Hz, 1H), 6.36 (dd, *J* = 17.02, 1.58 Hz, 1H), 5.78–5.92 (1H, m), 3.42–3.50 (4H, m), 3.01 (t, *J* = 4.81 Hz, 4H), 1.36 (9H, s).

4-(2-Acryloylaminopyrimidine-5-sulfonyl)piperazine-1-carboxylic Acid Benzyl Ester (25b). MS (ES⁺) *m/z* (M + 1) 432; δ_{H} (500 MHz, MeOD) 8.72–8.86 (2H, m), 7.11–7.27 (5H, m), 6.47–6.58 (1H, m), 6.37–6.46 (1H, m), 5.73–5.87 (1H, m), 4.98 (2H, s), 3.51 (4H, br s), 2.99 (4H, br s).

N-[5-(4-(Adamantane-1-carbonyl)piperazine-1-sulfonyl]pyrimidin-2-yl]acrylamide (25c). MS (ES⁺) *m/z* (M + 1) 460; δ_{H} (500 MHz, CDCl₃) 8.81 (2H, s), 8.21 (1H, s), 6.73 (dd, *J* = 16.96, 10.36 Hz, 1H), 6.43–6.59 (1H, m), 5.89 (d, *J* = 11.19 Hz, 1H), 3.74 (t, *J* = 4.58 Hz, 4H), 2.90–3.09 (4H, m), 1.91–2.00 (4H, m), 1.84 (d, *J* = 2.02 Hz, 7H), 1.54–1.75 (7H, m).

4-(4-Carboxybenzenesulfonyl)piperazine-1-carboxylic Acid *tert*-Butyl Ester. Diisopropylethylamine (2.0 mL, 10.8 mmol) was added in one portion to a stirred solution of piperazine-1-carboxylic acid *tert*-butyl ester (1.0 g, 5.38 mmol) in THF (20 mL) at room temperature. To this mixture was added 4-(chlorosulfonyl)benzoic acid (1.18 g, 5.38 mmol) portionwise, and the mixture was stirred at room temperature under a nitrogen atmosphere for 1 h. After this time the mixture was diluted with DCM (100 mL) and washed with water (50 mL) before being dried (MgSO₄), filtered, and concentrated to

give the title compound (1.41 g, 71% yield) as a white solid. MS (ES⁺) *m/z* (M + 23) 393.

4-[4-(Cyanomethylcarbamoyl)benzenesulfonyl]piperazine-1-carboxylic Acid *tert*-Butyl Ester (28n). Diisopropylethylamine (0.36 mL, 2.16 mmol) was added in one portion to a stirred solution of 4-(4-carboxybenzenesulfonyl)piperazine-1-carboxylic acid *tert*-butyl ester (0.2 g, 0.54 mmol), HATU (0.23 g, 0.59 mmol), and acetonitrile (0.061 g, 1.8 mmol) in DMF (5 mL), and the mixture was stirred at room temperature under a nitrogen atmosphere for 18 h. After this time the mixture was concentrated and the resulting residue diluted with DCM (100 mL) and washed with water (50 mL) before being dried (MgSO₄), filtered, and concentrated. The resulting residue was purified using flash column chromatography (elution, 70% ethyl acetate, 30% heptane) to give the title compound (0.1 g, 45% yield) as a white solid. MS (ES⁺) *m/z* (M + 23) 431; δ_H (500 MHz, DMSO-*d*₆) 9.50 (1H, br s), 8.10 (d, *J* = 8.44 Hz, 2H), 7.87 (d, *J* = 8.44 Hz, 2H), 4.36 (2H, s), 3.40 (4H, br s), 2.89 (t, *J* = 4.68 Hz, 4H), 1.34 (9H, s).

4-[4-(Cyanomethylcarbamoyl)benzenesulfonyl]piperazine-1-carboxylic Acid *tert*-Butyl Ester (28b). Oxone (0.12 g, 0.19 mmol) was added portionwise to a stirred solution of *N*-[4-(4-cyclopentanecarbonylpiperazine-1-sulfonyl)phenyl]acrylamide (28a, 0.05 g, 0.13 mmol) and sodium bicarbonate (0.05 g, 0.57 mmol) in a 1:1 mixture of acetone–water (2 mL), and the mixture was stirred at room temperature under a nitrogen atmosphere for 30 min. After this time the mixture was poured onto water (10 mL) and extracted with ethyl acetate (3 × 20 mL). The organic extracts were combined and washed with saturated sodium sulfite (20 mL) and brine (20 mL) before being dried (MgSO₄), filtered, and concentrated. The resulting residue was purified using flash column chromatography (elution, 1% methanol, 99% DCM) to give the title compound (0.1 g, 45% yield) as a white solid. MS (ES⁺) *m/z* (M + 23) 414; δ_H (500 MHz, CDCl₃) 7.94 (1H, s), 7.51–7.72 (4H, m), 3.64 (2H, br s), 3.48–3.57 (3H, m), 3.08 (t, *J* = 5.04 Hz, 1H), 2.86–2.97 (5H, m), 2.71 (quin, *J* = 7.84 Hz, 1H), 1.56–1.74 (7H, m), 1.41–1.53 (8H, m).

4-(4-Carboxymethylbenzenesulfonyl)piperazine-1-carboxylic Acid Benzyl Ester. Diisopropylethylamine (0.93 mL, 5.33 mmol) was added in one portion to a stirred solution of piperazine-1-carboxylic acid benzyl ester (0.47 g, 2.13 mmol) in THF (10 mL) at room temperature. To this mixture was added 4-(chlorosulfonyl)phenylacetic acid (0.5 g, 2.13 mmol) in one portion, and the mixture was stirred at room temperature under a nitrogen atmosphere for 1 h. After this time the solvent was removed under vacuum and the resulting residue was dissolved in DCM (50 mL) and washed with HCl (1M, 50 mL) before being dried (MgSO₄), filtered, and concentrated to give the title compound (0.72 g, 88% yield) as a white foam. MS (ES⁺) *m/z* (M + 1) 419.

4-[4-(2-Hydroxyethyl)benzenesulfonyl]piperazine-1-carboxylic Acid Benzyl Ester. Borane (1 M solution, 3.0 mL, 2.96 mmol) was added dropwise to a cool (0 °C), stirred solution of 4-(4-carboxymethylbenzenesulfonyl)piperazine-1-carboxylic acid benzyl ester (0.62 g, 1.48 mmol) in THF (5 mL), and the mixture was stirred at this temperature under a nitrogen atmosphere for 2 h. After this time the reaction mixture was diluted with ethyl acetate (50 mL) and washed with saturated sodium bicarbonate (50 mL) and water (50 mL) before being dried (MgSO₄), filtered, and concentrated. The resulting residue was purified using flash column chromatography (elution, 20% heptane, 80% ethyl acetate) to give the title compound (0.32 g, 54% yield) as a yellow oil. MS (ES⁺) *m/z* (M + 23) 426.

4-[4-(2-Oxoethyl)benzenesulfonyl]piperazine-1-carboxylic Acid Benzyl Ester. Pyridinium chlorochromate (0.05 g, 0.25 mmol) was added portionwise to a cool (0 °C), stirred solution of 4-[4-(2-hydroxyethyl)benzenesulfonyl]piperazine-1-carboxylic acid benzyl ester (0.1 g, 0.25 mmol) in DCM (5 mL) under a nitrogen atmosphere. The mixture was allowed to warm to room temperature before being stirred at this temperature overnight. After this time the reaction mixture was concentrated and the resulting residue was purified using flash column chromatography (elution, 60% heptane, 40% ethyl acetate) to give the title compound (0.025 g, 25% yield) as a white solid. MS (ES⁺) *m/z* (M + 23) 425.

4-[4-(3-Ethoxycarbonylallyl)benzenesulfonyl]piperazine-1-carboxylic Acid Benzyl Ester (28t). (Triphenyl-λ⁵-phosphanylidene)acetic acid ethyl ester (0.08 g, 0.24 mmol) was added portionwise to a stirred solution of 4-[4-(2-oxoethyl)benzenesulfonyl]piperazine-1-carboxylic acid benzyl ester (0.06 g, 0.16 mmol) in toluene (2 mL), and the mixture was stirred at room temperature under a nitrogen atmosphere for 24 h. After this time the reaction mixture was concentrated and the resulting residue was purified using flash column chromatography (elution, 60% heptane, 40% ethyl acetate) to give the title compound (0.028 g, 36% yield) as a white solid. MS (ES⁺) *m/z* (M + 23) 495; δ_H (500 MHz, DMSO-*d*₆) 7.63–7.75 (4H, m), 6.46–6.71 (2H, m), 5.01 (2H, s), 4.02–4.20 (2H, m), 3.41–3.54 (4H, m), 2.88 (4H, br s), 1.15–1.29 (3H, m).

4-[4-(2-Ethoxycarbonylvinyl)benzenesulfonyl]piperazine-1-carboxylic Acid Benzyl Ester (28s). MS (ES⁺) *m/z* (M + 23) 481; δ_H (500 MHz, DMSO-*d*₆) 8.06 (d, *J* = 8.20 Hz, 2H), 7.76–7.83 (3H, m), 7.27–7.44 (5H, m), 6.87 (1H, s), 5.08 (2H, s), 4.28 (q, *J* = 6.94 Hz, 2H), 3.54 (4H, br s), 2.92–3.03 (4H, m), 1.31–1.35 (2H, m).

4-[4-(3-Diazo-2-oxopropyl)benzenesulfonyl]piperazine-1-carboxylic Acid Benzyl Ester (28v). Thionyl chloride (0.47 mL) was added dropwise to a stirred solution of 4-(4-carboxymethylbenzenesulfonyl)piperazine-1-carboxylic acid benzyl ester (0.2 g, 0.47 mmol) in toluene (3 mL) at room temperature before being heated to reflux for 1 h. After this time, the mixture was cooled to room temperature and concentrated. The resulting residue was dissolved in ether (5 mL) and added portionwise to a 2 M solution of diazomethane in ether (20 mL), and the mixture was stirred at room temperature under a nitrogen atmosphere for 12 h. The resulting solid precipitate was collected by filtration, washed with ether (50 mL), and dried under vacuum to give the title compound (0.055 g, 26% yield) as a white solid. MS (ES⁺) *m/z* (M + 23) 465; HRMS (ES⁺) *m/z* 443.1393 (443.1389 calcd for C₂₁H₂₂N₄O₅S, M + H); ¹H NMR (500 MHz, DMSO) 7.96 (d, *J* = 8.24 Hz, 2H), 7.52 (d, *J* = 8.24 Hz, 2H), 7.33–7.15 (m, 5H), 6.127 (s, 1H), 5.02 (s, 2H), 3.81 (s, 2H), 3.56–3.51 (m, 4H), 2.92–2.85 (m, 4H); ¹³C NMR (126 MHz, DMSO-*d*₆) δ 191.7, 154.1, 141.0, 136.5, 133.1, 130.5, 128.4, 127.9, 127.6, 68.5, 54.9, 46.0, 45.6, 42.6 (br).

4-[4-(4-Diazo-3-oxobutyl)benzenesulfonyl]piperazine-1-carboxylic Acid Benzyl Ester (28u). MS (ES⁺) *m/z* (M + 23) 479; HRMS (ES⁺) *m/z* 457.1534 (457.1546 calcd for C₂₂H₂₄N₄O₅S, M + H); ¹H NMR (500 MHz, DMSO) 7.64 (d, *J* = 8.09 Hz, 2H), 7.50 (d, *J* = 8.09 Hz, 2H), 7.24–7.39 (m, 5H), 6.11 (br s, 1H), 5.02 (s, 2H), 3.47 (br s, 4H), 2.80–2.98 (m, 6H), 2.69 (br s, 2H).

4-(4-Nitrobenzenesulfonyl)piperazine-1-carboxylic Acid *tert*-Butyl Ester. Diisopropylethylamine (3.14 mL, 18.0 mmol) was added in one portion to a stirred solution of piperazine-1-carboxylic acid *tert*-butyl ester (3.05 g, 16.4 mmol) in DCM (20 mL) at room temperature. To this mixture was added 4-nitrophenylsulfonyl chloride (3.99 g, 18.01 mmol) portionwise, and the mixture was stirred at room temperature under a nitrogen atmosphere for 1 h. After this time the mixture was diluted with DCM (100 mL) and washed with water (50 mL) before being dried (MgSO₄), filtered, and concentrated to give the title compound (5.45 g, 90% yield) as a white solid. MS (ES⁺) *m/z* (M + 1) 372.

1-(4-Nitrobenzenesulfonyl)piperazine. Trifluoroacetic acid (25 mL) was added dropwise to a cool (0 °C), stirred solution of 4-(4-nitrobenzenesulfonyl)piperazine-1-carboxylic acid *tert*-butyl ester (5.45 g, 16.6 mmol) in DCM (25 mL) under a nitrogen atmosphere. The mixture was allowed to warm to room temperature and stirred overnight at this temperature. After this time the mixture was concentrated to give the title compound (3.95 g, 99% yield) as a yellow solid. MS (ES⁺) *m/z* (M + 1) 272.

1-[4-(4-Nitrobenzenesulfonyl)piperazine-1-yl]propenone. 1-(4-Nitrobenzenesulfonyl)piperazine (0.5 g, 1.9 mmol) was dissolved in THF (5 mL). To this was added diisopropylethylamine (0.98 mL, 5.7 mmol) in one portion followed by the dropwise addition of acryloyl chloride (0.16 mL, 2.09 mmol), and the mixture was stirred at room temperature under a nitrogen atmosphere for 3 h. The THF was removed under vacuum, and the resulting crude material was diluted with DCM (20 mL) and washed sequentially with NaOH (1 M solution,

10 mL), HCl (1 M solution, 10 mL), and brine (10 mL) before being dried (MgSO_4), filtered, and concentrated to give the title compound (0.22 g, 37% yield) as a white powder. MS (ES^+) m/z ($M + 1$) 326.

1-[4-(4-Aminobenzenesulfonyl)piperazin-1-yl]propenone. 1-[4-(4-Nitrobenzenesulfonyl)piperazin-1-yl]propenone (0.22 g, 0.68 mmol) was suspended in a 5:1 mixture of ethanol and water (30 mL). To this solution was added iron powder (0.44 g, 1.8 mmol) followed by saturated ammonium chloride solution (1 mL), and the mixture was heated to 80 °C for 3 h. After this time, the reaction mixture was cooled to room temperature and filtered through a pad of Celite, the Celite was washed with ethanol (10 mL) and ethyl acetate (50 mL), and the solution was concentrated under vacuum. The resulting residue was partitioned between DCM (50 mL) and water (20 mL). The organic layer was separated, dried with MgSO_4 , filtered, and concentrated to afford the title compound (0.18 g, 89% yield) as a white solid. MS (ES^+) m/z ($M + \text{H}^+$) 296.

[4-(4-Acryloylpiperazine-1-sulfonyl)phenyl]carbamic Acid Benzyl Ester (27). Diisopropylethylamine (0.22 mL, 1.2 mmol) was added in one portion to a stirred solution of 1-[4-(4-aminobenzenesulfonyl)piperazin-1-yl]propenone (0.18 g, 0.6 mmol) in THF (10 mL) at room temperature. To this mixture was added benzyl chloroformate (0.13 mL, 0.72 mmol) portionwise, and the mixture was stirred at room temperature under a nitrogen atmosphere for 1 h. After this time the mixture was diluted with DCM (100 mL) and washed with water (50 mL) before being dried (MgSO_4), filtered, and concentrated. The resulting residue was purified using flash column chromatography (elution, 100% ethyl acetate) to give the title compound (0.021 g, 8% yield) as a white solid. MS (ES^+) m/z ($M + 1$) 430; δ_{H} (250 MHz, $\text{DMSO}-d_6$) 10.31 (1H, s), 7.58–7.76 (4H, m), 7.26–7.53 (5H, m), 6.69 (dd, $J = 16.75, 10.36$ Hz, 1H), 6.03 (dd, $J = 16.75, 2.28$ Hz, 1H), 5.63 (dd, $J = 10.51, 2.28$ Hz, 1H), 5.17 (2H, s), 3.50–3.69 (4H, m), 2.84 (t, $J = 4.72$ Hz, 4H).

Incubations in Hepatic Microsomes. Test compound (1 μM) was incubated in 0.5 mg/mL of pooled male rat, mouse, or human liver microsomes (obtained commercially) in 0.1 M phosphate buffer at 37 °C. After the mixture was prewarmed for 5 min, reactions were initiated by the addition of NADPH (1 mM). Aliquots (80 μL), samples were taken from the incubation at 0 (control), 5, 10, 20, and 40 min, and the reaction was immediately terminated by adding the aliquot into 80 μL of acetonitrile containing an analytical internal standard (IS). Samples were centrifuged and the supernatant fractions analyzed by LC–MS/MS with multiple reaction monitoring (MRM). All incubations were performed in duplicate using testosterone as the positive control. The MRM area response ratio of the analyte over IS for time = 0 min control was set to 100%. The relative decrease in MRM area ratio intensity over time against that of the control (percent parent decrease) was used to determine the half-life ($t_{1/2}$) of memantine in the incubation. Half-life values were calculated from the relationship $t_{1/2}$ (min) = $-0.693/\lambda$, where λ is the slope of the ln concentration vs time curve. The intrinsic clearance (Cl_{int}) was calculated as $\text{Cl}_{\text{int}} = (0.693 \times \text{incubation volume } (\mu\text{L})) / (t_{1/2} \text{ (min)} \times \text{mg of microsomal protein})$.

Bidirectional Caco Permeability. CacoReady 24-transwell plates with plated Caco cells were purchased from Advantec and were prepared for the experiments following manufacturer's instructions. Test compound and reference compounds (propranolol, digoxin, and vinblastine) were added to either the apical or basolateral chambers of the transwell plate assembly at a concentration of 10 μM prepared in Hanks' balanced salt solution containing 25 mM HEPES (pH 7.4). Lucifer yellow (LY) was added to the donor buffer in all wells to assess viability of the cell layer. Since LY cannot freely permeate lipophilic barriers, results are rejected when a high degree of LY transport (>100 nm/s) was observed. After 1 h of incubation at 37 °C, aliquots were taken from both chambers and added to acetonitrile containing an analytical internal standard in a 96-well plate. Concentrations of compound in the samples were measured by high performance liquid chromatography/mass spectrometry (LC–MS/MS).

P_{app} values were calculated from the relationship $P_{\text{app}} = ([\text{compound}]_{\text{acceptor final}} \times V_a) / (A \times \text{time}([\text{compound}]_{\text{donor initial}}))$,

wherein V_a is the volume in the acceptor compartment and A is the surface area on the cell membrane.

The efflux ratio (Er) was calculated from the relationship $\text{Er} = P_{\text{app}}(\text{B to A}) / P_{\text{app}}(\text{A to B})$, wherein the following assay acceptance criteria were used: propranolol, $P_{\text{app}}(\text{A}>\text{B}) \geq 20$ ($\times 10^{-6}$ cm/s); vinblastine, $P_{\text{app}}(\text{A}>\text{B}) < 5$ ($\times 10^{-6}$ cm/s) with $\text{Er} \geq 5$; Lucifer yellow permeability of ≤ 100 nm/s.

Kinetic Solubility (2% DMSO). By use of a 10 mM stock solution of each compound in 100% DMSO, dilutions are prepared to a theoretical concentration of 200 μM in phosphate buffered saline (PBS), pH 7.4 (2% DMSO final concentration), and in 100% DMSO. An aliquot of the 200 μM DMSO solution is then further diluted to 10 μM , and all dilutions ($n = 2$ in 96-well plates) were allowed to equilibrate at room temperature on an orbital shaker for 2 h. The PBS dilutions are filtered using a Multiscreen HTS solubility filter plate (Millipore), and filtrates are analyzed by LC–UV and LC–MS. The concentration of compound in the PBS filtrate is determined by comparing the UV absorbance peak with that of the two DMSO dilutions which are used as calibration standards. Mass spectrometry is used to confirm the presence of the expected molecular ion in the UV peak measured. The effective range of the assay is 5–200 μM , and compounds returning values close to the upper limit may have much higher solubility.

Plasma Protein Binding. Compounds (10 μM) are added to plasma ($n = 2$) and dialyzed, using a 96-well equilibrium dialysis device (HT Dialysis), against phosphate buffered saline (pH 7.4) for 6 h at 37 °C. After incubation the contents of each plasma and buffer compartment are removed and mixed with equal volumes of control buffer or plasma as appropriate to maintain matrix similarity for analysis. Plasma proteins are then precipitated by the addition of acetonitrile containing analytical internal standard and centrifuged, and the supernatant is removed for analysis by mass spectrometry (LC–MS/MS). The percentage drug bound is determined using the following relationship, where total plasma concentration and free concentration are the MS responses obtained from analysis of the plasma and buffer compartments, respectively: % bound = $(\text{total plasma concentration} - \text{free concentration}) \times 100 / \text{total plasma concentration}$. Compound recovery in the assay and stability in plasma were determined simultaneously in the same assay.

■ ASSOCIATED CONTENT

● Supporting Information

Interaction profile diagrams of TG2 with peptide 1 generated using the fragment molecular orbital (FMO) method and k_{inact}/K_i versus IC_{50} correlation data for TG1, TG3, and FXIIIa consisting of data tables and attending graphs. This material is available free of charge via the Internet at <http://pubs.acs.org>.

■ AUTHOR INFORMATION

Corresponding Author

*Phone: (310) 342-5518. Fax: (310) 342-5519. E-mail: john.wityak@chdifoundation.org.

■ ACKNOWLEDGMENTS

The authors thank Wayne Thomas and Jonathan Austin for DMPK profiling of program compounds.

■ ABBREVIATIONS USED

TG2, transglutaminase 2; FXIIIa, factor XIIIa; HD, Huntington's disease; HTS, high-throughput screening; GSH, glutathione; DMPK, drug metabolism and pharmacokinetics; MALDI ToF MS, matrix-assisted laser desorption/ionization time of flight mass spectrometry; MM, molecular mechanics; QM, quantum mechanical; FMO, fragment molecular orbital; SBDD, structure-based drug discovery; PIE, pair interaction energies; HEK, human embryonic kidney 293;

HEK-TG2, human embryonic kidney cells stably expressing TG2; PMSF, phenylmethylsulfonyl fluoride

REFERENCES

- (1) Greenberg, C. S.; Birckbichler, R. H. Transglutaminases: multifunctional cross-linking enzymes that stabilize tissues. *FASEB J.* **1991**, *5*, 3071–3077.
- (2) Im, M.-J.; Riek, P.; Graham, R. A novel guanine nucleotide-binding protein coupled to the $\alpha 1$ -adrenergic receptor. *J. Biol. Chem.* **1990**, *265*, 18952–18960.
- (3) Lai, T.-S.; Slaughter, T.; Peoples, K.; Hettasch, J.; Greenburg, C. Regulation of human tissue transglutaminase function by magnesium–nucleotide complexes. *J. Biol. Chem.* **1998**, *273*, 1776–1781.
- (4) Hasegawa, G.; Suwa, M.; Ichikawa, Y.; Ohtsuka, T.; Kumagai, S.; Kikuchi, M.; Sato, Y.; Saito, Y. A novel function of tissue-type transglutaminase: protein disulfide isomerase. *Biochem. J.* **2003**, *373*, 793–803.
- (5) Appelt, D. M.; Kopen, G. C.; Boyne, L. J.; Balin, B. J. Localization of transglutaminase in hippocampal neurons: implications for Alzheimer's disease. *J. Histochem. Cytochem.* **1996**, *44*, 1421–1427.
- (6) Aeschlimann, D.; Kaupp, O.; Paulsson, M. Transglutaminase-catalyzed matrix cross-linking in differentiating cartilage: identification of osteonectin as a major glutaminyl substrate. *J. Cell Biol.* **1995**, *129*, 881–892.
- (7) Mastroberardino, P. G.; Farrace, M.; Viti, I.; Pavone, F.; Fimia, G.; Melino, G.; Kodolfo, C.; Piacentini, M. Tissue transglutaminase contributes to the formation of disulphide bridges in proteins of mitochondrial respiratory complexes. *Biochim. Biophys. Acta* **2006**, *1757*, 1357–1365.
- (8) Molberg, O.; McAdam, S.; Sollid, L. Role of tissue transglutaminase in celiac disease. *Journal of Paediatr., Gastroenterol. Nutr.* **2000**, *30*, 232–240.
- (9) Mangala, L.; Mehta, K. Tissue Transglutaminase (TG2) in Cancer Biology. In *Transglutaminases: The Family of Enzymes with Diverse Functions*; Mehta, K., Eckert, R., Eds.; Karger: Basel, Switzerland, 2005; pp 125–138.
- (10) Siegel, M.; Khosla, C. Transglutaminase 2 inhibitors and their therapeutic role in disease states. *Pharmacol. Ther.* **2007**, *115*, 232–245.
- (11) Jeitner, T.; Pinto, J.; Krasnikov, B.; Horswill, M.; Cooper, A. Transglutaminases and neurodegeneration. *J. Neurochem.* **2009**, *109*, 160–166.
- (12) Stamnaes, J.; Pinkas, D. M.; Fleckenstein, B.; Khosla, C.; Sollid, L. M. Redox regulation of transglutaminase 2 activity. *J. Biol. Chem.* **2010**, *285*, 25402–25409.
- (13) Liu, S.; Cerione, R. A.; Clardy, J. Structural basis for the guanine nucleotide-binding activity of tissue transglutaminase and its regulation of transamidation activity. *Proc. Natl. Acad. Sci. U.S.A.* **2002**, *99*, 2743–2747.
- (14) Pinkas, D.; Strop, P.; Brunger, A.; Khosla, C. Transglutaminase 2 undergoes a large conformational change upon activation. *PLoS Biol.* **2007**, *5*, 2788–2796.
- (15) Pardin, C.; Gillet, S. M. F. G.; Keillor, J. W. Synthesis and evaluation of peptidic irreversible inhibitors of tissue transglutaminase. *Bioorg. Med. Chem.* **2006**, *14*, 8379–8385.
- (16) Watts, R. E.; Siegel, M.; Khosla, C. Structure–activity relationship analysis of the selective inhibition of transglutaminase 2 by dihydroisoxazoles. *J. Med. Chem.* **2006**, *49*, 7493–7501.
- (17) Griffin, M.; Mongeot, A.; Collighan, R.; Saint, R. E.; Jones, R. A.; Coutts, I. G. C.; Rathbone, D. L. Synthesis of potent water-soluble tissue transglutaminase inhibitors. *Bioorg. Med. Chem. Lett.* **2008**, *18*, 5559–5562.
- (18) Duval, E.; Case, A.; Stein, R. L.; Cuny, G. D. Structure–activity relationship study of novel tissue transglutaminase inhibitors. *Bioorg. Med. Chem. Lett.* **2005**, *15*, 1885–1889.
- (19) Ozaki, S.; Ebisui, E.; Hamada, K.; Goto, J.-I.; Suzuki, A. Z.; Terauchi, A.; Mikoshiba, K. Potent transglutaminase inhibitors, aryl β -aminoethyl ketones. *Bioorg. Med. Chem. Lett.* **2010**, *20*, 1141–1144.
- (20) Case, A.; Stein, R. L. Kinetic analysis of the interaction of tissue transglutaminase with a nonpeptidic slow-binding inhibitor. *Biochemistry* **2007**, *46*, 1106–1115.
- (21) Mastroberardino, P. G.; Iannicola, C.; Nardacci, R.; Bernassola, F.; DeLaurenzi, V.; Melino, G.; Moreno, S.; Pavone, F.; Oliverio, S.; Fesus, L.; Piacentini, M. Tissue transglutaminase ablation reduces neuronal death and prolongs survival in a mouse model of Huntington's disease. *Cell Death Differ.* **2002**, *9*, 873–880.
- (22) Bailey, C.; Johnson, G. Tissue transglutaminase contributes to disease progression in the R6/2 Huntington's disease mouse model via aggregate-independent mechanisms. *J. Neurochem.* **2005**, *92*, 83–92.
- (23) Chun, W.; Lesort, M.; Tucholski, J.; Faber, P. W.; MacDonald, M. E.; Ross, C. A.; Johnson, G. V. W. Tissue transglutaminase selectively modifies proteins associated with truncated mutant huntingtin in intact cells. *Neurobiol. Dis.* **2001**, *8*, 391–404.
- (24) Ruan, Q.; Quintanilla, R. A.; Johnson, G. V. Type 2 transglutaminase differentially modulates striatal cell death in the presence of wild type or mutant huntingtin. *J. Neurochem.* **2007**, *102*, 25–36.
- (25) Cariello, L.; de Cristofaro, T.; Zanetti, L.; Cuomo, T.; Di Maio, L.; Campanella, G.; Rinaldi, S.; Zanetti, P.; Di Lauro, R.; Varrone, S. Transglutaminase activity is related to CAG repeat length in patients with Huntington's disease. *Hum. Genet.* **1996**, *98*, 633–635.
- (26) Lai, T.-S.; Liu, Y.; Tucker, T.; Daniel, K. R.; Sane, D. C.; Toone, E.; Burke, J. R.; Strittmatter, W. J.; Greenberg, C. S. Identification of chemical inhibitors to human tissue transglutaminase by screening existing drug libraries. *Chem. Biol.* **2008**, *15*, 969–978.
- (27) Schaertl, S.; Prime, M.; Wityak, J.; Dominguez, C.; Munoz-Sanjuan, I.; Pacifici, R.; Courtney, S.; Scheel, A.; Macdonald, D. A profiling platform for the characterisation of transglutaminase 2 (TG2) inhibitors. *J. Biomol. Screening* **2010**, *15*, 478–487.
- (28) Huber, M.; Rettler, I.; Bernasconi, K.; Frenk, E.; Lavrijsen, S. P.; Ponc, M.; Bon, A.; Lautenschlager, S.; Schorderet, D. F.; Hohl, D. Mutations of keratinocyte transglutaminase in lamellar ichthyosis. *Science* **1995**, *267*, 525–528.
- (29) Boeshans, K. M.; Mueser, T. C.; Ahvazi, B. A three-dimensional model of the human transglutaminase 1: insights into the understanding of lamellar ichthyosis. *J. Mol. Model.* **2007**, *13*, 233–246.
- (30) Seitz, R.; Duckert, F.; Lopaciuk, S.; Muszbek, L.; Rodeghiero, F.; Seligsohn, U. ETRO working party on factor XIII questionnaire on congenital FXIII deficiency in Europe: status and perspective. *Semin. Thromb. Hemostasis* **1996**, *22*, 415–425.
- (31) MacFaul, P. A.; Morley, A. D.; Crawford, J. J. A simple in vitro assay for assessing the reactivity of nitrile containing compounds. *Bioorg. Med. Chem. Lett.* **2009**, *19*, 1136–1138.
- (32) Simeonov, A.; Jadhav, A.; Thomas, C. J.; Wang, Y.; Huang, R.; Southall, N. T.; Shinn, P.; Smith, J.; Austin, C. P.; Auld, D. S.; Inglese, J. Fluorescence spectroscopic profiling of compound libraries. *J. Med. Chem.* **2008**, *51*, 2363–2371.
- (33) Lor, L. A.; Schneck, J.; McNulty, D. E.; Diaz, E.; Brandt, M.; Thrall, S. H.; Schwartz, B. A simple assay for detection of small-molecule redox activity. *J. Biomol. Screening* **2007**, *12*, 881–890.
- (34) Kitaura, K.; Ikeo, E.; Asada, T.; Nakano, T.; Uebayasi, M. Fragment molecular orbital method: an approximate computational method for large molecules. *Chem. Phys. Lett.* **1999**, *313*, 701–706.
- (35) Fedorov, D. G.; Kitaura, K. Extending the power of quantum chemistry to large systems with the fragment molecular orbital method. *J. Phys. Chem.* **2007**, *111*, 6904–6914.
- (36) Ahvazi, B.; Boeshans, K. M.; Rastinejad, F. The emerging structural understanding of transglutaminase 3. *J. Struct. Biol.* **2004**, *147*, 200–207.
- (37) Yee, V. C.; Pedersen, L. C.; Trong, I. L.; Bishop, P. D.; Stenkamp, R. E.; Teller, D. C. Three-dimensional structure of a transglutaminase: human blood coagulation factor XIII. *Proc. Natl. Acad. Sci. U.S.A.* **1994**, *91*, 7296–7300.
- (38) Halim, D.; Caron, K.; Keillor, J. W. Synthesis and evaluation of peptidic maleimides as transglutaminase inhibitors. *Bioorg. Med. Chem. Lett.* **2007**, *17*, 305–308.

(39) Boyd, M. J.; Crane, S. N.; Robichaud, J.; Scheigetz, J.; Black, W. C.; Chauret, N.; Wang, Q.; Massé, F.; Oballa, R. M. Investigation of ketone warheads as alternatives to the nitrile for preparation of potent and selective cathepsin K inhibitors. *Bioorg. Med. Chem. Lett.* **2009**, *19*, 675–679.

(40) McConoughey, S. J.; Basso, M.; Niatsetskaya, Z. V.; Sleiman, S. F.; Smirnova, N. A.; Brett C. Langley, B. C.; Mahishi, L.; Cooper, A. J. L.; Antonyak, M. A.; Cerione, R. A.; Li, B.; Starkov, A.; Chaturvedi, R.; Beal, M. F.; Coppola, G.; Geschwind, D. H.; Ryu, H.; Li, X.; Lismaa, S. E.; Pallos, J.; Pasternack, R.; Hils, M.; Fan, J.; Lynn A. Raymond, L. A.; Marsh, J. L.; Thompson, L. M.; Ratan, R. R. Inhibition of transglutaminase 2 mitigates transcriptional dysregulation in models of Huntington disease. *EMBO Mol. Med.* **2010**, *2*, 1–22.

(41) Chun, W.; Lesort, M.; Tucholski, J.; Faber, P. W.; MacDonald, M. E.; Ross, C. A.; Johnson, G. V. W. Tissue transglutaminase selectively modifies proteins associated with truncated mutant huntingtin in intact cells. *Neurobiol. Dis.* **2001**, *8*, 391–404.

(42) Jeitner, T. M.; Matson, W. R.; Folk, J. E.; Blass, J. P.; Cooper, A. J. L. Increased levels of γ -glutamylamines in Huntington disease CSF. *J. Neurochem.* **2008**, *106*, 37–44.

(43) Verdonk, M. L.; Cole, J. C.; Hartshorn, M. J.; Murray, C. W.; Taylor, R. D. Improved protein–ligand docking using GOLD. *Proteins: Struct., Funct., Genet.* **2003**, *52*, 609–623.

(44) Schmidt, M. W.; Baldrige, K. K.; Boatz, J. A.; Elbert, S. T.; Gordon, M. S.; Jensen, J. H.; Koseki, S.; Matsunaga, N.; Nguyen, K. A.; Su, S.; Windus, T. L.; Dupuis, M.; Montgomery, J. A. General atomic and molecular electronic structure system. *J. Comput. Chem.* **1993**, *14*, 1347–1363.

(45) Suenaga, M. Facio: new computational chemistry environment for PC GAMESS. *J. Comput. Chem. Jpn* **2005**, *4*, 25–32.

(46) Suenaga, M. Development of GUI for GAMESS/FMO Calculation. *J. Comput. Chem. Jpn* **2008**, *7*, 33–53.

(47) Labute, P. The generalized Born/volume integral implicit solvent model: estimation of the free energy of hydration using London dispersion instead of atomic surface area. *J. Comput. Chem.* **2008**, *29*, 1693–1698.